Chemical Engineering Journal 264 (2015) 899–935

Contents lists available at ScienceDirect

Chemical Engineering Journal

journal homepage: www.elsevier.com/locate/cej

Review

# Review on the physicochemical treatments of rice husk for production of advanced materials

N. Soltani, A. Bahrami, M.I. Pech-Canul*, L.A. González

*Centro de Investigación y de Estudios Avanzados del Instituto Politécnico Nacional Cinvestav-Saltillo, Av. Industria Metalúrgica No. 1062 Parque Industrial Saltillo-Ramos Arizpe, Ramos Arizpe, Coahuila 25900, Mexico*

## HIGHLIGHTS

- Applications of rice husk and its derivatives.
- Study the available technologies for production of SiC, pure Si, $Si_3N_4$, $Mg_2Si$, $SiO_2$ from rice husk.
- Explanation of different furnaces for production of rice husk ash.
- Study the available technologies for production of activated carbon from rice husk.

## ARTICLE INFO

*Article history:*
Received 30 July 2014
Received in revised form 23 October 2014
Accepted 6 November 2014
Available online 3 December 2014

*Keywords:*
Rice husk ash (RHA)
Silicon-based materials
Physicochemical treatments
Agricultural waste materials
Pyrolysis
Carbon active

## ABSTRACT

Recently, much attention has been focused on the utilization of plant biomass to produce engineering materials, encompassing the technological/scientific aspects as well as the economic, environmental and social issues. Amongst the variety of agricultural wastes or biomasses available, rice-husk (RH) occupies a preeminent position, not only in terms of its amount produced worldwide, but also because of its unique chemistry-related features. In this sense, some attempts have been made to produce advanced materials – including $SiO_2$, SiC, $Si_3N_4$, elemental Si, $Mg_2Si$ and more recently, active carbon –, using RH. The production of those mentioned advanced materials depends largely on the treatments used (physical and/or chemical) and the reactions involved in the process, such as pyrolysis, carbothermal and reduction processes. In this contribution, a critical review on the processing and application of rice husks (RHs) for the production of various silicon-based materials and of active carbon is presented. The review addresses the different processing methods, the effects of various process parameters on the pyrolysis stage, the influence of physical, chemical and thermal treatments, activating conditions and activated carbon consolidation mechanisms. A flow chart with all the possible routes to produce $SiO_2$ was purposely constructed.

© 2014 Elsevier B.V. All rights reserved.

## Contents

1. Introduction . . . . . 900
2. Biofibers from agricultural by-products for industrial applications . . . . . 901
    2.1. Rice husk . . . . . 901
3. Application of rice husk . . . . . 903
    3.1. Absorbent. . . . . 903
    3.2. Coatings . . . . . 904
    3.3. Pigment . . . . . 904
    3.4. Cement industry . . . . . 904

---

* Corresponding author. Tel.: +52 (844) 4 38 96 00x8678.
*E-mail addresses:* martin.pech@cinvestav.edu.mx, martpech@gmail.com (M.I. Pech-Canul).

http://dx.doi.org/10.1016/j.cej.2014.11.056
1385-8947/© 2014 Elsevier B.V. All rights reserved.

- 3.5. Insulator . . . . 905
- 3.6. Rubber . . . . 905
- 3.7. Electronics . . . . 905
- 3.8. Energy . . . . 905
- 3.9. Production of potential reinforcement for fabrication of MMCs and CMCs . . . . 906

4. Production of silica . . . . 907
   - 4.1. Furnace/reactor for production of RHA . . . . 908
     - 4.1.1. Rotary kiln . . . . 908
     - 4.1.2. Fluidized bed process . . . . 908
     - 4.1.3. Inclined grate furnace . . . . 909
     - 4.1.4. Cyclonic furnace . . . . 909
   - 4.2. Effect of temperature on the structure of obtained silica from rice husk . . . . 910
   - 4.3. Pre-purification of thermal treated rice husk . . . . 912
   - 4.4. Post-purification of thermal treated rice husk . . . . 914
     - 4.4.1. Precipitation of silica from the sodium silicate solution through acid treatment . . . . 914
     - 4.4.2. Precipitation of silica from sodium solution through injection of $CO_2$ . . . . 915
   - 4.5. Precipitation of silica with $NH_4F$ . . . . 915
   - 4.6. Hydrothermal process . . . . 915
     - 4.6.1. High-temperature hydrothermal process . . . . 915
     - 4.6.2. Low-temperature hydrothermal process . . . . 915
   - 4.7. Microbial fermentation . . . . 916
5. Silicon carbide . . . . 916
   - 5.1. Vapor–liquid–solid (VLS) . . . . 917
   - 5.2. Frank mechanism (whisker growth from vapor phase) . . . . 917
   - 5.3. SiC formation from rice husk . . . . 917
     - 5.3.1. Pyrolysis of rice husk at lower temperature . . . . 917
     - 5.3.2. Carbothermal reaction of rice husk at higher temperature . . . . 918
   - 5.4. Effect of different parameters on SiC formation . . . . 918
     - 5.4.1. Distribution of silica in rice husk . . . . 918
     - 5.4.2. Effects of catalysts . . . . 919
     - 5.4.3. Effect of atmosphere on SiC formation . . . . 920
     - 5.4.4. Effect of chemical pre-treatment of rice husk . . . . 921
     - 5.4.5. Effect of crystallinty of $SiO_2$ and C . . . . 921
     - 5.4.6. Effect of milling of starting materials . . . . 921
6. Preparation of nano SiC . . . . 922
   - 6.1. Utilization of agricultural waste materials as source for carbon . . . . 922
   - 6.2. Arc plasma reactor . . . . 922
   - 6.3. Microwave heating . . . . 922
7. Silicon nitride . . . . 923
   - 7.1. $Si_3N_4$ formation through carbothermal reduction and nitridation of rice husk . . . . 923
     - 7.1.1. Effect of catalysts on $Si_3N_4$ formation . . . . 924
   - 7.2. $Si_3N_4$ formation through chemical vapor deposition . . . . 925
8. High purity silicon . . . . 925
9. Magnesium silicide ($Mg_2Si$) . . . . 926
10. Activated carbon . . . . 927
    - 10.1. Physical activation . . . . 927
    - 10.2. Chemical activation . . . . 928
    - 10.3. Microwave heating technology . . . . 929
11. Summary and conclusions . . . . 929

Acknowledgments . . . . 930
References . . . . 930

---

## 1. Introduction

Since the 1990s, natural fibers started to emerge rapidly for industrial applications. Several authors have reported recent progresses in the use of natural fibers (rice husk (RH), bagasse, breadfruit, coconut shell and coir, etc.) in composites. Natural fiber composites offer environmental advantages such as reduced dependence on non-renewable energy/material sources, lower pollutant emissions, lower greenhouse gas emissions, enhanced energy recovery, and end of life biodegradability of components [1]. Based on source and origin of natural fibers, they are classified into three large groups: animal, vegetable and mineral natural fibers. Due to the wide usage of vegetables and to their vast availability and renewability in short time periods as compared to the others, in this review paper whenever the term “natural fibers” appears in the text, we are referring to the vegetable ones, which are extracted from plants.

Depending on the part of the plant where they are extracted from, natural fibers can be classified into three categories. When determining the properties of natural fibers, one has to keep in mind that variability in properties depends on the growing environment: temperature, humidity, soil composition, air, age and body of the plant all affect the height of the plant, density and the strength of its fibers, etc. In addition, the way the plants are harvested and processed results in a variation of properties. Rice husk is a major agricultural by-product in rice growing countries like China and India, with 33% and 22% of the global rice harvest, respectively. Unique large-tonnage waste material from cultivation and processing of crops, dissimilarity in the composition and properties to some other plant wastes makes it as a potential material.

The world rice harvest is estimated in 500 million tons per year. Considering that 20% of the grain is husk, and 20% of the husk after combustion is converted into ash, a total of 20 million tons of ash can be obtained. The ash contains potassium, sodium, magnesium, calcium, iron, and phosphorus, as well as considerably smaller quantities of copper, iron, manganese, etc. A large quantity of the world production of rice husk and rice husk ash remains as an unused waste material. As a result, a large number of possible industrial applications of rice husk ash has been investigated. Extensive research has been carried out on the preparation, properties and applications of RHA during the last three decades and many scientific investigations and patents have been published on this subject.

In this contribution, authors critically analyze the past and present research work carried out so far on the processing and application of rice-husk for the production of various silicon-based engineering materials and in addition, of active carbon. The work addresses the different processing methods, the effects of various process parameters on the pyrolysis stage, the influence of physical, chemical and thermal treatments, activating conditions and mechanisms of active carbon consolidation. Albeit a number of scientific/technical review articles related to the use of rice-husk for the development of adsorbents, for polymer green composite constituents and for energy applications, have been published, and with the exception of the work by Sun et al. [2] no attempt has been made to discuss in a comprehensive way the potential of rice husk for the production of advanced materials, within the framework of the materials chemistry perspective. It should be pointed out that other agricultural residues have also been proposed for the production of advanced materials, but due to their low $SiO_2$ content in the ash, they have not been considered for further studies.

In this publication, authors make an attempt to gather information from the oldest to the most recent developments regarding the methods to produce silicon-based material from rice husk. More specifically, the paper is aimed at discussing in depth about the effect of different catalysts, heat treatments, pretreatments and different procedures for the preparation of silicon-based materials, like $SiO_2$ (nanosilica), SiC (nano SiC), $Si_3N_4$, Si, and $Mg_2Si$ (in decreasing order of importance). It also includes the different extraction routes and the methods for enriching and purifying silica in prior and post heat treatment methods. Three main identified routes for silica extraction are summarized in a flow diagram purposely designed for this contribution. The characteristics and operation conditions of the different furnace/reactor systems for silica preparation from rice husk are also presented. The production of active carbon from rice husk under special conditions in two different methods (either physical or chemical activation) is also addressed.

## 2. Biofibers from agricultural by-products for industrial applications

Natural fibers consist of three major components: cellulose, hemicellulose and lignin. Based on the types of fibers and the plant source, the relative portion of these components may vary. Cellulose is a homopolymer of glucose, while hemicellulose is a heteropolymer consisting of hexose (glucose, mannose, and galactose) and pentose sugars (xylose and arabinose) [3]. Cellulose is a semicrystalline polysaccharide and is responsible for the hydrophilic nature of natural fibers. Hemicellulose is a fully amorphous polysaccharide with a lower molecular weight compared to cellulose. The amorphous nature of hemicelluloses comes from the fact that it is partially soluble in water and alkaline solutions. Lignin is an amorphous polymer that does not contain carbon sources. However, it provides rigidity to the structure of the plant. Unlike hemicelluloses, lignin is composed mainly of aromatic compounds, having a small or insignificant influence on the absorption of water [4]. The mechanical properties of fibers directly relates to their elemental composition, components, structure and internal defects. The percentage of cellulose influences the structure and properties of fibers such as tensile strength, electrical resistivity, density, modulus, and crystallinity. However, it should not be generalized to all kinds of fibers. Those with higher cellulose content and higher degree of polymerization of cellulose have better mechanical properties. By increasing the content of lignin and decreasing the length-to-diameter ratio ($l/d$) of individual cells, the mechanical properties deteriorate while extensibility of fibers increases. High $l/d$ ratio of banana and pineapple fibers in comparison with other plants results in the production of long fibers. The $l/d$ ratio of rice straw, wheat straw and corn husk are smaller than those of the former, therefore relatively finer fibers can be formed through the processes while coir has thick individual cells and therefore cannot form fine fibers. Under stress, tensile failure shows two modes: intercellular or intracellular. For instance in banana and pineapples intercellular fracture occurs and fibers give the higher modulus and tensile strength but lower breaking elongation in comparison with coir fibers. On the other hand, it has been reported that the hollow tubular (cellular) structure of the plant fibers provides excellent insulation against heat and noise for automobile applications [5].

Natural fibers (derived from vegetables) can be classified into four groups depending on the part from which they are extracted:

1. Fruit: This kind of fibers are extracted from the fruits of the plant, they are lightweight and hairy, and allow the wind to carry the seeds.
2. Bast: They are found in the stems of the plant, providing the plant its strength. Usually they run across the entire length of the stem and are therefore very long.
3. Leaf: This kind of fibers are extracted from the leaves; they are sturdy and form part of the plant's transportation system.
4. Stalk: These fibers are composed of a slender or an elongated structure that holds up an argon or another part of the body.

Fig. 1 presents a flowchart, showing a classification of natural sources depending on the parts from which they are obtained.

Table 1 summarizes the physical and mechanical properties as well as the chemical composition of the aforementioned natural fibers [6–11].

Because of its low price and more silica content, as compared to the other natural fibers, rice husk has been found suitable for a wide range of manufacturing and application oriented processes. Accordingly, the current critical review focuses on the application and production of silicon-based materials derived from rice husk.

### 2.1. Rice husk

Amongst the various biomasses, with abundant and renewable energy sources, rice husk is not only a potential source of energy, but also a value-added by product [12]. In the last decades, there were many reasons associated with rice husk for not being used effectively like (1) lack of awareness of its potential by farmers and industry persons, (2) socio-economic problems, (3) penetration of technology, (4) lack of environmental concerns, and etc. Solution to the problems associated with utilization of this solid waste needs to be addressed both in quality and quantity aspects. Recently the efforts have centered mostly in the utilization of rice husk to reduce the cost of industrial processing, but due to its hard surface, high silicon content, small bulk density, and not being easily decomposed by bacteria, rice husk residues constitute a dra-

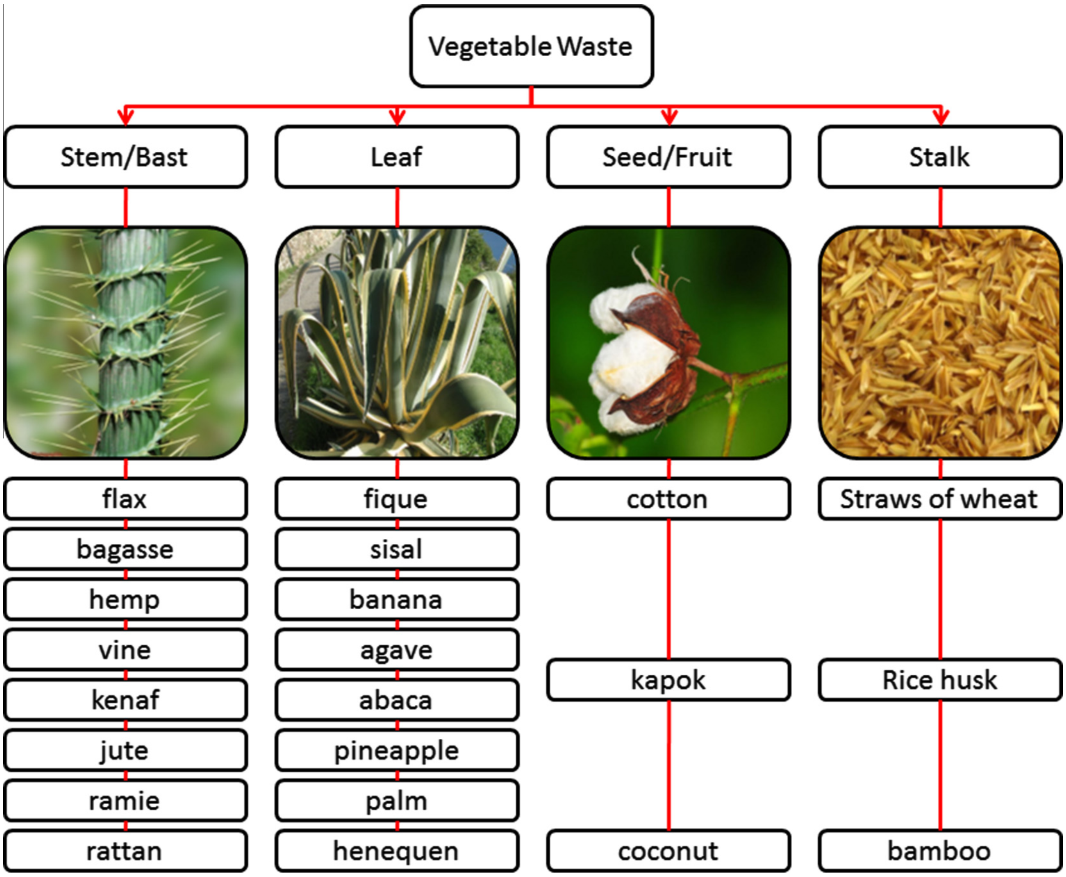

**Fig. 1.** Classification of vegetable source based on the parts from which they are derived.

**Table 1**
Component percentage, physical and mechanical properties of some natural fibers [6–11].

| Natural fiber name | Cellulose | Hemicellulose | Lignin | Ash | Mechanical properties | | | Density (g/cm$^3$) | Moisture (wt.%) |
|---|---|---|---|---|---|---|---|---|---|
| | | | | | Tensile strength (N/mm$^2$) | El. at break% | Young modulus (GPa) | | |
| Ramie | 68–91 | 13.1–16.7 | 0.6–0.7 | 1 | 560–915 | 3.0 | 5.5–12 | 1.5 | 8.5 |
| Flax | 65 | 16 | 2.5 | 3.4 | 344–1035 | 3.0 | 26–28 | 1.3 | 4 |
| Coconut | 32.65 | 7.65 | 59.4 | 5.1 | 150–180 | 20–40 | 4–6 | 0.6–1 | 27.1 |
| Abaca | 56–63 | 20–25 | 7–9 | 3 | 400 | 3.4 | 14 | 1.5 | 14 |
| Banana | 70 | 6–8 | 12 | 1.2 | 529–914 | 1–3.7 | 27–32 | 1.45 | 13.5 |
| Hemp | 70.2–74.4 | 18–22.4 | 3.7–5.7 | | 350–800 | 1.6–4 | 30–60 | 1.48 | 8 |
| Pineapple | 64.35 | 13.85 | 4.6 | 0.04 | 360–749 | 2.8 | 24–35 | 1.45 | 91.35 |
| Kenaf | 53–57 | 15–19 | 5.9–9.3 | 2–5 | 400–700 | 25–50 | 1.7–2.1 | 1.3 | 17 |
| Baggase | 30.2 | 56.73 | 13 | 4.1 | 170–290 | 3–7 | 15–19 | 0.12 | 8.8 |
| Rice husk | 34.4 | 24.3 | 19.2 | 15–20 | – | – | – | 0.55 | 6.5 |
| Corn cob | 45 | 29.3–35 | 13.7–15 | 1–3 | – | – | – | 0.5–0.7 | 9 |
| Oil palm | 56.03 | 27.51 | 20.48 | 2.4 | 248 | 25 | 3.2 | 0.7–1.55 | 1.72 |
| Bamboo | 26–43 | 30 | 21–31 | 1.7–5 | 500–740 | 25 | 30–50 | 0.64 | 6.2 |
| Cotton | 82.7 | 5.7 | – | 0.82–2 | 300–700 | 6–8 | 6–10 | 1.51 | 8.5 |
| Sisal | 67–78 | 7–11 | 10–24 | 0.6–1 | 300–500 | 2–5 | 10–13 | 1.33 | 11 |

matic source of pollution which can alter the ecosystem [13]. Because of this, numerous criticisms and complaints have been reported. In addition, the burned rice husk is associated with carcinogenic and bio-accumulative effects, resulting in silicos is syndrome, in other words, a general adverse effect to health. Furthermore, on the one hand, it has been reported that the utilization of RH in electric power generation is linked to the release of a large number of greenhouse gases that can be a threat to human's health and environment [14]. On the other hand, it has been reported elsewhere that unlike fossil fuels, rice husk can be used for reducing the greenhouse effect because trees absorb $CO_2$ as they grow and this carbon is released when the biomass is combusted. Thus, the net amount of $CO_2$ added to the atmosphere during energy production through the use of biomass (RH) over the entire life cycle is nearly zero [15].

Rice husks contain organic substances and 20% of inorganic material. The main elemental components of RH are C 37.05 wt.%, H 8.80 wt.%, N 11.06 wt.%, Si 9.01 wt.% and O

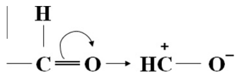

**Fig. 2.** Electromeric effect in components of hemicelluloses [16].

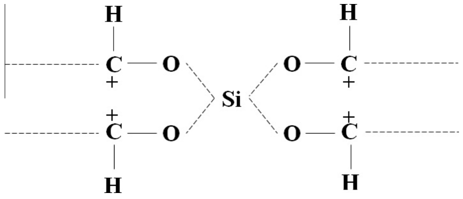

**Fig. 3.** Possible bonding of silicon with carbohydrate in rice husk [16].

**Table 2**
Calculated contents of silicon and $SiO_2$ [16].

| Organic constituent | $SiO_2$ (wt.%) | Silicon (wt.%) |
|---|---|---|
| D-Xylose | 5.179 | 2.421 |
| L-Arabinose | 0.225 | 0.225 |
| Methyl glucoronic acid | 0.3465 | 0.162 |
| D-Glucose | 0.145 | 0.068 |
| Total | 6.1515 | 2.876 |

35.03 wt.%. The contents of RH are hemicellulose 24.3%, cellulose 34.4%, lignin 19.2%, ash 18.85%, and the else substance 3.25% [10]. The monomeric components of hemicelluloses (monosaccharides) are resources for producing large-scale commodities such as xylose, activated carbon, and silicon dioxide, which become polar due to an electromeric effect. The electromeric effect operates as shown in Fig. 2 [16].

This type of electron transfer is brought into play only under the influence of an attacking reagent. Therefore it seems that in rice husk, in addition to free $SiO_2$, silicon is bonded with monosaccharides [16]. Cellulose, ($C_6H_{10}O_5$), the main constituent of rice husk, being a polysaccharide, does not seem to possess considerable bonding property. Lignin, which exists with cellulose, is mostly inert and therefore it is also not expected to be suitable for bonding [16–18]. The possible bonding of silicon with four monosaccharide molecules is shown in Fig. 3.

Based on the assumption that four monosaccharide molecules react with one atom of silicon (as silicon is tetravelent), the percentages of silicon that can remain bonded with different monomeric components of hemicelluloses (monosaccharides) have been shown in Table 2.

Johar et al. [19] reported that cellulose fibers and cellulose nanocrystals can be extracted from rice husk. They purified the cellulose by removing lignin and hemicelluloses from rice husk fibers with an alkali solution. The bleaching process is completed by adding a buffer solution of acetic acid, aqueous chlorite and distilled water. Then, the acid hydrolysis treatment was conducted by sulphuric acid. Most nanocrystal cellulose displayed a diameter and aspect ratio in the range of 15–20 nm and 10–15, respectively. Fig. 4 shows the typical structures of rice husk after each step of the experiment.

## 3. Application of rice husk

India, Pakistan, Bangladesh, Sri Lanka, Australia, Thailand, Indonesia, and USA were pioneers in the utilization of rice husk during 1970–1985, which were supported by government and other organizations. Unique characteristics of rice husk in comparison with other agricultural residues, such as high silica contents (87–97 wt.% $SiO_2$), high porosity, lightweight and very high external surface area make it a valuable material for industrial applications. Fig. 5 depicts some of the applications of rice husks in different industrial fields, taking advantages of special characteristics of rice husk.

### *3.1. Absorbent*

The presence of heavy metals like iron, manganese, nickel, arsenic, cadmium and some anions such as nitrate and fluoride in aquatic systems is a very serious problem and related to the prevalence of some diseases like renal failure, liver cirrhosis, hair losses, cancer, and chronic diseases. Heavy metals are dangerous for living organisms because of their stability, toxicity, and tendency to accumulating in the environment. Adsorption using activated carbon has been found to be an attractive process for the removal of heavy metals from industrial effluents. However, the cost of activated carbon and the loss of adsorption efficiency after regeneration of the exhausted activated carbon have limited its use in effluent waste water treatment. Therefore, alternative low-cost, non-conventional adsorbents such as bagasse fly ash (BFA), rice husk ash, peat, lignite, bagasse pith, wood, saw dust, etc. have been proposed for the treatment of effluents [20,21]. Adsorption properties of rice husk have been studied because of its low price and richness in silica.

Experimental results done on the adsorption behavior of phosphate-treated rice husk (PRH) in case of Ni (II), Zn (II), Cd (II) and Cr (VI) showed that adsorption of Ni (II) and Cd (II) are significant [22], while the investigation by Rocha et al. [23] showed that the adsorption order was Cd (II) > Cu (II) > Zn (II) > Hg (II) on the rice straw. In addition, adsorption column methods show the complete removal of both As (III) and As (V) with rice husk ash [24,25]. It has also been reported that RHA can remove chromium (III) ion from aqueous solutions, but is not very efficient [26].

It has been reported that RHA produced by heating rice husks at 300 °C adsorbs more gold thiourea than the conventionally used activated carbon [27] and also is an effective adsorbent for the removal of Brilliant Green (BG) [13] and Congo Red [28] from aqueous solution.

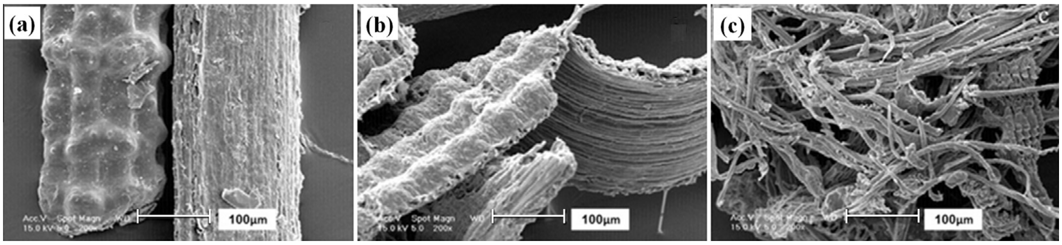

**Fig. 4.** Scanning electron micrograph of (a) untreated rice husk fibers, (b) alkali-treated rice husk fibers, and (c) bleached rice husk fibers [19].

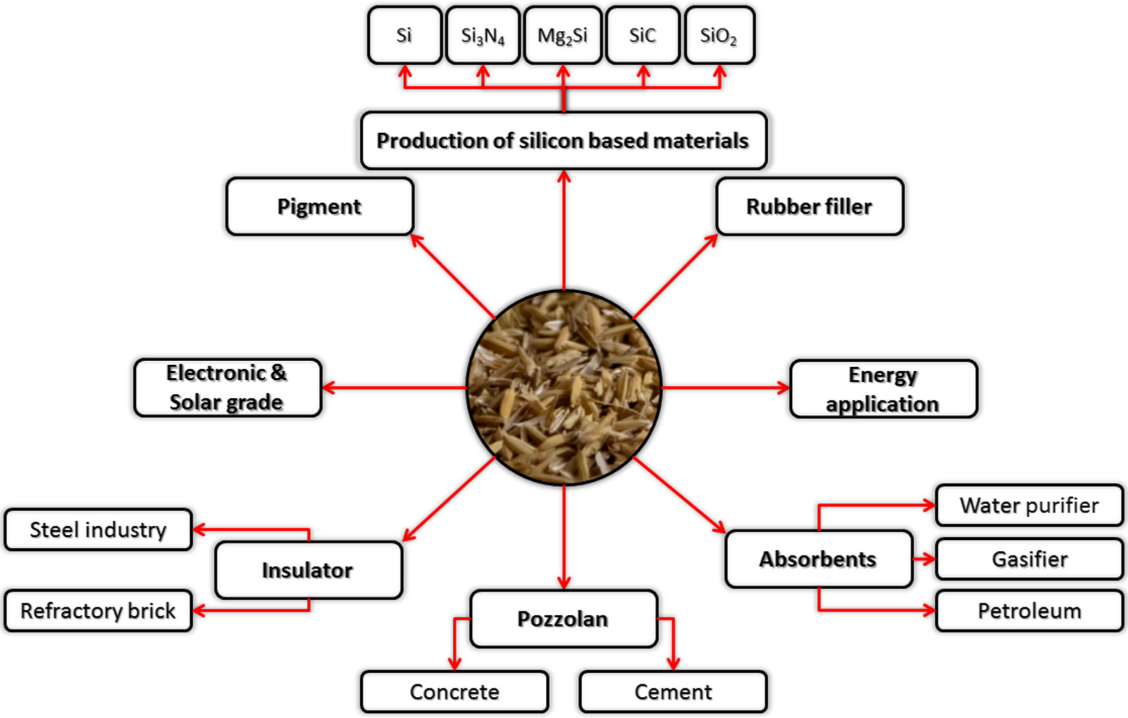

**Fig. 5.** Schematic of applications of derived rice husk.

In addition to the above-mentioned environmental threats, the utilization of dyes in industries such as textiles, rubber, paper, plastics, cosmetics, etc., to color the products is a serious problem for the environment. The dyes are invariably left as the major waste in these industries. Many of the organic dyes are hazardous and may affect aquatic life and even the food chain. For example, malachite green, a common silk and cotton-dyeing agent, has been found to be highly toxic in mammalian cells and acts as a liver tumour-enhancing agent. The removal of dyes is an essential task for environmental protection. Although activated carbon is the most widely used adsorbent for this purpose because of its extended surface area, microporous structure, high adsorption capacity and high degree of surface reactivity, the problems associated with it makes activated carbon a somewhat undesirable adsorbent. Abdelwahab et al. [29] have used activated rice husk to adsorb dyes from aqueous solutions. The result demonstrated that the maximum adsorption capacity was ~13 mg of dye per one gram of dry rice husk. The rice husk also can be used as low-cost and effective sorbent for the removal of direct F. Scarlet (anionic dye Direct Red 23 (DR23)) from aqueous solution. In addition, aluminum hydroxide-coated rice husk ash can remove fluoride from drinking water [30].

Proctor and Palaniappan [31] found that a silicate material derived from rice husk ash was capable of binding lutein from soy oil in hexane at room temperature. Acid washing lowered the ash pH and enhanced lutein adsorption by the ash. In the case of gas adsorption it was reported that absorbent prepared from rice husk ash such as RHA/CaO/$CeO_2$, RHA/CaO, RHA doped with copper and RHA-lithium based have a high capacity in sulfur dioxide ($SO_2$), NO and $CO_2$ absorption [32–36]. In addition, with the aim of lowering manufacturing cost and green synthesis for $CO_2$ absorbant, a series of polyethyleneim-immobilized unimodel and/or biomodal porous silicas were prepared from rice husk ash with biopolymer of chitosan as a pore structure-directing agent [37]. Zeng and Bai reported that TEPA-impregnated mesoporous silica from rice husk treated at 400 °C exhibits a good $CO_2$ adsorption capacity of 173 mg/g adsorbent under 10% $CO_2$ at 75 °C. The porous silica was synthesized by the hydrothermal treatment method using the silicate supernatant extracted from RHA and cetyltrimethyl ammonium bromide (CTAB) as the silica precursor and structure-directing template, respectively [38].

### 3.2. Coatings

The presence of RHA in epoxy paints as steel coating can enhance wear resistance, scratch resistance, and elongation. It seems that this type of filler in epoxy paints increases paint plasticity [39]. In addition, rice husk ash can be used as natural silica ($SiO_2$) source for surface improvement of paper to gain better printability. This coating layer surface will reduce the ink penetration into the paper structure by reducing coating permeability, hence improved water fastness [40].

### 3.3. Pigment

The synthesis of yellow pigment [(Pr, Zr) $SiO_4$] using RHA to study the possibility of an agricultural waste as silica precursor, was evaluated by Bondioli et al. [41]. This pigment is normally produced by calcining a mixture of monoclinic zirconia ($ZrO_2$) and silica ($SiO_2$) in the stoichiometry of zircon, together with the coloring ion precursor ($Pr_6O_{11}$) and one or more mineralizers, i.e. NaF, NaCl or $MgCl_2$. The fabrication of $ZrSiO_4$–$Fe_2O_3$ inclusion through solid state reactions between the mineralizer and both silica (from rice husk) and iron oxide precursors was reported by Andreola and co-workers [42].

### 3.4. Cement industry

Substantial research has been carried out on the use of amorphous silica in the manufacture of concrete. RHA is used in the manufacture of low cost building blocks and in the production of high quality cement in two areas. Ordinary Portland Cement (OPC) is expensive and unaffordable to a large portion of the world's population. Since OPC is typically the most expensive constituent of concrete, the replacement of a proportion of it with RHA offers improved concrete affordability, particularly for low-cost housing in developing countries. The use of pozzolan as alternatives for common Portland cement has been practiced in the past few decades either for cost reduction, performance and durability enhancement, or environmental reasons [43]. Pozzolans are siliceous and aluminous materials, which in themselves possess little or no cementing property. It can be chemically reacted with calcium hydroxide in presence of moisture, at ambient temperature to form compounds possessing cementitious properties [44]. Pozzolanic materials are added to cement to fix the free lime by clinker silicates during their hydration. It results in insolubility of free lime in water, in some instances providing a stronger bond than cement without RHA. The amorphous silica in rice husk ash reacts with $Ca(OH)_2$ to form C–S–H gel ($Ca_{1.5}SiO_{3.5} \times H_2O$) in presence of water at temperature around 30 °C. When this product is heated up, it losses the water, but maintains an amorphous form up to 750 °C. The ultrafine size makes it excellent filler which goes into the micro voids giving high strength to the concrete [45].

Besides, the corrosion performance of concrete can be improved by addition of rice husk ash. As mentioned above, the rice husk ash forms a calcium silicate hydrate gel around the cement particles, which is highly dense and less porous. This will prevent the cracking of the concrete and protect it from corrosion by not allowing any leaching agents to break down the material. The study done by Saraswathy and Song [46] found that the incorporation of RHA up to 30% replacement level reduces the chloride penetration, decreases permeability, and improves strength and corrosion resistance properties.

### 3.5. Insulator

Because of the low thermal conductivity of rice husk ash, it can be used as a raw material for the thermal insulators in a FireBrick. The thermal conductivity of ceramic materials is attributed to crystalline lattice vibrations, or phonons [47]. Fabrication of RHA with the highest flux content, results in characteristics like coarse grains, higher residual carbon content, and low crystallinity. Coarse grains are favorable for formation of porous structures. By increasing the porosities content thermal conductivity decreases. Porous refractories have air entrapped in their pores and this acts as a non-heat conducting material. The amount of the entrapped air increases with porosity of the refractory and hence its thermal conductivity decreases [48]. RHA is also used during the production of high quality flat steel. For instance, RHA is used for insulation of molten metal in tundish and ladle in slab caster. The temperature of molten metal in the ladle is around 1400 °C. When the metal flows from ladle to tundish, the temperature drops to around 1250 °C. This reduction in temperature leads to choking and causes breakdown in the slab caster. Because of separation of RHA as a coating over the molten metal in the ladle and tundish, it forms a coating that maintains the temperature. Therefore, it reduces the breakdown time of the casting. Moreover, it prevents rapid cooling of steel and ensures uniform solidification in casting process [48].

### 3.6. Rubber

Many attempts have been made to use rice husk ash as filler for natural and synthetic rubbers. These kinds of composites have experienced an enormous growth in the automotive industry due to environmentally friendliness, renewability of these fibers, good sound abatement capability, and improved fuel efficiency resulted from the reduced weight of the components. In one of these attempts, Haxo and Mehta [49] revealed the possibility of using ground RHA obtained by a special burning condition as moderately reinforcing filler for styrene-butadiene rubber (SBR), ethylene–propylene–diene elastomer (EPDM), and natural rubber (NR). The results demonstrated that this filler does not adversely affect either the vulcanization characteristics or aging behavior of mentioned materials. On the other hand, Oui et al. [50] investigated the effects of filler loading on the properties of RHA-filled natural rubber (NR) materials compared with those of commercial fillers. They found that both grades of RHA, low- and high-carbon contents, provided inferior mechanical properties (tensile strength, modulus, hardness, abrasion resistance, and tear strength) compared with those of reinforcing filler such as silica and carbon black.

Fuad et al. [51] reported that incorporation of RHA into polypropylene led to an increased flexural modulus of the composites, whereas tensile strength, elongation and impact strength decreased. Siriwardena et al. [52–54] studied the effect of dynamic vulcanization and influence of filler loading of white rice husk ash (WRHA)-filled on different polymer blends. They reported that WRHA-filled blends can be dynamically vulcanized to achieve enhanced properties in a manner similar to that of the unfilled blends. Several researchers studied the poor strength properties resulting from a lack of adhesion between the hydrophobic polymer and hydrophilic filler. They used coupling or compatibilizing agents to improve dispersion, adhesion and compatibility for systems containing hydrophilic cellulose and a hydrophobic polymer. These agents modified the interface by interacting with both the fiber and the polymer, thus forming a link between the components [55–57].

### 3.7. Electronics

Biocon Ltd. in Australia have carried out work on purifying amorphous RHA but can only get to about 99.9% purity at a great cost, and thus Biocon considers that there are no real market opportunities with silicon chips [58]. However, The Indian Space Research Organization has successfully developed technology for producing high purity precipitated silica from RHA, which has a potential use in the computer industry. American and Brazilian scientists developed methods to extract and purify silicon with the aim of using it in semiconductors manufacture [59]. Some companies are purifying RHA into silica suitable for several industries, including silicon chip manufacture [60–62]. Moreover, Bose et al. [63] indicated that magnesium silicide prepared by alloying of 99.9% purity polycrystalline silicon obtained from rice husk ash and high-purity magnesium powder, has potential applications as a semiconductor devices.

### 3.8. Energy

The fact that the present energy use is largely dependent on fossil fuels makes future sustainable development very difficult. There are drastic changes in the composition and behavior of our atmosphere due to the rapid release of polluting combustion products from fossil fuels. There are large quantities of residues, associated with agricultural production and processing industries that can be used for energy production. Unlike fossil fuels, which are limited in availability, these residues are not only abundantly available, but also renewable [64]. Rice husks, as a renewable source of energy, can provide a continuous supply of liquid and gaseous fuels through thermochemical conversion processes. Fig. 6 illustrates the main conversion technologies that have been used or are under development for the production of secondary energy carriers. Combustion (domestic heating, combined heat and power (CHP), and co-combustion), gasification (large-scale and small-scale), and pyrolysis are known as the main thermochemical conversion pathways, while fermentation and transesterification are

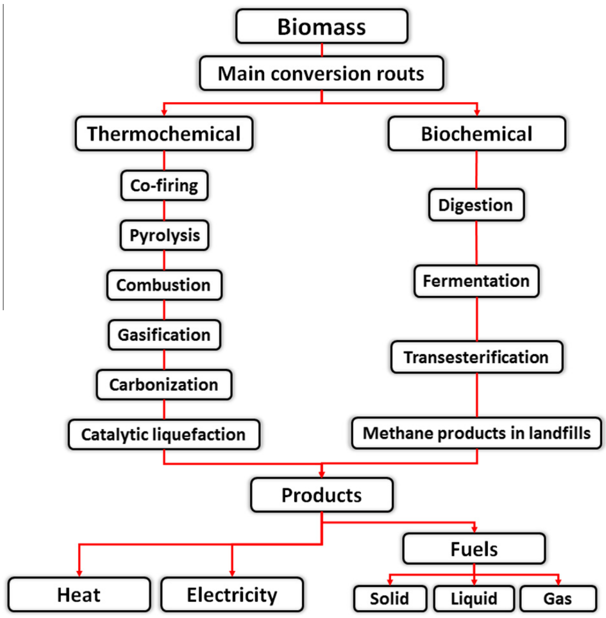

**Fig. 6.** Major conversion technologies for converting biomass into useful energy carriers [66].

the most common biochemical conversion pathways for ethanol and biodiesel production [65,66].

The combustion temperature of rice husk is lower than that of fossil fuel combustion therefore, it is anticipated that there will be lower $NO_x$ emissions. Since biomass contains little sulphur compared to coal, it is also expected that there will be lower $SO_x$ emissions [67,68]. Moreover, rice husk has an average lower heating value (LHV) of 13–16 MJ/kg, which in comparison is about one-third of that for furnace oil, one-half that of good quality coal and comparable with sawdust, lignite and peat. Due to its relatively high calorific value, the combustion of rice husk is autogenously (self-sustaining) and this minimizes the requirements for auxiliary fuel. Apart from offering the benefits of energy recovery, the combustion of rice husk in thermal treatment units will also solve its disposal problem. It is also more environmental friendly as the combustion process reduces the greenhouse effect by converting emissions that would have been methane due to its slow-rotting into the less potent greenhouse gas carbon dioxide [69]. Gasification as a process of converting carbonaceous materials into gaseous products using a gasifying medium such as air, oxygen, steam and etc., that was suggested by Ghaly et al. [70] as an alternative to combustion of low density biomass materials. Some authors have claimed that fluidized bed combustion, with excellent heat and mass transfer characteristics, seems to be a suitable technology for converting rice husk and other agricultural residues into energy [71,72]. The turbulence due to fluidization in the bed can break the rigid ash skeleton to make the trapped carbon available for conversion, although rice husk is difficult to be fluidized due to its cylindrical shape, nongranular and flaky nature. However, fluidization behavior of rice husk was improved when it mixed with other solid particles, such as silicon sand and coal forming a multi solid system. Rice husk ash can easily be removed from the fluidized bed by entrainment in the gas stream, from which it can be collected by a particle-separating system [73]. The main goal of the gasification process is the production of a combustible gas that enriched in CO, $H_2$ and $CH_4$ with medium to high LHV which is suitable for further exploitation in internal combustion engines and turbines [74]. Bed temperature as one of the most important parameters that affects heating value and produced gas composition which should be maintained between 650 and 850 °C [75], besides two other processing parameters should be satisfied, actual air to biomass weight ratio divided by stoichiometric air to biomass weight ratio (ER) and steam to biomass ratio. These ratios should be fixed between the range of 0.2–0.4 [76] and 1.35–4.04 [77], respectively.

### *3.9. Production of potential reinforcement for fabrication of MMCs and CMCs*

Because of the high silicon content in RHs, more extensive studies have been conducted in the past few decades – as compared to other wastes – that have significantly widened its utilization. At present, RHs are the raw materials for the production of a series of silicon-based materials including $SiO_2$, SiC, $Si_3N_4$, $Mg_2Si$ and carbon enriched materials which can be used in metal matrix (MMCs) and ceramic matrix (CMCs) composites [78–82].

For instance, in the original work by Das et al. [83] rice husk ash was used as a reinforcing phase in aluminum–silicon alloys to investigate the effects of second phases on the alloy solidification behavior. A reactive infiltration processing of SiC/Fe–Si composites using preforms made of coked rice husks and SiC powder in different proportions is reported by Zhu et al., in which the $FeSi_2$ alloy was used as the infiltrating liquid material. The incorporation of SiC was conducted in order to improve the wetting and infiltration of the preforms by the alloyed Fe–Si and thus engineer the mechanical properties of the composites.

Because of their scientific and industrial significance, the following paragraphs are devoted to silicon carbide (SiC) ceramic matrix composites, specifically, to some previous investigations where RHA has been used for synthesis of these important materials, although other ceramic matrix composites and different fabrication routes have also been included in this review.

The liquid silicon infiltration (LSI) route in which liquid Si is commonly driven to infiltrate into carbon porous preforms – or a mixture of carbon and SiC powders –, and to react with the carbon, is a promising method to fabricate SiC ceramic composites. $SiC_w$/SiC–Si composites were fabricated by the infiltration of molten Si into porous preforms prepared from pyrolyzed RHs containing SiC whiskers, particles, and carbon. While the amorphous carbon would react with molten Si and form new SiC phases, the SiC whiskers in the preform are expected to remain and act as reinforcement in the composites. The Vickers hardness, flexural strength, elastic modulus, and fracture toughness of the $SiC_w$/SiC–Si composites infiltrated at 1550 °C were 18.8 ± 0.6 GPa, 450 ± 40 MPa, 354 ± 2 GPa, and 3.5 ± 0.3 MPa $m^{1/2}$, respectively [84].

Addition of Mo powder in different proportions to pyrolyzed rice husk up to 11 wt.% was found to cause a suitable residual stress in the material, and thus enhanced the fracture toughness of the composite to 4.1 MPa $m^{1/2}$ [85]. By the reaction of the Mo powder and the pyrolyzed carbon in the preform with molten Si, $MoSi_2$ and SiC can be formed at a much lower infiltration temperature than that for SiC–$MoSi_2$ composites using Mo–Si alloys as infiltration materials [86,87].

Recently, it has been considered that multi-carbide ceramics based on $B_4C$ and SiC have the potential to provide enhanced mechanical properties compared with those of the single-carbide ceramics. For instance, SiC–$B_{12}$(C, Si, B)$_3$–$MoSi_2$ composites have been prepared by the infiltration of molten Si into porous preforms prepared from pyrolyzed RH including SiC whiskers and particles, amorphous carbon and $B_4C$, as well as a little amount of Mo. Molten Si is supposed to react with carbon and $B_4C$ in the preform, forming new carbides. It is also expected that the SiC whiskers and particles in the preforms will remain intact and will preserve their properties in the composites. It is intended that by the reaction with Si, the addition of Mo gives place to $MoSi_2$ formation,

**Table 3**
Utilization of rice husk in ceramic and metal matrix composite materials.

| Composite | Fabrication route | Starting material | Observations | Refs. |
|---|---|---|---|---|
| Si–SiC composite | Self-propagating high temperature synthesis (SHS) | Powder mixture of rice husk ash – activated carbon-Mg | Microstructure and chemical composition | [89] |
| Ferrite composite using $SiO_2$ | At high temperature treatment under nitrogen atmosphere | Pyrolyzed rice husk – $Fe(NO_3)3\cdot9H_2O$ | Enhanced adsorption ability for acid orange II | [90] |
| Al alloy-rice husk ash | Stir casting technique | A356.2 Al alloy | Good interfacial bond between matrix and rice husk ash particles, increment in UTS, hardness and wear resistance | [91,92] |
| Alumino silicate composites (ASC) | | Aluminum hydroxide-rice husk ash-NaOH, $Na_2SiO_3$ boric acid | Good Compressive strength in 3 vol% $H_2SO_4$ solution | [93] |
| Aluminum-4mass% copper/alumina | Powder forging | Aluminum, copper, and rice husk ash silica | Maximum hardness of 44 HRA | [94] |
| Al–Si–Fe/Rice husk ash | Double stir casting method | Ferrosilicon, rice husk ash particle, aluminum | High strength | [95] |
| Alumina–Mullite–Silicon Carbide Composite | In situ by carbothermal reduction | $Al_2Si_2O_7\cdot2H_2O$, $SiO_2$ powder, rice husk ($SiO_2$) and activated carbon | Obtaining $Al_2O_3$–$Al_6Si_2O_{13}$–SiC composite with the whiskers SiC | [96] |
| Aluminum alloy-rice husk ash | Casting | Rice husk, LM 13 alloy, Mg | | [83] |
| Magnesium composite with magnesium silicide | Powder metallurgy(solid-state reaction) | Rice husk silica particles with magnesium powder | High density and hardness | [97] |
| Carbon/silica composite | Carbonizing and hot-pressing | Rice husk | Maximum bulk density and Vickers hardness at sintering temperature of 800 °C | [98] |
| $SiC_w/MoSi_2$–SiC | Liquid Si infiltration (LSI) | Rice husks – Mo powder | High elastic modulus and fracture toughness | [85] |
| $Al/MgAl_2O_4$ | In situ | Microsilica, rice husk ash, pure Al, Mg | Microstructural observations | [99] |
| SiC/Fe–Si | Reactive infiltration | Cocked rice husks, SiC powder, $FeSi_2$ alloy | High Vickers hardness, elastic modulus, three-point flexural strength and indentation fracture toughness | [100] |
| Nano-composites of RHA-10Sn10Ti RHA-10Sn RHA-10Ti | Sol–gel technique | $SnCl_2\cdot2H_2O$, HCl $TiCl_3$, Rice husk ash, cetyltrimethylammonium bromide, $HNO_3$, NaOH | High photocatalytic activity | [101] |
| Nano-composite SiC/$Si_3N_4$ | Carbothermal reduction | Rice husk ash | | [102] |
| Nanocomposite $TiO_2$–$SiO_2$ | Sol–gel | Rice husk | High UV absorption efficiency | [103] |
| Magnesium composite alloys dispersed with $Mg_2Si$ | Extrusion | HCl solution, Rice husk, AZ31 alloy powder | Having high hardness and Young's modulus. | [104] |
| SiCw/SiC–Si composite | Si liquid Infiltration | Rice husk, carbon, silicon | High Vickers hardness, flexure strength, elastic modulus, and fracture toughness | [84] |
| AlSi10Mg/RHA | Stir casting | Rice husk ash with different size ranges (50–75, 75–100 and 100–150 μm), AlSi10Mg alloy | Better wear properties, the coarser and the more rice husk ash, the lower wear rate | [105] |
| Al/SiC/RHA | Pressureless infiltration | Recycled aluminum form beverage containers, SiC, rice husk ash | Presence of the rice husk ash prevent degradation of composite through the formation and subsequent hydration of $Al_4C_3$ | [106] |

which would be advantageous to the overall properties of the composites. This is because $MoSi_2$ is a less brittle phase compared with Si and has a high melting point (2030 °C), thus favoring the high-temperature performance of the composite [88]. A summary of different fabrication routes and types of ceramic- and metal-matrix composites, starting from rice husk is presented in Table 3 [83–85,89–106].

The following sections are devoted to get an insight into the different processing methods, the effects of various process parameters on the pyrolysis stage, the influence of physical, chemical and thermal treatments and mechanisms on synthesis of different silicon based materials including $SiO_2$, SiC, $Si_3N_4$, elemental Si, and $Mg_2Si$.

## 4. Production of silica

Various methods have been reported in the literatures for preparing silica materials, such as plasma synthesis [107], chemical vapor deposition [108], sol–gel processing [109], micro emulsion processing [110], combustion synthesis [111] and hydrothermal technique [112]. The traditional industrial method of preparing silica is that sodium carbonate powder reacts with quartz sand at high temperature to form sodium silicate, and then the obtained sodium silicate reacts with sulfuric acid in order to precipitate silica. This method was hazardous to the environment because of production of 0.23 ton carbon dioxide ($CO_2$), 0.74 ton sodium sulfate and 20 tons waste water during the preparation of 1 ton of silica by using 0.51 ton of sulfuric acid and 0.53 ton of sodium carbonate. In recent years, one of the world's primary concerns is the "greenhouse" effect, especially relating with $CO_2$ [113]. The main disadvantages of the traditional technique are the high-energy consumption and the high levels of pollution. The processes produce large quantities of $CO_2$ and inorganic salts, which have limited their large-scale commercial applications and violated the principle of sustainable development. It is believed that a cheaper and environmental benign route to produce silica powder with desirable materials attracts much more attention. Therefore, nowadays most of the attention is focused on the utilization of biomasses as silica rich source. A content of 65% silica in rice husk ash – produced during burning of rice husk in order to generate energy –, makes this waste material an economically viable raw material for production of silica gels and powders [114]. Silica has been

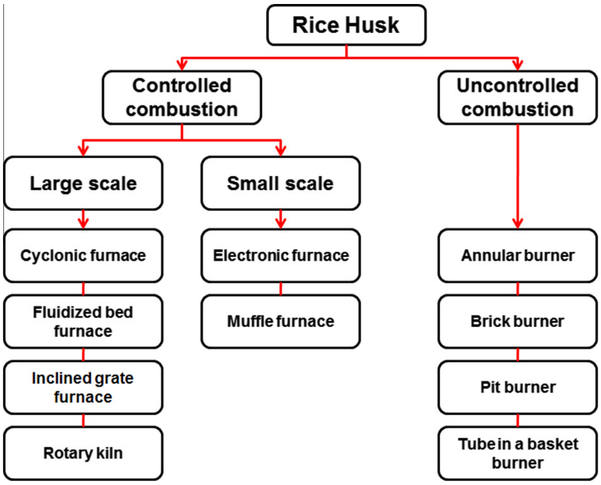

**Fig. 7.** Production of rice husk ash by thermal treatment [117].

widely used in vegetable oil refining [115], pharmaceutical products, detergents, adhesives, chromatograph column packing and ceramics [116].

Depending on the combustion process and RH composition, the rice husk ash may have different colors, which could be, high carbon char, low carbon gray ash, carbon-free pink and white ash. By using different treatment temperatures, pre- and post-purification with different agents (acids, bases, etc.), different structures and purities can be obtained.

### 4.1. Furnace/reactor for production of RHA

In most of processes used for the preparation of ceramic phases from rice husk, furnaces play a vital role. The combustion of rice husk can be divided into two groups: controlled and uncontrolled. It should be mentioned that for production of rice husk ash in large scale, controlled combustion procedures should be chosen. Because of importance of furnaces that work under controlled combustion in production of high purity and activated rice husk ash and also applying special techniques in controlled combustion furnaces, in this part cyclonic furnace, fluidized bed furnace, inclined grate furnace and rotary kiln are introduced [117]. Fig. 7 illustrates the division of thermal production of rice husk ash into two kinds of combustion.

#### 4.1.1. Rotary kiln

When rice husk is used as a heat resource, it is necessary to blow air to achieve the highest possible combustion temperature. However, almost all of the rice husk ash obtained by such procedure is crystalline and very low chemically active. It therefore has few practical uses. Because no method was available for low-cost industrial production of rice husk ash exhibiting high activity, there was a need for developing one. In the batch method for producing active rice husk, a hollow platform having very small holes is placed on an enclosed floor slab. A chimney is erected on the hollow platform in communication with the interior of the hollow platform; a cone of rice husk is formed around the chimney to completely cover the hollow platform. The rice husk at the small holes is ignited for smolderingly incinerating the rice husk into carbonized rice husk, and the carbonized rice husk, and the latter is allowed to self-burn into ash. In the continuous method for producing active rice husk ash, downstream and upstream rotary kilns are connected in tandem; heating of the upstream rotary kiln is controlled to a temperature for burning rice husk into ash. Rice husk is supplied to the upstream rotary kiln to be smolderingly incinerated into carbonized rice husk, then the carbonized rice husk is supplied to downstream rotary kiln to be burned into ash, and finally, the resulting active husk ash is discharged from the downstream rotary kiln [118].

In summary, since this procedure first carbonizes rice husk by burning it in an incineration furnace without flaming and then burns the carbonized rice husk into ash, it enables easy production of white rice husk ash exhibiting excellent chemical reactivity. The schematic of rotary kiln furnace is presented in Fig. 8.

#### 4.1.2. Fluidized bed process

In case of completion of mixing and heat transformation during the combustion of rice husk, in comparison with the other processes, the fluidized bed process is more practical. Therefore, through modern fluidized bed process, it is possible to produce rice husk ash with consistently low ash content (<4%), at a very small residence time (<2 min) in the combustion chamber. A simple fluidized-bed reactor consists of a chamber containing a bed of inert particles such as sand, supported by a distributor plate. Pressurized

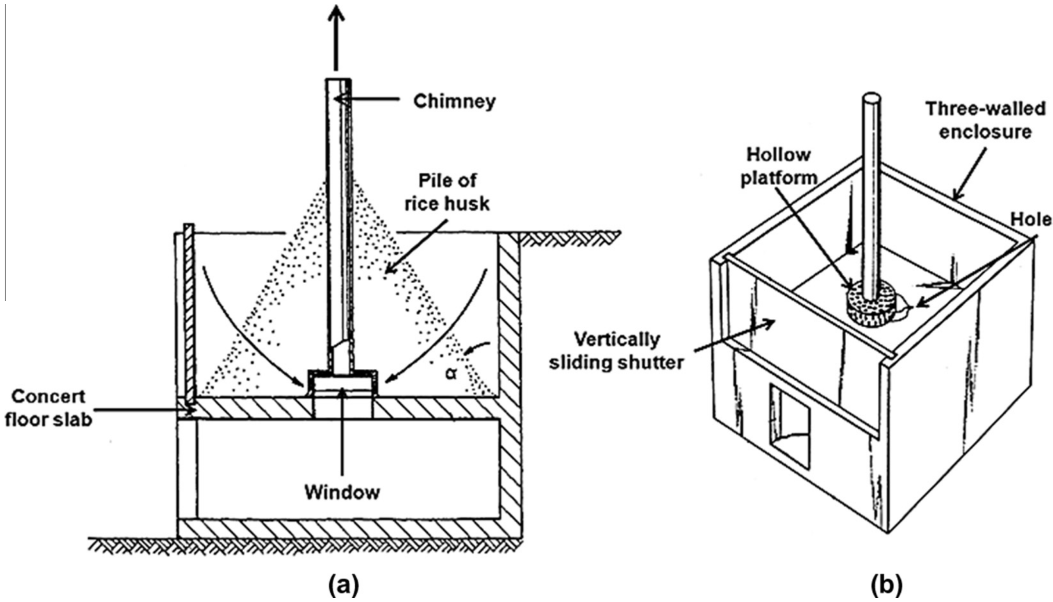

**Fig. 8.** (a) Sectional view of rotary kiln furnace and (b) perspective view of rotary kiln furnace [118].

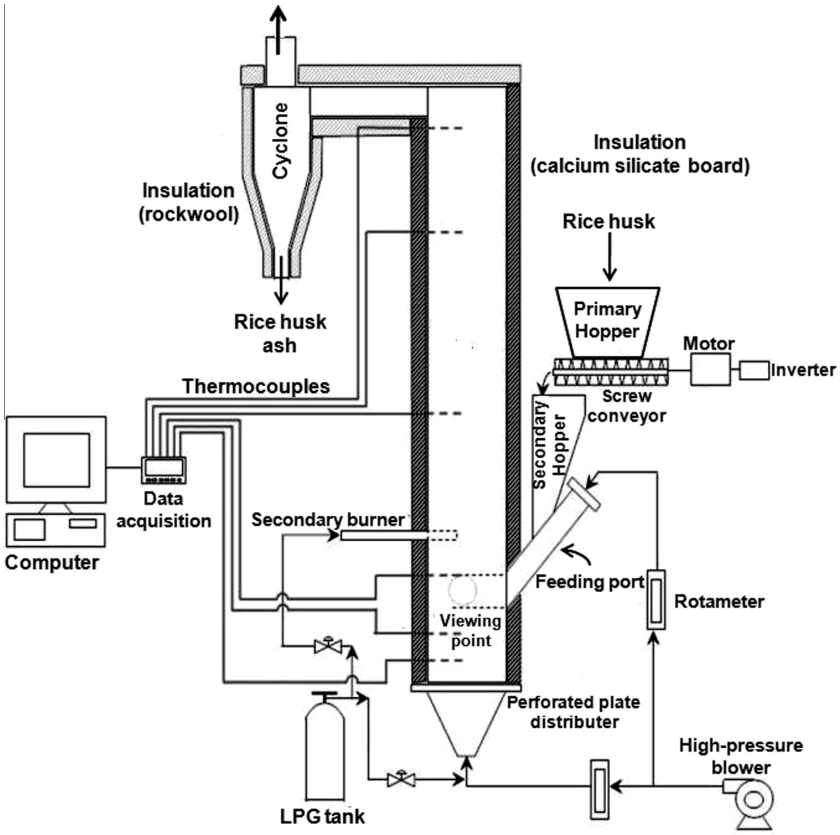

**Fig. 9.** Schematic diagram of the fluidized bed combustor system developed by Rozainee et al. [120].

air is passed through the distributor plate and the velocity of the air is progressively increased to support the entire weight of the bed by the fluid drag on the bed particles due to the upward flowing air. The bed is then said to be incipiently fluidized, and it exhibits fluid-like properties above this particular velocity, called minimum fluidization velocity [64,119]. Because of being exothermic reaction with high calorific value, the external heating is required only during the start-up of the combustion of rice husk; the process is later self-sustaining (autogenous). The process can be operated continuously for large-scale operation. Rice husk ash is easily removed from the fluidized bed by entrainment in the gas stream, from which it can be separated by a simple particle separating system such as cyclone. The control of critical process parameters, such as temperature and residence time is achieved through the control of the ratio of air and rice husk feed in the fluidization chamber. The main advantage of the process is its flexibility to produce rice husk ash of different grades (level of carbon content) depending upon the market demand [117]. Fig. 9 depicts a schematic of fluid bed process developed and utilized by Rozainee et al. [120] in order to produce high purity silica from rice husk.

In addition to the abovementioned attributes of fluidized bed technology, applying this procedure is associated with other significant advantages and disadvantages as follows:

- Continuous and self-sustainable combustion.
- High combustion intensity.
- Better ash composition and no ash sintering or ash removal problem.
- Lower operating temperature range.
- Optimum opportunities for temperature control.
- Easier ash removal, no clinker formation.
- Less excess air, higher $CO_2$ in flue gas.
- Simple operation, quick start-up.
- Fast response to load fluctuations.
- Fluidization of the rice husk and husk char seems to be difficult, unless it is mixed with sand and/or char and/or ash to form a multi-solid system [64,120,121].

### *4.1.3. Inclined grate furnace*

Inclined grate furnace consists of a hull-feeding component, a combustion chamber, and an ash precipitation chamber. It is simple in construction and operation. The air for combustion is supplied by the suction of the dryer fan, while the fuel supply is facilitated by the vibration of a feeder connected by a wire to the fan shaft. However, it has incomplete combustion and inefficient ash separation so that ash and sparks are partially sucked by the fan into the dryer plenum. Despite of similar performance of inclined grate furnace to flat-bed dryers, the former has more durable steel parts than the later, particularly the grate, which is made of mild steel. Two furnace designs are shown in Fig. 10, both with inclined grates. The box-type furnace does not work appropriately for settling ashes as the furnace with cylindrical chamber and center pipe [122].

### *4.1.4. Cyclonic furnace*

In the cyclonic furnace designed and tested by Singh et al. [123] husk and air were introduced tangentially to the cyclone chamber. The air kept the husk rotating in circular motion and accelerated combustion in the chamber. It took initial time for the furnace to attain a self-supporting spontaneous ignition of the husk. The burner was then shut off and the furnace was allowed to run for more given time to obtain the steady state condition. For recording the temperatures at different points in the furnace as shown in

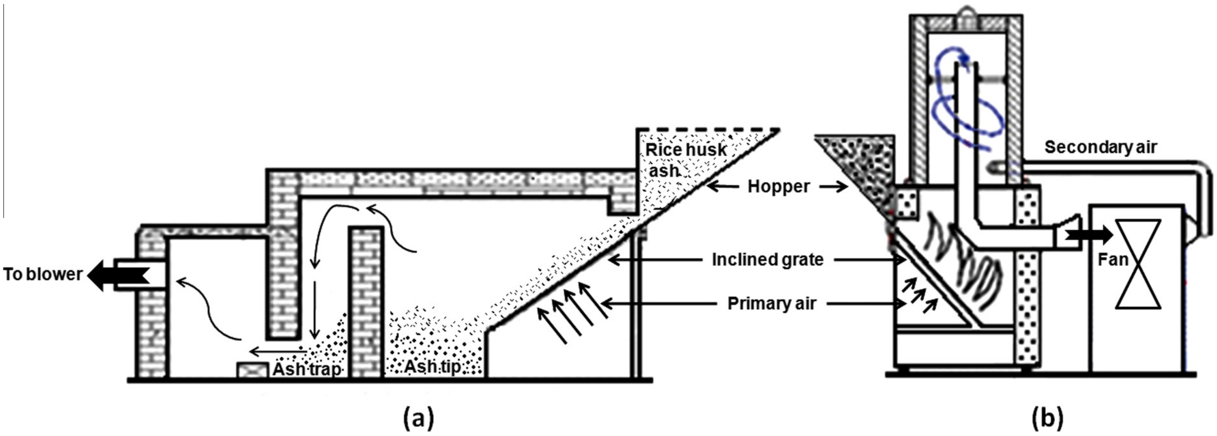

**Fig. 10.** (a) Schematic of the box-type inclined grate furnace and (b) schematic of the furnace with cylindrical combustion chamber [122].

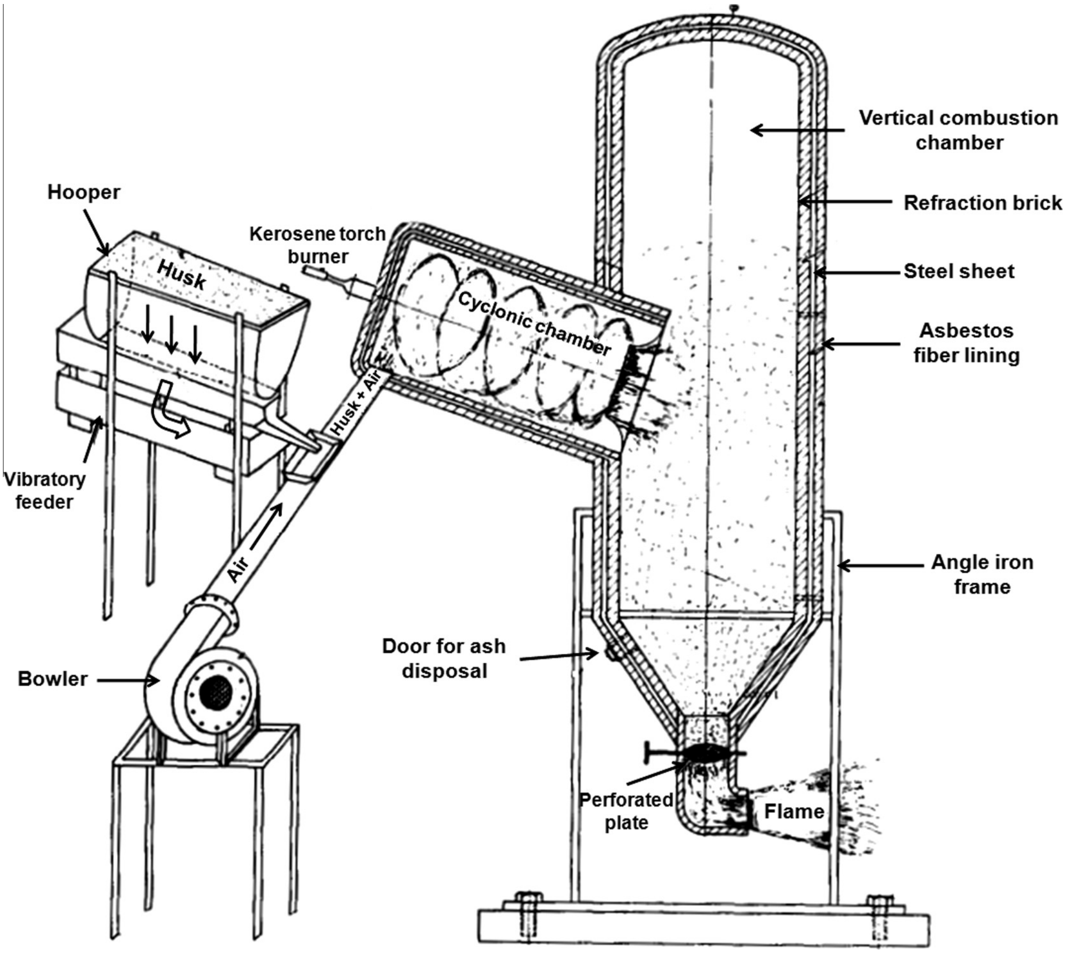

**Fig. 11.** Schematic of cyclonic furnace [123].

Fig. 11, thermocouples were used, which were connected to a temperature recorder. A burner with compressor was also attached to the cyclone for firing the furnace. The inside of the furnace was lined with a mixture of fire-clay and refractory bricks. The ash was trapped behind a perforated cast iron plate provided in the outlet of the conical bottom. The removal of ash was done intermittently through a side opening. In general, the designation of system includes determination of the volume of the cyclone furnace, selection of blower capacity, thickness of insulation and the feeding mechanism. A schematic diagram of the experimental furnace designed by Singh et al. is shown in Fig 11.

### *4.2. Effect of temperature on the structure of obtained silica from rice husk*

Calcination of rice husk in static air at temperatures below 800 °C, leads to the amorphous nature of silica, while crystalline silica occurs at temperatures above 900 °C [45].

**Table 4**
Density and silica content of calcined rice husks [124].

| Temperature (°C) | Density (g/cm$^3$) | $SiO_2$ (wt.%) |
|---|---|---|
| Untreated rice husk | 0.559 | 25.81 |
| 500 | 1.825 | 83.66 |
| 600 | 1.923 | 91.50 |
| 700 | 1.938 | 91.85 |
| 800 | 1.960 | 92.90 |

Yalcin et al. [124] showed that density and silica content increase by increasing temperature; also they indicated that an increase of oxygen partial pressure helped to reduce carbon and increment in $SiO_2$ content to 98.32%. Density measurements, silica content of untreated rice husk, and calcined rice husks at 500, 600, 700, 800 °C (for 4 h) are given in Table 4.

Fig. 12 shows the structure of rice husk ash extracted through different incineration temperatures. RHA300 (incinerated at 300 °C) (Fig. 12a) reveals the porous structure of the adsorbent surface and shows the 'corn cob' structure [125]. The SEM structures of RHA500 and RHA700 are shown in Fig. 12b and c, respectively. Cell walls around pores are fractured and elongated on heating and somewhat ordered reticulated backbones are exposed due to burning off of less dense materials. RHA700 showed less-fractured internal structure and thicker cell walls, giving fewer pores than RHA500. Heating to 900 °C (RHA900) results in a somewhat "glassy" appearance with smooth small pores (Fig. 12d) and the internal backbones appear to be fused together.

The XRD patterns of RHAs are shown in Fig. 13. The broad smooth hump between 15° and 35° ($2\theta$) in the diffractogram in Fig. 13(a–d) is a characteristic feature of amorphous material, indicating that pyrolysis converted the crystalline cellulose structure to amorphous, random, disordered structure, potentially capable of adsorption. When the temperature increases from 500 to 700 °C, there is a little increase of peak intensity at 22° ($2\theta$). Heating to 900 °C increased the intensity of peaks at 22° ($2\theta$), in addition, other peaks were observed at 43°, 45°, 47° and 49° ($2\theta$). This augment in crystal organization would affect the available surface area, resulting in restriction of adsorption capability.

Phase analyses of RHA powders show that by increasing temperature, three crystalline phases are formed, namely, cristobalite, tridymite and quartz in RHA. By increasing the temperature up to 900 °C, the unburned carbon can be removed from the ashes [126], but this leads to the crystallization of the ash from amorphous silica into cristobalite or tridymite. More investigations have been devoted on the formation of cristobalite and tridymite [127–129]. It has been reported that transformation to β-quartz occure at 573–870 °C, β-tridymite at 870–1470 °C, and β-cristobalite at 1470–1710 °C [127]. It has also been reported in the literatures that formation of crystalline phase is accelerated by the presences of potassium oxide ($K_2O$) in the RH. Moreover, by increasing the concentration of potassium, crystallization of tridymite tends to take a place. Silica is able to incorporate "stuffing cation" such as $Na^+$, $K^+$, and $Ca^{2+}$, into cavities of six-membered rings of $SiO_{4/2}$ tetrahedral. Indeed, these inclusions involve particularly the valence compensating elements and require an open structure for transformation of silica to crystalline forms. Quartz, which is the densest of the structures, cannot accommodate additional elements, while tridymite is the only silica polymorph with the lowest density phase that is able to accommodate interstitial $K^+$ cations into its big cavities. Therefore, the addition of $K^+$ cations to silica stabilizes the tridymite structures.

It has been found that some kinds of metal oxides especially potassium oxide, contained in RHA cause the surface melting of $SiO_2$ particles and accelerate the crystallization of amorphous $SiO_2$ into cristobalite and tridymite. Moreover, alkali metal impurities cause the remained carbons in ashes, originated in organics, after burning rice husk. This is because the eutectic reaction between alkali metals and $SiO_2$ element occurs during burning, and the carbon remains in the melt $SiO_2$ and causes the crystallization of rice husk ash at lower temperature [130–133].

In an investigation on the effect of temperature on the morphology and phase transformations of nano-crystalline silica obtained from rice husk, Sarangi et al. reported a graph of the variation of crystallite size of the calcined materials as a function of temperature [134]. This profile shows two regimes: the first one, for temperatures between 500 and 700 °C, corresponds to a situation where the crystallite size grows slowly with temperature. The second one, for temperatures higher than 700 °C, the aggregation effects become very important producing a significant growth in the crystallite size. The aggregation processes, produced by the condensation of the silanol groups ($\equiv$Si—OH), become important

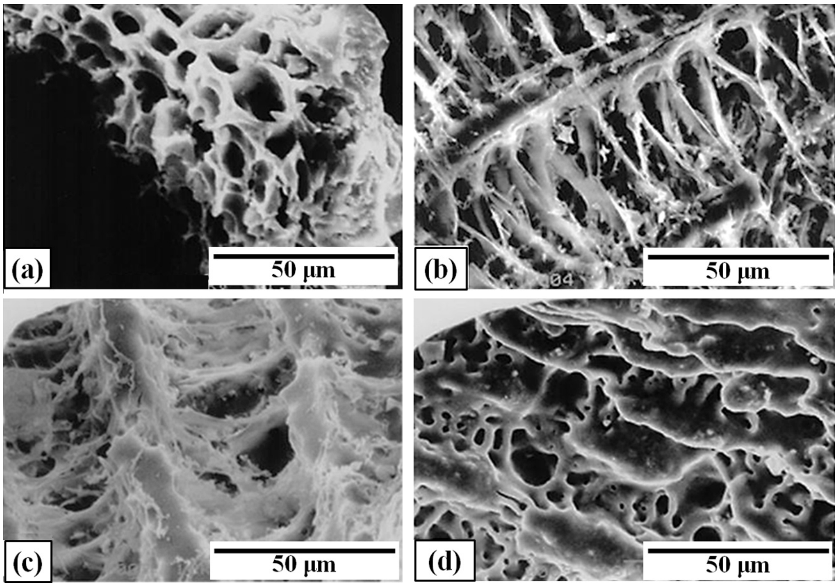

**Fig. 12.** SEM micrographs of rice husk ashes (RHAs); (a) RHA300, (b) RHA500, (c) RHA700 and (d) RHA900 [125].

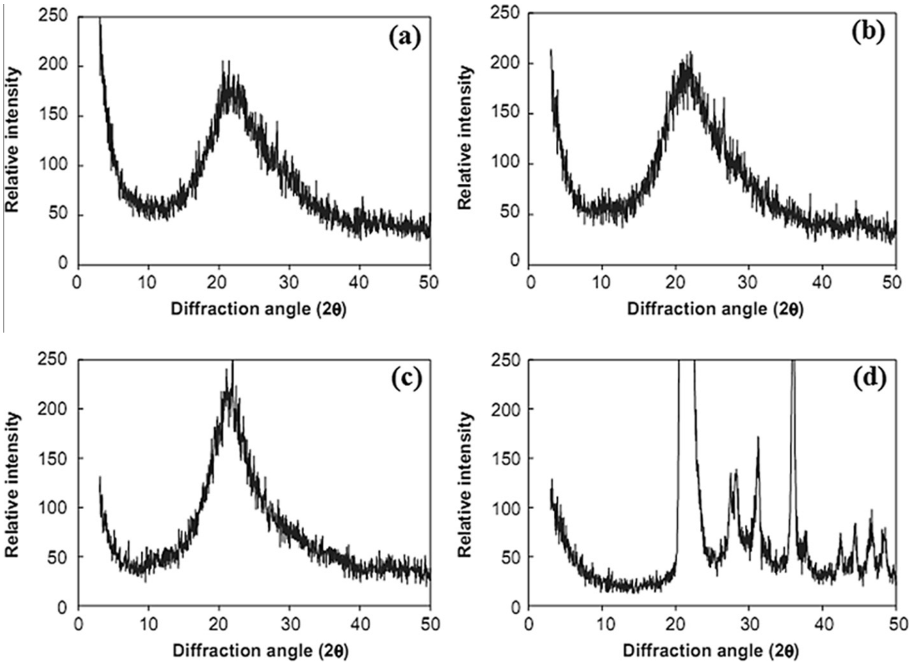

**Fig. 13.** X-ray diffraction patterns of rice husk ashes (RHAs); (a) RHA300, (b) RHA500, (c) RHA700 and (d) RHA900 [125].

for temperatures higher than 700 °C. It is also showed crystallite size increases from 4.87 to 18.61 nm with increase in temperature from 700 to 1100 °C mainly due to agglomeration.

### 4.3. Pre-purification of thermal treated rice husk

Many authors have suggested that leaching and boiling of rice husk with a solution of HCl, $H_2SO_4$, $H_3PO_4$, $HNO_3$, $NH_4OH$ and NaOH before heat treatment at different ranges of temperature and time can be so effective in accelerating the hydrolysis of cellulose and hemicelluloses contained in rice husks and removing most of the metallic impurities. This allows producing ash-silica completely white in color, with high specific surface area [16,130,135–139].

Xiong et al. [140] carried out the preliminary leaching of rice husk with a solution of hydrochloric acid before the combustion. It was found that pretreatment is necessary to obtain relatively pure silica (~99.5%) with a high specific surface area (~260 $m^2$/g). This treatment was very effective for removing most of the impurities. By increasing the temperature up to 1000 °C, only the amorphous phase was detected in diffractograms. This means some leached out ions from the husks favored the crystallization of untreated RHA. Umeda and co-worker [141] also obtained the high purity silica ashes with 99.3% when using a dilute $H_2SO_4$ acid leaching and high temperature combustion.

Chakraverty et al. [135] have studied the effect of different acids and their concentration on the combustion product of rice husk. HCl, $HNO_3$ and $H_2SO_4$ were used for leaching of the rice husk before combustion. Table 5 presents the effect of acids and their concentrations on the impurity reduction. As it can be seen the leaching effect of HCl is superior to that of $H_2SO_4$ and $HNO_3$ for removing the metallic ingredients. It was reported that, acid leaching of rice husk in dilute HC1 (1 N) helps in producing ash completely white in color.

They also evaluated the TG, DTG and DTA analyses of the untreated and acid-treated husks [142] (see Fig. 14). The TG analysis revealed three distinct stages of mass loss, namely, removal of moisture, release of volatile matter and burning of combustible material. The removal of moisture took place at temperatures ranging from 40 to 150 °C. The volatile matter released from untreated

**Table 5**
Effect of acid leaching of husk on removal of metallic constituents from rice husk [135].

| Treatment | Metallic constituents as oxides (ppm) | | | | | | | | |
|---|---|---|---|---|---|---|---|---|---|
| | Na | K | Ca | Fe | Mg | Mn | Zn | Cu | Total |
| Untreated | 5125 | 11750 | 7042 | 946 | 2562 | 1192 | 179 | 31 | 28827 |
| 1 N HCl treated | 46 | 50 | 58 | 362 | 187 | 19 | 19 | 6 | 747 |
| 3 N HCl treated | 33 | 33 | 46 | 262 | 146 | 7 | 19 | 6 | 552 |
| 5 N HCl treated | 25 | ND | 25 | 146 | 125 | 3 | 19 | 6 | 349 |
| 11.3 N HCl treated | 12 | ND | 8 | 129 | 125 | 3 | 17 | 6 | 300 |
| 1 N $H_2SO_4$ treated | 87 | 25 | 2500 | 233 | 729 | 25 | 102 | 12 | 3713 |
| 4.5 N $H_2SO_4$ treated | 92 | 25 | 2417 | 225 | 646 | 25 | 98 | 6 | 3534 |
| 9 N $H_2SO_4$ treated | 75 | 25 | 2500 | 229 | 625 | 19 | 85 | 6 | 3564 |
| 18 N $H_2SO_4$ treated | 75 | 50 | 2667 | 217 | 625 | 24 | 83 | 6 | 3747 |
| 36 N $H_2SO_4$ treated | 117 | 100 | 3333 | 221 | 437 | 171 | 98 | 6 | 4483 |
| 4.5 N $HNO_3$ treated | 17 | 25 | 19 | 500 | 83 | 19 | 17 | 8 | 688 |
| 9 N $HNO_3$ treated | 8 | 25 | 11 | 442 | 83 | 12 | 12 | 6 | 599 |
| 18 N $HNO_3$ treated | 4 | 25 | 7 | 392 | 62 | 6 | 12 | HD | 508 |
| 1 N HCl + 4.5 $HNO_3$ | 4 | 25 | 3 | 375 | 52 | 12 | 19 | 6 | 496 |

ND = Not Detected.

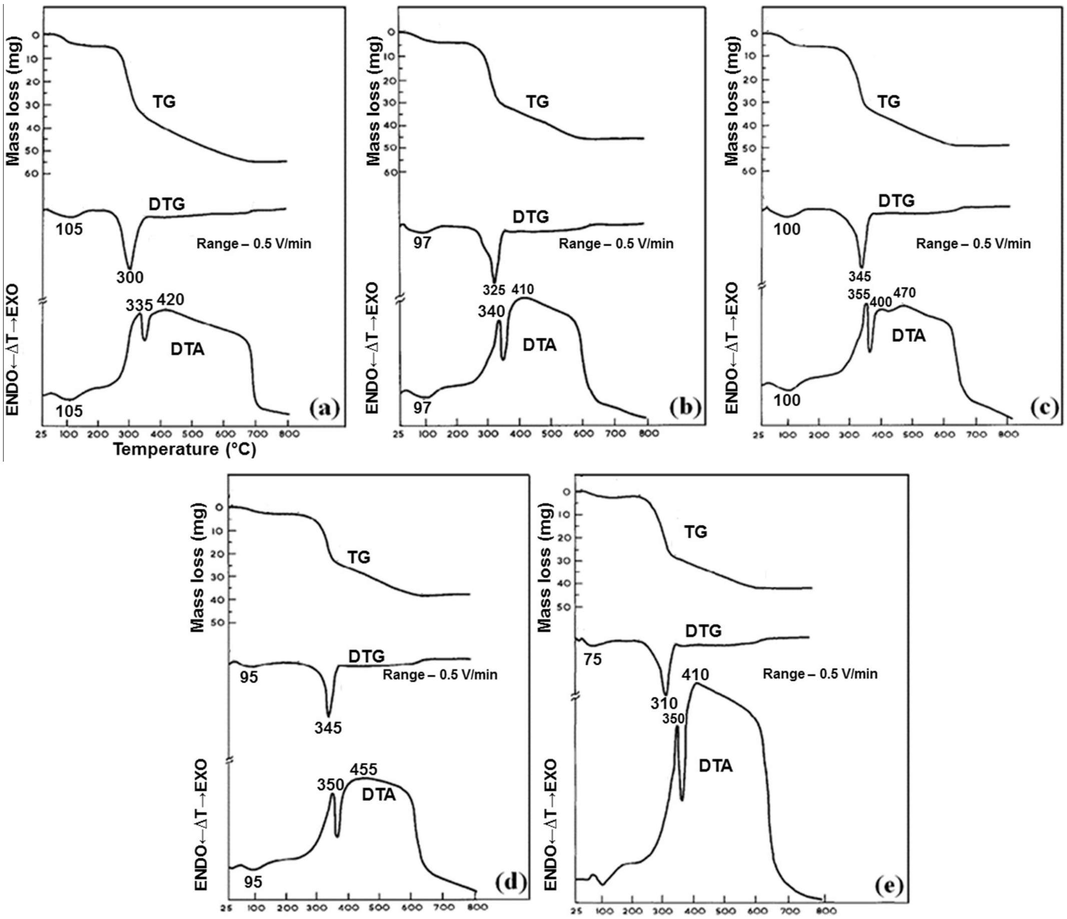

**Fig. 14.** TG, DTG and DTA curves of (a) untreated rice husk, (b) treated with 1 N HCl, (c) treated with 3 N HCl, (d) treated with 5 N HCl and (e) treated with 4.5 N $H_2SO_4$ [142].

husk is in the range of 215–350 °C, while that for acid-treated husk is in the range of 225–375 °C. In the last stage of mass loss that corresponds to the combustion process, DTA records exothermic peaks for untreated rice husk at 690 °C, for treated husk with 1 N and 5 N HCl at 630 and 650 °C, respectively and for 5.5 N $H_2SO_4$ at 645 °C. This shows that treatment with acids of lower concentration is desirable and the final temperature of combustion in this stage decreased with acid-treatment of the husk. However, Carmona et al. [137] showed that activation energies for thermal degradation of acid treated rice husk are higher than those from untreated rice husk. It has been reported that the presence of alkaline and earth-alkaline metals lower the activation energy for thermal degradation of rice husk and decrease the final temperature conversion to silica [143]. Liou et al. [144] also showed the weight loss as a function of heating time at a heating rate of 5 °C/min for rice husk decomposing in $N_2$ and air environment. They showed that the amount of volatile matter evolved in air is greater than that from the $N_2$. By increasing the temperature up to 1500 °C in argon atmosphere, rice husk is converted to SiC at 1375 °C and nothing occurs in weight loss; whereas, in the air atmosphere, weight loss continues [145].

A strong acid leaching treatment, however, is significantly hazardous to environment and human life, and causes an increase of the process cost. Therefore, there are some attempts to use an environmentally benign, harmless to human and economically effective process in order to obtain high-purity $SiO_2$ from rice husk [146].

Umeda and Kondoh [146,147] used a carboxylic acid (citric acid) leaching in order to produce high purity silica. It was reported that by using this acid and hydrolyzing above 200 °C, the metallic impurities such as Na, K, Ca, Mg, Fe, Cu, etc could be also removed from the husks via a chelate reaction between carboxyl groups (–COOH) and the metal elements. After acid leaching, it was necessary to supply a suitable amount of air to complete organics combustion. Thus, high-purity amorphous silica material with 99% or more purity were prepared from rice husks by applying the citric acid leaching treatment and burning process at 800 °C in air. In general, the investigation by Real et al. [130] showed that leaching of rice husks with an acid solution before their combustion would yield silica powder of high specific surface area. However, if the acid leaching was performed after combustion, the specific surface area of silica would be poor.

In some processes besides acid leaching, alkaline treatment was done to purify the rice husk. Ding and Su [148] reported production of native in-situ mastoid $SiO_2$, which in terms of crystal structure is different with the other crystalline $SiO_2$. The first step of their experiment was processing of rice husk with 30% $H_2O_2$ and 10% HCl mixture and then purifying of rice husk with alkaline water compounds 30% ammonia ($NH_3 \cdot H_2O$). The main purpose of pretreatment was to remove the Na, Mg, Ca, Mn, Al, Fe, Zn and other elements with acidic water; another purpose was to remove Na, Cl, P, S and other elements with alkaline water. After heating of dried rice husk at the temperature of 600 °C in a resistance furnace for 10 h, the native white silica was obtained. Eventually, nano-$SiO_2$ white powder was obtained by using ultrasonic fragmentation method. Patel et al. [16] have shown $NH_4OH$ as very weak alkali, cannot dissolve $SiO_2$ and all the $SiO_2$ remains intact. The amount of carbon decreased to 76 wt.% in $NH_4OH$.

Javed and co-workers [149] used $KMnO_4$ as oxidizing agent for preparation of high purity amorphous silica. They mixed rice husk ash with 0.001 N solution of potassium permanganate for 30 min and then dried it in oven at 105 °C for 24 h. It was found that $KMnO_4$ reduces the cellulose and organic contents of the rice husk and acts as an oxidizing agent during thermal degradation. Contribution of cellulose reduction and organic contents and availability of sufficient oxygen both helps thermal degradation of rice husk and produces high purity amorphous silica.

In addition to acid leaching, deionized water can be used as leaching agent. Shen et al. [150] proposed a leaching procedure with deionized water followed by the low calcination temperature and the short calcination times (at 600 °C in 0.5 h) in order to prepare more active amorphous silica from the rice husk. Fig. 15 shows a plot of pore size distribution calculated using the Barrett–Joyner–Halenda (BJH) method. The water-rinsed husk sample shows a narrow peak at the pore diameter of about 3 nm, slightly smaller than that of acid-leached husk sample, which has a value of 3.5 nm. Liou et al. also showed that water rinsed husk has a specific surface area of only 1.45 $m^2/g$, whereas that of the acid leached husk is increased to 10.39 $m^2/g$. The result indicates that the acid can help to decompose the organic matter in the rice husk [144].

### 4.4. Post-purification of thermal treated rice husk

#### 4.4.1. Precipitation of silica from the sodium silicate solution through acid treatment

Through low-temperature alkali extraction, purified silica from amorphous rice husk ash can be obtained. The solubility of amorphous silica at pH = 10 and below is very low and with the increasing the pH, the solubility increases. This unique solubility behavior makes silica extractable in pure form of silica gel by solubilizing it under alkaline conditions, subsequently precipitating it at a low pH and eventually, drying it.

Valchev and co-workers [79] evaluated the purification of silica from rice husk ash using caustic soda at high pressure. Reaction between NaOH and $SiO_2$ was conducted at temperature in the range of 180–200 °C and pressure ranging from 6 to 8 atmospheres. With burning, the rice husk at 650 °C, high reaction pressures can be avoided. The reaction is:

$$SiO_2 + 2NaOH = Na_2SiO_3 + H_2O \tag{1}$$

Precipitating silica from sodium-silicate is induced using sulphuric acid at temperature of 90–100 °C at atmospheric pressure.

$$Na_2SiO_3 + H_2SO_4 = SiO_2 + Na_2SO_4 + H_2O \tag{2}$$

Then, the obtained silica was purified in order to remove the sulphate impurities. The purity and surface of obtained silica were reported 98% and 150 $m^2/g$, respectively. Kalapathy et al. [151] proposed an improved method for production of silica from rice husk ash with lower sodium. They evaluated producing silica in the form of sodium silicate by adjusting the pH to 4 and 7 with different reagents like citric acid, oxalic acid, or hydrochloric acid solution and compare the purity of silica xerogels produced. Comparison between these procedures shows that at pH = 4, gelation is slower and hence sodium ions diffuse readily out of gel matrix and therefore, the content of sodium is lower in comparison with pH = 7. In both the silica precipitated using citric and oxalic acid solution has lower sodium content in comparison with the silica produced using hydrochloric acid. This can be due to the differences in the size of these sodium salts. Because of smaller size of sodium chloride, it can be absorb on to the surface of micropores in the silica, and it cannot be washed out from the silica matrix resulting in higher concentration of sodium. However, Liou et al. [152] concluded that larger salts may become embedded in the gel matrix, and hence are not washed out from the gels. They studied the effect of different gelation pH from 1 to 11 on silica surface area. It has been shown that silica surface strongly depends on pH value. By decreasing pH, silica surface increases. They showed gelation does not occur at pH less than 3. At pH 3, solid starts to precipitate, whereas gel formation is low. Silica yields gradually increase with increasing pH, with a maximum yield occurring at around pH 7. When the pH is greater than 8, formed gels are unstable and partially redissolved. At pH 11, these gels dissolve almost entirely in water. On the other hand, gelation pH has a great effect on porosity and particle size of produced silica. When pH increases from 3 to 7, particle size and porosity increase because, during gel formation, a polycondensation reaction may occur in the following two consecutive paths [153].

$$(OH)_3Si - OH + OH^- = (OH)_3Si - O^- + H_2O \tag{3}$$

$$(OH)_3Si - OH + (OH)_3Si - O^- = (OH)_3Si - O - Si(OH)_3 + OH^- \tag{4}$$

where the $OH^-$ plays an important catalyst role. In the acidic regime, reduced gelation pH leads to the conversion of siloxane bonding (Si–O–Si) to silanol bonding (Si–OH) and gel formation is slow. In this situation, silica is composed of smaller primary particles and, therefore, possesses high surface area. In the basic regime, the formation of a siloxane linkage from surface silanol groups creates negative charges between silica particles and leads to increased electrostatic repulsion [154]. The charge catalyzes the particle to further growth, resulting in increased particle size with increasing pH. This result causes increased porosity and decreased surface area of samples.

Porous silica with high specific surface area has been obtained by Li et al. [155,156]. Pyrolyzed rice husk has been boiled in NaOH

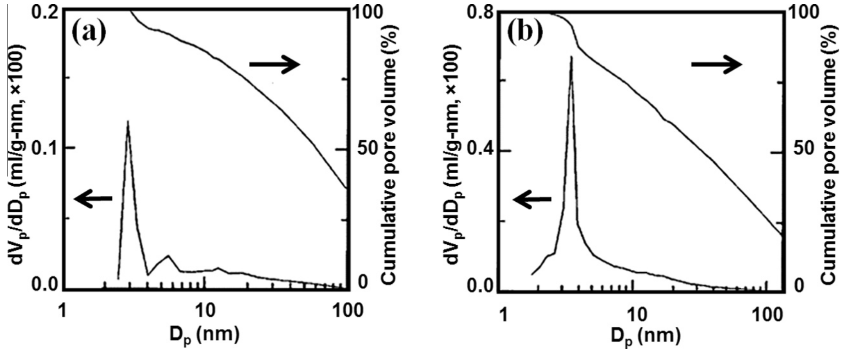

**Fig. 15.** Differential pore size and cumulative pore volume distribution before and after thermal decomposition of specimens, (a) water-rinsed husk and (b) acid-leached husk [144].

solution for 3 h to yield sodium silicate solution. pH value was adjusted by ortho-phosphoric acid ($H_3PO_4$) to 9.0. Next, polyethylene glycol (PEG) was dissolved in this solution. The acid was again added dropwise to decrease the pH value to 4.9 and finally calcined at 500 °C for 1 h. It has been also shown that the amount of PEG used for preparation significantly affects the textural properties of the porous silica. By decreasing pH to 3.2 significantly increased the amount of PEG incorporated into the silica-PEG composites, and hence more pores were generated in the lower pH sample when the PEG was destroyed by calcination. The specific surface can be reached to 1018 $m^2/g$.

#### 4.4.2. Precipitation of silica from sodium solution through injection of $CO_2$

It was reported that by using carbon dioxide at a specific flow rate with continuous stirring, silica could be precipitated from the sodium silicate solution. The precipitated silica is filtered, washed with water to remove the soluble salts and then dried. Addition of calcium caused formation of calcium carbonate and sodium hydroxide. The resulting solution is filtered to remove the solid calcium carbonate. A typical characteristic of silica precipitated is that it is amorphous in nature and the purity is above 98%. The surface area is about 150–200 $m^2/g$ [157]. An [158] introduced another green route for purification of silica powders. In this method, RHA was added into HCl solution, followed by a treatment with a solution of HF and $H_2SO_4$. Then, certain concentration of $Na_2CO_3$ solution was added into the reactor under vigorous stirring for 4 h. The obtained filtrate was kept at 85 °C, and $CO_2$ injects into the reactor through a tube for 60 min. The purity of obtained silica was 98.20%. The yield of silica is affected by different factors such as impregnation ratio of $Na_2CO_3$ to rice husk ash, extraction and carbonation time and concentrations of $Na_2CO_3$ (as silica extraction reagent). Optimal conditions for three factors, impregnation ratio, extraction and carbonation time, were found to be 5:1, 4 h and 60 min, respectively. They showed that the yield of silica gradually increased with the increasing of $Na_2CO_3$ concentration, and reached the maximum value (72.52%) at the concentration of 20 wt.% $Na_2CO_3$. Further increment of $Na_2CO_3$ concentration did not give an increase in silica yield. This outcome can be explained as follows: the reactions (5, 6 and 7) occur in the $Na_2CO_3$ solution, and the concentrations of $HCO_3$ and $OH^-$ increase with the increasing of $Na_2CO_3$ concentration. The increment of $OH^-$ leads to more silica leached out from RHA, therefore, the content of $SiO_3^{2-}$ increased, which accelerated the process of the reaction (6). Thus, the yield of silica was gradually increased. However, the solubility of $HCO_3^-$ is weaker than that of $CO_3^{2-}$, and the increasing of $HCO_3^-$ leads to the separating out of silica in the residue before filtering the suspension. Therefore, the yield of silica slightly decreased when the concentration of $Na_2CO_3$ was above 20 wt.%.

$$CO_3^{2-} + H_2O \leftrightarrow HCO^{3-} + OH^- \qquad (5)$$

$$2OH^- + SiO_2 \leftrightarrow SiO_3^{2-} + H_2O \qquad (6)$$

$$CO_2 + SiO_3^{2-} + H_2O = SiO_2 \cdot H_2O + CO_3^{2-} \qquad (7)$$

### 4.5. Precipitation of silica with $NH_4F$

Ma et al. [159] proposed the recyclable technology for preparation of silica powder using rice husk ash and $NH_4F$. By dissolving silica into 5 mol/l $NH_4F$ solution at a reaction temperature of 110 °C for 3 h, $(NH_4)_2SiF_6$ and $NH_3$ are produced. Addition of $(NH_4)_2SiF_6$ solution to $NH_3{\cdot}H_2O$ causes precipitation of high purity spherical silica powder with the diameter of 50–60 nm. The process of silica dissolution and precipitation is described by reactions (8) and (9), respectively.

$$6NH_4F + SiO_2 \rightarrow (NH_4)_2SiF_6 + 4NH_3 + 2H_2O \qquad (8)$$

$$(NH_4)_2SiF_6 + 4NH_3 + (n+2)H_2O \rightarrow 6NH_4F + SiO_2 \downarrow + nH_2O \qquad (9)$$

### 4.6. Hydrothermal process

The hydrothermal process has been widely used for the synthesis of a vast range of solid-state compounds such as oxides, sulfides, halides, and non-oxide nanomaterials with specific shapes and sizes, as well as for the synthesis of new solids. Nowadays, the hydrothermal process has become an important technique for the synthesis of various kinds of inorganic materials, such as functional oxide molecular zeolites, and other microporous phases.

Hydrothermal process can be considered as constituent process for the base and acid treatments. Due to its intrinsic advantages such as benign environment due to dissolving of some gases, such as $CO_2$, nitrogen oxides, and sulfur oxides in water, versatile chemistry, enhanced reaction rate, and economic cost, it is viable method to produce high purity silica from rice husk at industrial levels. In this respect, a hydrothermal process might have the opportunity to turn into a powerful technique for the synthesis of valuable silica materials from raw rice husk. According to different experimental conditions and reaction mechanisms, two hydrothermal processes can be classified: (1) a high-temperature hydrothermal process and (2) a low-temperature hydrothermal process [160–164].

#### 4.6.1. High-temperature hydrothermal process

Hydro thermo-baric process was used [165,166] to achieve pure silica from rice husk. Hydro thermo-baric purification refers to a process that utilizes single or heterogeneous phase reactions in aqueous media at high temperature ($T > 243$ °C) and pressure ($P > 3$ MPa) to cause leaching or solutionizing of oxide impurities as well as degradation of organic compounds of rice husk. The theory behind the process is that water as a sole aqueous medium, can be dissociated at high temperatures and pressures, forming hydronium (hydrated proton or protonized water) ($H_3O^+$) ion as well as the hydroxyl ($OH^-$) ion. Thus, this acid–base system is capable of reacting with basic and acidic oxides as well as the organic components (the hemicellulose, cellulose and lignin). Except for phosphorous oxide that tends to remain in the solid phase in large quantities, most of the impurities existing in the rice husk can be removed after 30 min. Silica possessed high surface area, retained amorphous structure, and has nanometric particle size, though the product have some residual carbon adsorbed onto its surface.

#### 4.6.2. Low-temperature hydrothermal process

Mochidzuki et al. [167] treated rice husk under hydrothermal conditions in autoclave and steam-explosion processes. The rice husk ash obtained by this method exhibited some properties that are different from those obtained by conventional techniques. The results show that the hydrothermal reaction hardly affected the local silicate structures within the temperature range tested (<240 °C). Regarding the Si local structure, it consisted not only of Q4 network but also Q3 and Q2 units, which the rice husk originally possess. Q4, Q3 and Q2 correspond to the silicon oxygen tetrahedral frameworks [$^*Si(OSi)_4$], silanol groups [$(OH)^*Si(OSi)_3$] and silanediol groups [$(OH)_2{}^*Si(OSi)_2$], respectively. For instance, Q4: is the $SiO_4$ anionic group, or a silicon atom with four surrounding oxygen atoms arranged to define the corners of a tetrahedron. A silanol (Q3) is a functional group in silicon chemistry with the connectivity Si–O–H. It is related to the hydroxy functional group (C–O–H) found in all alcohols. It is suggested that the hot-water-treatment residue is applicable to the preparation of water–glass like materials that are required in some liquid-phase syntheses of inorganic materials, e.g., an advanced production system of mesoporous silicate.

### 4.7. Microbial fermentation

Rohatgi and co-workers [168] suggested a method to release of silica-rich particles from rice husk by microbial fermentation. Rice husk, obtained from a local dehusking mill in Bhopal (India) was subjected to microbial fermentations using a locally isolated species of white rot fungus, Cyathus. Fermentation of the rice husk was carried out for a period of 60 days under standardized conditions of substrate availability and growth temperature. They reported that after harvesting the fermented husk and air dried at 80 °C, rice husks was sieved through different sized sieves to separate the small particles emancipated from the organic fibrous material during microbial fermentation. Then they were burned at 450 °C. The results showed that fermentation resulted in a decrease in organic matter and increment in $SiO_2$ content. The $SiO_2$ content of the fermented husk was also found to be higher in smaller sieve size fractions in comparison to the untreated one. Because of utilization of mechanical sieving in their investigation, released silica-rich particles separate easily. Extracting $SiO_2$ was more efficient when more effective techniques like floatation are explored to separate silica-rich particles. Microbial fermentation could be advantageously used for producing $SiO_2$ particles from rice husk for commercial applications.

Production of silica nano-particles by Californian-red worms through a bio-digestion process of rice husk has been proposed by Estevez et al. [169]. Worms were fed with rice husk for 5 months. The excreted humus was neutralized by using $CaCO_3$ and calcined at different temperatures (500, 600, 700 °C) and then digested with a mixture of two acids (HCl and $HNO_3$ in a ratio 1:3 vol.). The size of the silica particles was in the range from 55 to 250 nm depending on calcination temperatures. It was found that to obtain single silica nano-particles; the calcined temperature should be lower than 600 °C.

In summary, the structure and properties of obtained silica are sensitive to the methods chosen to produce it from rice husk. Depending on the temperature or chemical treatments selected, the results can be different, from amorphous to distinct crystal phases. Fig. 16 summarizes most of the procedures used for the production of silica from rice husk.

## 5. Silicon carbide

Composite materials reinforced with silicon carbide have been the subject of considerable interest in recent years. Silicon carbide has been increasingly considered for improving the strength, stiffness, wear and corrosion resistance, etc [170,171]. High strength and stiffness values in combination with large aspect ratios provide whiskers of silicon carbide effective means to reinforce modern metal and ceramic matrix composite materials. They can be incorporated into metal matrices, usually by melt infiltration or powder metallurgy.

Silicon carbide has many polytypes arising from the different schemes of stacking layers of C and Si atoms; the most common (α-SiC, 4H) is formed at temperatures greater than 1700 °C and has a modified hexagonal crystal structure (wurtzite). The beta configuration (β-SiC, 3C) exhibits a zinc-blende crystal structure (diamond), and can be formed at temperatures below 1700 °C [172]. Structure and stacking sequence for 4H-SiC (ABAC...), 3C-SiC (ACBA...) and 6H-SiC (ABCACB...) are shown in Fig. 17.

Conventionally silicon carbide is manufactured from coal and quartz sand in electric furnace by the Acheson process at high temperature (around 2400 °C) [173]. The large grain size of product (>1 mm) decreases the sinterability of the powder. Fine silicon carbide particles can be obtained by sol–gel techniques and plasma chemical vapor deposition at a submicrometer size. Carbothermal reaction of silica can yield SiC particles easily. The primary problem of the carbothermal reduction process is the particle size of reactants and the need for an intimate contact among them. The size of SiC particles can be optimized through the appropriate control of the particle size of silica and carbon in the reaction mixture. During the last four decades, much attention has been paid to the use of rice husks as starting material for the production of silicon carbide (particles and whiskers). Lee and Cutler did the first synthesis of SiC from RHs in the 1970s. However, many improvements have been made in further studies, to the point where complete industrialization of this technology has been achieved. Due to innumerable reasons, rice rice husk shows the encouraging potential for being used as a starting material for production of SiC particles at a relatively low temperature (~1500 °C), much lower than indicated by thermodynamic and kinetic calculations. Some of them are facile converting of cellulosic component of RH to carbon upon pyrolysis, richness in silica (up to 28% in some varieties), high surface area and intimate contact available from carbon and silica in the RH [174].

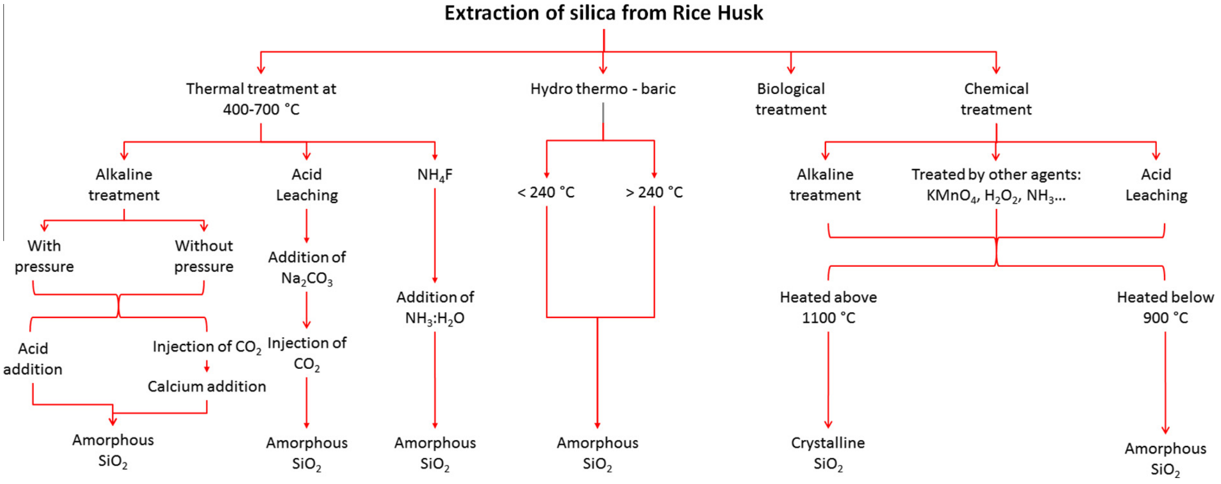

**Fig. 16.** Different procedures, used for producing silica with different structure from rice husk.

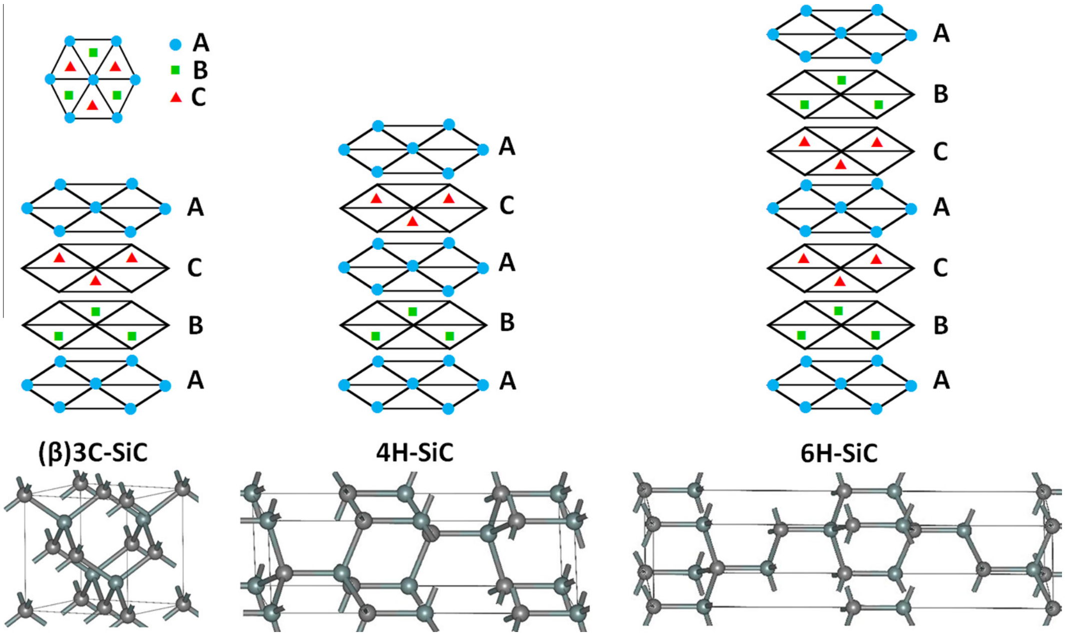

**Fig. 17.** Structure and the staking sequence of major SiC polytypes [172].

By choosing the optimum conditions for processing parameters, both whiskers and particles will be formed. Separation of whiskers from the particulates can be achieved by liquid–liquid separation, froth flotation, selective flocculation, liquid extraction and surface chemical methods [175,176].

A whisker is usually defined as a single crystal of very high aspect ratio, i.e. ratio of length to diameter, with $l/d > 10$ and a diameter in the range $0.01\ \mu m < d < 10\ \mu m$. Such crystal shapes are highly non-equilibrium, with very large surface area to volume ratios. In order for such a structure to be obtained there must be kinetic factors, which promote a highly one-dimensional crystal growth [177,178]. Two mechanisms have been suggested for whiskers growth starting from silica and carbon in rice husk [179]:

### 5.1. Vapor–liquid–solid (VLS)

In this mechanism, the presence of a small liquid droplet acts as a preferred site for whisker growth at the tip of each whisker. Metallic impurities in rice husk are able to act as catalysts in inducing the growth of SiC. Upon heating, the catalysts decompose, and metallic silicides in the form of liquid eutectic droplets are formed, capable of dissolving carbon. The abundance of cavities can be observed in whiskers that result from the entrapment of carbon monoxide gas evolved during the rapid growth period. The absence of the cavities observed outside the whisker core region can be attributed to the lateral growth at slower rates [180]. Milewski et al. and Petrovic [181,182] did provide a more detailed analysis of the VLS mechanism.

### 5.2. Frank mechanism (whisker growth from vapor phase)

In this mechanism, whiskers include one or more screw dislocations parallel to their growth axes. The steps or ledges due to the dislocations at the whisker tips provide the energetically favored sites for growth to continue. Frank mechanism was ruled out due to the absence of axial screw dislocations in any of the whiskers [183]. It has been shown that the whiskers contain discrete regions of high and low planar defect density. Obtaining SiC at low temperature might be associated with planar defects in SiC whiskers. The regions of low defect density were identified as 3C-SiC, whereas the regions of high defect density were consistent with a mixture of SiC polytypes, with the 3C and the 6H polytypes being the most predominant as a result of the formation of microtwins [184].

### 5.3. SiC formation from rice husk

There are several reports, which explain all aspects of formation of SiC from rice husk [185–194]. In most of the cases, the formation of SiC is carried out in two steps. The rice husks are pyrolyzed in the absence of air at a temperature of 700–900 °C and then fired at temperatures of 1500 °C in an inert or reducing atmosphere [195]. Therefore, the carbon/silica ratio of the pyrolyzed rice husks plays a vital role in the formation of silicon carbide. Liou showed the carbonization of raw rice husk under nitrogen atmosphere. By comparing the carbon/silica molar ratio in the carbonized husk, it was found that the carbon/silica molar ratio increased with increasing the heating rate and the micropore, mesopore and total pore volume decrease with increasing the heating rate. The theoretical molar ratio of carbon to silica is 2 for the formation of $Si_3N_4$ and 3 for SiC [144].

#### 5.3.1. Pyrolysis of rice husk at lower temperature

Because the main constituents of biomass materials are celluloses (C) and lignin (L), the pyrolysis reaction reflects the behavior of these two raw organic materials during the process [196,197]. The pyrolysis process at the first stage includes decomposition or depolymerization of celluloses and lignin into the same intermediates (I) that may be organic material of smaller molecular weight; then both gaseous volatiles (V1 and V2) are released from individual pyrolysis reactants (C and L). There is an overlap of decomposition of celluloses and lignin in the first stage. Since the lignin is more difficult to decompose than cellulose, greater activation energy is observed in the last period of the first stage. In the second stage, the residual organic matter (regarded as intermediates, I) is further pyrolyzed to form other volatile species (V3), tar and char (P); the latter is composed of a pure mixture of carbon and silica [197] (see Fig. 18). This material has very high porosity and may

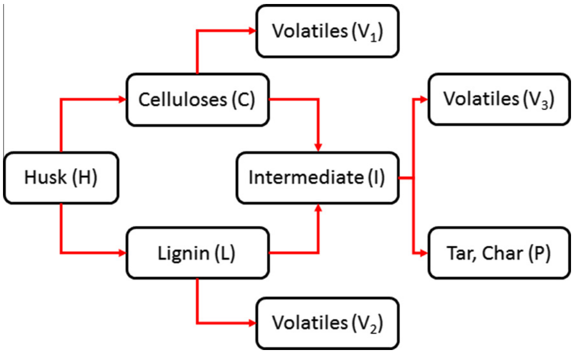

**Fig. 18.** The pyrolysis process of rice husk at low temperature [197].

be used as a starting material for the synthesis of silicon carbide and silicon nitride [198].

### 5.3.2. Carbothermal reaction of rice husk at higher temperature

It has been reported that the four following stages occur during carbothermal reaction: (i) crystallization of silica to form cristobalite (1000–1200 °C), (ii) graphitization of amorphous carbon (>1300 °C), (iii) formation of SiC whiskers (1200–1400 °C) and (iv) formation of SiC particulates (α and β) at higher temperature (>1400 °C) [199]. The change in the structure from whiskers to particles was due to coagulative recrystallization of whiskers. Two factors that control the carbothermal reaction is the production of CO and SiO during the process. It was reported that formation of CO is a desirable condition for formation of silicon carbide whiskers ($SiC_W$). As long as silica and carbon are in contact, the SiO can be produced. As time passes they no longer remain in contact. The CO that is produced by reaction (10), reacts with SiO to form SiC and $CO_2$. By controlling the release of SiO vapor, the formation of $SiC_w$ from rice husks increases. The SiO absorbed in the pores of carbon tends to form SiC particles [173].

$$SiO_2\ (s) + C\ (s) = SiO\ (g) + CO\ (g) \tag{10}$$

$$SiO\ (g) + 3CO\ (g) = SiC\ (s) + 2CO_2\ (g) \tag{11}$$

$$SiO\ (g) + 2C\ (s) = SiC\ (s) + CO\ (g) \tag{12}$$

$$CO_2\ (g) + C\ (s) = 2CO\ (g) \tag{13}$$

The FT-IR spectrum of carbonized rice husk contains several absorption bands, which have been assigned to individual structural units as listed in Table 6.

**Table 6**
Absorption bands in the FT-IR spectra and their assignment.

| Region (cm$^{-1}$) | Assigned to | Refs. |
|---|---|---|
| 3600–3100 | O—H stretching | [200,316] |
| 3000–2850 | C—H stretching | [316,317] |
| 1600 | Aromatic C—C vibrations activated by neighboring oxygen groups | [318] |
| 1500–1415 | C—H deformation | [200,316] |
| 1500–1200 | $CH_2$, $CH_3$, $Si(CH_3)$, $C(CH_3)$ | [319] |
| 1500–1000 | Aromatic C=C skeletal vibration | [200] |
| 2150 | C≡C | [320] |
| 1360–1310 | C—C and C=O skeletal vibration | [200] |
| 1100–1000 | Si—O stretching | [321–323] |
| 970 | SiC (reflection) | [324] |
| 898–825 | Characteristic Si—C bonds appears beside Si—O vibrations | [318] |
| 825–800 | Antisymmetric Si—C stretching | [321,325] |
| 780 | Si—C | [326] |
| 460, 796, 1093 | Characteristic of Si—O bonds | [201,318] |

FT-IR spectra of samples heated to 1240 °C showed that some unsaturated C–C bonds (1360–1310 cm$^{-1}$) and carbonyl groups (1500–1415 cm$^{-1}$) were formed. When it pyrolyzed at a higher temperature (1275 °C) these compounds progressively transformed to aromatic and condensed aromatic compounds, corresponding to the 1600 cm$^{-1}$ band. This results in a rapidly growing three-dimensional network polymer, which continuously grows by trapping small reactive pyrolysis products [200]. As the temperature is increased from 1240 to 1275 °C, a change in absorption at 1100 cm$^{-1}$ (corresponding to the vibration of Si–O bond) with respect to that at 900 cm$^{-1}$ (Si–C–O) is observed. There tends to be stronger absorption at 900 cm$^{-1}$ for the samples heat-treated to higher temperature, or Fe pretreated. The absorption ratios of the bands Si–O/Si–C–O may be indicative of the progressive transformation from silica to SiC [201,202].

Silicon carbide (Si-SiC) also was synthesized by self-propagating high temperature synthesis (SHS) from a powder mixture of rice husk ash-C-Mg under pressure of 0.5 MPa. The overall chemical reactions can be expressed as [89,203]:

$$2SiO_2\ (s) + C\ (s) + 4Mg = SiC\ (s) + Si\ (s) + 4MgO\ (s) \tag{14}$$

During SHS process, the mixture of $SiO_2$, Mg and C may have interacted to form some possible compounds as the following intermediate chemical reactions.

$$SiO_2\ (s) + 2Mg = Si\ (s) + 2MgO\ (s) \tag{15}$$

$$Si\ (l) + C\ (s) = SiC\ (s) \tag{16}$$

$$SiO_2\ (s) + C\ (s) = SiO\ (g) + CO\ (g) \tag{17}$$

$$SiO\ (g) + 2C\ (s) = SiC\ (s) + CO\ (g) \tag{18}$$

## 5.4. Effect of different parameters on SiC formation

By controlling both nucleation and growth of SiC whiskers, the obtainment of SiC can be increased. The thermodynamics and kinetics aspects, temperature, gas flow rates, availability and concentration of growth species, Si/C ratio and a free space to grow are some of the important parameters that should be considered. It has been recognized that the final purification, morphology, structure, and size of SiC ceramic phases depend largely on the chosen processing conditions and additives. Herein, the effects of some of these parameters and additives are discussed.

### 5.4.1. Distribution of silica in rice husk

Composition and topography of both husk surfaces and their internal tissues are important factors for the properties and performance of composite products. Silica distribution plays the main role in formation of SiC. Although, silica exists in all over the rice husk, X-ray point analysis shows that silica is more highly concentrated in regions corresponding to dome-shaped protrusions and adjoining sloping areas (i.e. protruding inter-dome regions) [204]. A representative FE-SEM image and the results of X-ray point analysis are shown in Figs. 19 and 20 [204]. The letters (a, b, c,...) in the *X* axis in Fig. 20 correspond to the silica distribution at various locations in the FE-SEM micrograph of Fig. 19.

The XPS and XRD results indicate that silicon in raw rice husk is bonded to organic material. The SEM analysis of the converted rice husks shows that the part of the rice husk that is rich in carbon (organic material) tends to form a SiC skeleton structure, whereas the part that is rich in silica is the main source of SiO for the formation of SiC whiskers. By growing the whiskers on a carbon surface, the tip of the whisker would no longer be in contact with carbon. The whiskers that formed by the VLS (vapor–liquid–solid) mechanism generally show spherical tips. It confirms that the growth of

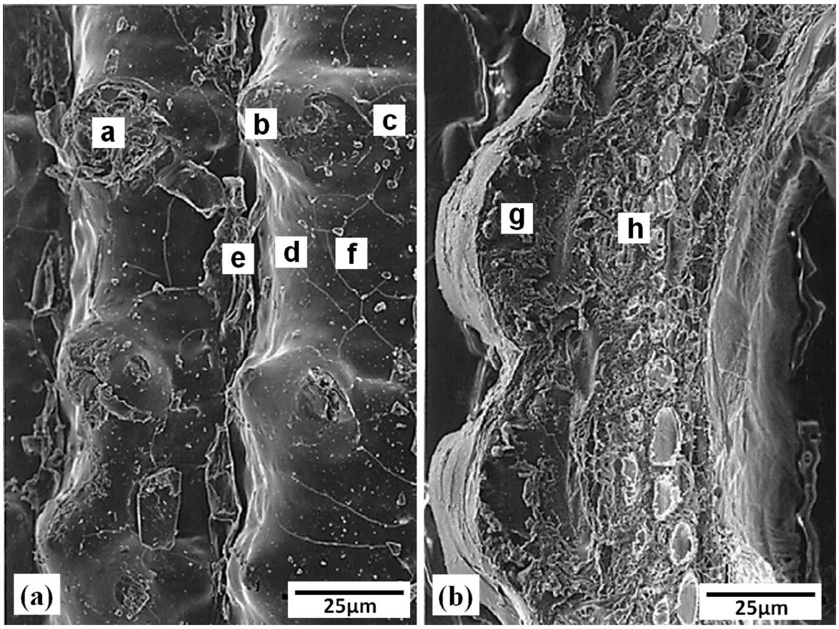

**Fig. 19.** High magnification FE-SEM view of outer surface and cross section of rice husk. The points indicated by letters (a–h) were analyzed by X-ray point analysis for silica concentration, as shown in Fig. 20 [204].

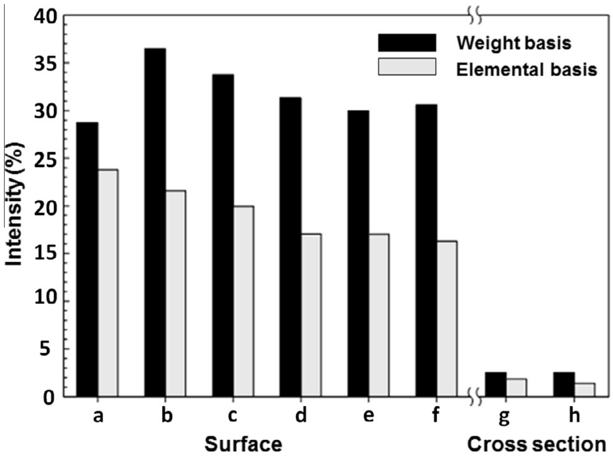

**Fig. 20.** Silica distribution using X-ray point analysis at various locations on the outer surface and within internal tissues of rice husk [204].

SiC whiskers occurs mainly by reaction between SiO and CO [205–207].

### 5.4.2. Effects of catalysts

Analysis of the progression of reaction rate, morphology of the whisker formed, evolution of gases during reaction, crystal size and intermetallic phases, leads to conclusion of a reaction mechanism based on the formation of an M-Si-C liquid phase, which is essential for the nucleation and growth of the SiC whiskers. Catalysts and reaction mechanism, which are involved in the formation of whiskers at elevated temperatures, play complex roles. The effect of catalytic elements in chemical reactions above 600–800 °C are rarely reported [208]. In sight of the melting points of the catalysts, it is likely that their role predominates below 1000 °C. The metallic catalyst may be accelerating reactions between $SiO_2$ and carbon, thus increasing the formation of SiC. During this reaction, it is necessary to flush out the oxygen constantly by argon flow in order to avoid the reverse reaction, namely, oxidation of SiC. In addition, the reduced metal catalyst particles may re-oxidize if the oxygen is not eliminated.

Therefore, it can be said that the progress of the reaction depends on how quickly the oxygen can be removed [209]. The unification of a catalyst greatly increases the reaction rate up to three times that for the un-catalyzed reaction. Different types of catalysts, such as Fe, Co, Ni, Pd, and Cr, have been used in order to achieve high production rate and desirable morphology. It has been reported that iron, cobalt, and nickel are good catalysts for the synthesis of SiC and that their effect is more remarkable for short reaction times. The effect of different catalysts on the formation of SiC from burned rice husks was studied over a temperature range of 1200–1600 °C and the increment in proportion of β-phase from 95% to 99% was observed. Although, using cobalt as a catalyst causes producing larger crystal sizes and nickel increases reaction rate more than other catalysts, the general behavior of the catalysts are very similar [173]. The increasing order of catalytic activity is Ni > Co > Fe > un-catalyzed, whereas for SiC crystal size is Co > Fe > Ni > un-catalyzed. In the investigation by Krishnaro [210] cobalt has been found to accelerate the formation of total SiC (particulate and whiskers) and decrease the formation of SiC whiskers from mixture of silica–carbon black. Cobalt acts as a strong catalyst to the gasification of carbon and decreases the crystallization of carbon black. In the presence of cobalt catalyst, rapid heating has been shown to form larger quantities of SiC whiskers. Without any catalyst, rapid heating has resulted in the formation of SiC particulates. The effect of Fe content on the formation of SiC from rice husk was investigated by Mansour et al. [211]. They reported that the amount of SiC increases with increase in the Fe/$SiO_2$ ratio, up to a limiting value of 0.07 [173]. Martinez et al. [206] evaluated the effects of two different catalysts ($CoCl_2{\cdot}6H_2O$ and $FeCl_2{\cdot}4H_2O$ with $NH_4OH$ as a Fe precipitation agent) on the production of SiC-based materials. It was found that the optimum condition was developed using $FeCl_2{\cdot}4H_2O$ as a catalyzer at 1370 °C. Mansour et al. [211] also reported elsewhere that by addition of iron to the rice husk the volatile matter evolved during the carbonization process would be increased. Furthermore, the iron could also act as an inhibitor for the crystallization of silica and carbon, leading to an increase in the rate of silicon carbide formation at higher temperatures. Platinum loaded SiC samples were found to be very active by Singh et al. [212] observing a 100% conversion of CO to $CO_2$ at temperature as low as 175 °C in the experiment. The activity of the platinum-doped samples did not change with increase in temperature up to 700 °C; however, the high performance observed was attributed to the uniform distribution of platinum on the surface of SiC particles. Kermarec and co-workers [213] reported that the catalysts added as metal hydroxides are first converted to the oxide at around the coking temperature and are subsequently reduced to the metal particles using hydrogen, CO and $C_nH_m$ molecules as:

$$Ni(OH)_2 \rightarrow NiO \rightarrow Ni^0 \tag{19}$$

The zero-valent metal particles can impart a high catalytic property.

Raman et al. [214] increased the yield of $SiC_w$ from a mixture of rice husk, textile grade polycarbonitrile (PAN) and boric acid. PAN was used as an external carbon source in the pyrolysis of rice husks to synthesize $SiC_w$. The carbon from PAN is an active form of carbon and is produced in situ, and helps in the carbothermal reduction of silica. In addition, boric acid as catalyst enhances the migration of silica particles, resulting in an efficient contact between silica and carbon. By increasing the temperature, boric acid melts with decomposition to give $B_2O_3$·$B_2O_3$ can be mixed with silica due to the formation of a liquid phase, and this helps in bringing silica and carbon in close contact and result in the formation of $SiC_w$ at 1450 °C. Krishnarao and Godkhindi [170] found that addition of $Si_3N_4$ to black milled ash causes in an increment in the formation of SiC whiskers and a reduction in the temperature of conversion to 1200 °C. Silicon nitride is converted to SiC rapidly at and above 1300 °C.

### 5.4.3. Effect of atmosphere on SiC formation

The chamber atmosphere and the gas flow rate play significant roles in determining the structure of the final product and the amount of CO and SiO produced, respectively. Furthermore, the increment in gasification rate causes an increase in the surface area of carbon, and thus leads to a high total porosity and adsorption capacity of carbon. Therefore, the gasification rate should be controlled. As mentioned before, the produced carbon monoxide during pyrolysis and SiO control the structure of SiC into whiskers. If the CO gas produced is derived away from the reaction zone rapidly under high gas flow rate, the SiO gas will also be carried away, thus preventing the growth of whiskers. On the other hand, if the gas flow rate is too slow, most of the CO gas will be concentrated at the reaction zone and thus inhibiting the reaction to form SiC. In addition, fast moving gases can also destabilize the liquid droplet at the whisker tip and hinder whisker growth [180,215]. The effect of the atmosphere used during pyrolysis, i.e. argon, vacuum was investigated by Zawrah et al. [216]. As it is clear from Fig. 21, the pyrolyzed samples in vacuum exhibited higher SiC peaks intensity than those pyrolyzed in argon atmosphere. During pyrolyzing in argon atmosphere, the furnace chamber pressure increases because of the development of CO produced from the reactions between silica and carbon. Increasing the pressure around the silica and carbon, according to reaction (10) in presence of higher temperature leads to increasing the crystallinity and the stability of both reactants and consequently leads to decreasing the formation of SiC. In other words, increasing the pressure results in augmenting the free energy and the stability of the material according to reaction (10) and the following thermodynamics equations:

$$\Delta G = \Delta G^0 + \Delta nRT\ln(p/p^0) \tag{20}$$

where $\Delta G^0 = G_{SiO} + G_{CO} - G_{SiO_2}$ ($\Delta n = 2$, $R$ = gas constant, $T$ = temperature, $P$ = final pressure, $p°$ = initial pressure) [217,218].

In contrast, it was found that the pyrolysis in vacuum guarantees the lower pressure around the reactants and consequently increases the formation of SiC at temperature around 1550 °C due to increment of intimate contact between $SiO_2$ and C. Moreover Radhakrishna and Sanghi [179] reported that vacuum prevents whisker growth since it removes the vapors containing the whisker growth species. Sarangi et al. [219] showed in high-vacuum at ~1400 °C, high crystalline β-SiC particles of very fine size formed along with some amount of unreacted silica in less than 5 min.

Fig. 22 shows the relationship between the stable condensed phases, log $P_{N2}$, log $P_{CO}$ and the temperature for the Si–C–N–O system. The atmosphere was considered to be composed of $N_2$ and CO, which was formed by the reaction between $O_2$ in the $N_2$ gas cylinder and carbon black. It indicates that at the heating temperature (1400 °C) and high $N_2$ pressure the α-$Si_3N_4$ phase is stable [220]. As it can be seen, by controlling $N_2$ pressure and temperature, it is possible to reach SiC. However, Ekelund and Forsluhbnd [221] reported that an increase in $N_2$ pressure does not have any effect

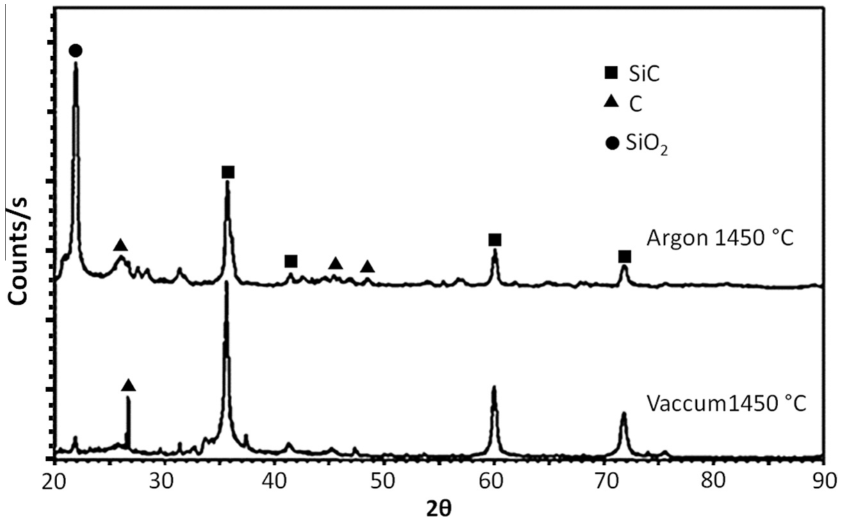

**Fig. 21.** XRD patterns of SiC prepared from coarse rice husk ash (as is) pyrolyzed at temperature of 1450 °C in argon and vacuum atmosphere [216].

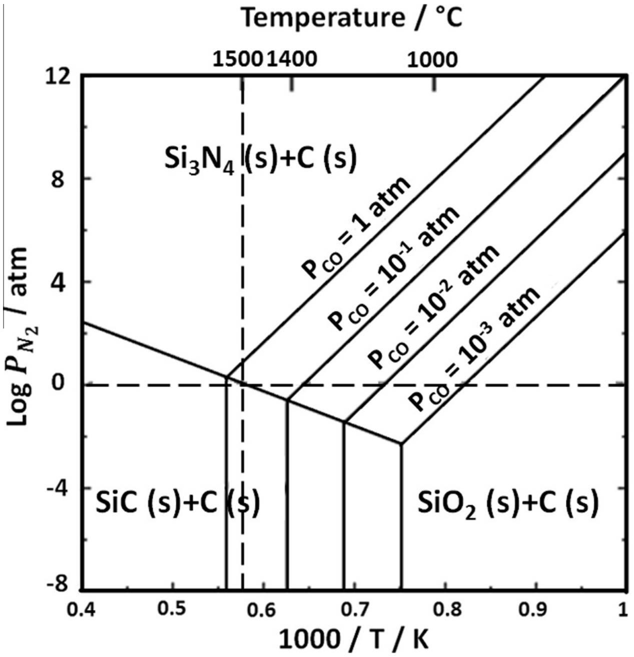

**Fig. 22.** Relationship between the stable condensed phases, log $P_{N2}$, log $P_{CO}$, and temperature in the Si–C–N–O system [221].

on carbothermic nitridation processes in contrast to thermodynamic prediction, as shown in Fig. 22 [221].

It has been reported that the pyrolysis of rice husk in nitrogen atmosphere at 1550 °C led to the formation of SiC–$Si_3N_4$ nanocomposite. The reported amount of formed SiC was higher than the amount of $Si_3N_4$ [102]. Nitridation of rice husk can be represented by the following reactions:

$$SiO_2\ (s) + C\ (s) = SiO\ (g) + CO\ (g) \tag{21}$$

$$SiO_2\ (s) + CO\ (g) = SiO\ (g) + CO_2\ (g) \tag{22}$$

The subsequent reaction is:

$$SiO\ (g) + 2/3N_2\ (g) = 1/3Si_3N_4\ (s) + 1/2O_2\ (g) \tag{23}$$

$$1/2O_2\ (g) + C\ (s) = CO\ (g) \tag{24}$$

$$SiO\ (g) + C\ (s) + 2/3N_2\ (g) = 1/3Si_3N_4\ (s) + CO\ (g) \tag{25}$$

In another investigation, Krishnarao and co-workers [191] pyrolyzed rice husks without pre-coking in a graphite resistance heating furnace at 1100–1400 °C in nitrogen atmosphere. They reported the formation of good quality (needle-type) SiC whiskers without the detection of $Si_3N_4$. While, small quantities of $Si_2N_2O$ were formed at 1100–1200 °C. The formation of silicon oxynitride can be eliminated as long as carbon is present in excess or at least in the stoichiometric ratio. The results also illustrated that by increasing the reaction chamber pressure, the crystallinity of silica and carbon in RHs increases, while formation of SiC whiskers decreases. Hydrogen can also be used, but offers no real advantage even though it might help to increase the SiO concentration by the reaction [179]:

$$SiO_2\ (s) + H_2\ (g) = SiO\ (g) + H_2O\ (g) \tag{26}$$

### 5.4.4. Effect of chemical pre-treatment of rice husk

It was reported that treating of rice husk with acid and pyrolyzing it in argon atmosphere increases the SiC contents [222]. The degree of crystallization decreases due to eliminating the impurities in the RH, resulting in higher purity of RHs with a porous structure. Because of porous structure of acid treated rice husk, the intimacy between silica and carbon eliminates. As a result of low degree of crystallization, carbon in treated rice husk can form and absorb a larger quantity of CO and SiO and the produced CO reacts with $SiO_2$ to form SiO. Thus, the SiC content in the pyrolyzed treated rice husk was higher than that in pyrolyzed untreated rice husks. The formation of SiC whiskers in acid treated rice husk is lower than in un-treated one. Patel and Prasanna [223] reported the formation of $Si_2N_2O$ from acid-treated RHs at 1300–1500 °C. Krishnarao [224] reported that by treating the pulverized burned RHs with aqueous solution of $CoC1_2$, the degree of crystallization of silica and carbon decreases. They claimed that $CoCl_2$ diffuses into the graphite and burned rice husk and opens up the layers of graphite by channeling. It has been reported that the SiC whisker formed in $CoCl_2$ treated burned rice husks is negligible. Alkali pretreatment has also been reported [16]. Patel et al. [16] also showed that the concentrated (>9 N) NaOH solution cannot penetrate through the holes of rice husk and the extraction of silica decreases. Mizuki et al. [80] proposed using an enzymatic method for formation of SiC. The ground treated powders of rice husk with NaOH were hydrolyzed with a mixture of Acucelase and Meicelasein acetate buffer (pH 4–5, 20 ml). After treatment with enzymes the precipitate was dried and pyrolyzed in a two-step process (at 500 °C for 1 h in $N_2$ atmosphere and 1600 °C for 1 h in Ar atmosphere). The cellulase treatment was developed to control excess carbon for silicon carbide formation from rice husks. Komatsu et al. [225] demonstrated that sieving is an easily controlled method; however, the yield of carbon-controlled rice husks (45.5%) was lower than that for the enzymatic method (54.0%).

### 5.4.5. Effect of crystallinty of $SiO_2$ and C

It has been found that under the same experimental conditions, formation of SiC from rice husk precursors depends on the characteristics of the rice husk raw material. The lowest yield and quality is obtained from pulverized black ash (ground black ash) because although the C/Si ratio of black ash is adequate for the reaction, the high aromaticity, less open structure, non-availability of void spaces and low CO formation, slow down the rate of the reaction. While mixtures of white ash and carbon black allow producing intermediate amounts and quality of SiC. The highest ones are typically obtained using raw rice husk [202,207], where sufficient carbonaceous substrate and large enough CO formed from degradation of cellulose in rice husks and sufficient void space in the husk bed were available. Liou [144] showed level of micropores in coked rice husk is higher than crystallite rice husk ash. Moreover, it was reported that the intensity of the SiC peak in the mixture of crystalline white ash with carbon (CWA + C) is higher than that of mixture of white ash and graphitized carbon (WA + GC). This outcome can be attributed to the production of a large quantity of CO by amorphous carbon. By increasing the heating rate, the carbon in (WA + GC) could absorb less quantity of SiO due to increasing the closed porosity. Thus, the intensity of the SiC peak in slowly heated (WA + GC) was higher than that in the rapidly heated sample [202].

### 5.4.6. Effect of milling of starting materials

It is believed that high-energy milling before carbothermic reduction has not altered the reaction mechanism of SiC formation and the involvement of gaseous phases, SiO and CO, in the formation of SiC but greatly enhanced the formation of materials [226–228]. High energy milling leads to the following changes to the $SiO_2$: (i) formation of amorphous phase in the reactants; (ii) low degrees of long-range order in the remaining crystalline reactants; (iii) large grain-boundary areas associated with ultrafine crystallites; (iv) high internal strains in the remaining crystalline reactants; (v) large specific surface areas; (vi) fine particle sizes; and (vii) intimate mixing of reactants at microstructural levels changes. (i) to (vii) can enhance SiC formation by increasing reaction kinetics via increased diffusivities, increased reaction areas, and decreased diffusion distance, whereas changes (i) to (vi) can also enhance SiC formation by increasing the free energy of the reactants [227]. Lakiza et al. [194] showed at temperature of about 1500 °C silica begins to evaporate from free surfaces of $SiO_2$ grains. With increasing specific surface of $SiO_2$ particles, the intensity of this process grows. $SiO_2$ and SiO vapors become adsorbed on the surface of carbon and are reduced by it to Si. The free silicon reacts, either directly or by a vapor–liquid–solid (VLS) mechanism with carbon, as a result SiC is formed. The effect of milling process on particle size of the prepared SiC was also investigated by Zawrah et al. [216]. They evaluated the effects of three rice-husk ash samples: coarse-grained rice husk ash, fine rice husk ash (hand-ground) and ball milled one. It was found that the particle sizes of the obtained SiC from ball milled materials were smaller than those prepared without milling at 1550 °C under vacuum. In addition they claimed that mechanical activation of the reactants (rice husk ashes) at room temperature by high-energy ball milling increases the reactivity of the reactants and dramatically reduces the temperature and time for the synthesis reaction of SiC.

## 6. Preparation of nano SiC

In the last decade, efforts have been made by various researchers to synthesize fine and pure SiC powder by alternative methods like sol–gel, plasma, laser, chemical vapor deposition (CVD), self-propagating high-temperature synthesis [229–233]. Nano-sized SiC rods have also been prepared using Si and C as the reactants at the temperature of 1200 °C. The availability of nano silicon carbide commercially could possibly promote more wide spread application of silicon carbide in industry by lower sintering pressure and/or temperature. However, the high cost of the powder may hinder the progress. Recently synthesis of nano SiC from rice husk was proposed in order to overcome the high production price of nano SiC through the conventional routes [234,235].

### *6.1. Utilization of agricultural waste materials as source for carbon*

Recently, formation and growth of SiC nano-wires from mixture of oil palm and rice husk ash as a carbon and silica sources, respectively was investigated by Chiew and Cheong [236]. Oil palm fibers have been reported with high carbon content and low ash content. It has been shown that the ratio of RHA to oil palm affects the growth mechanism. The growth mechanism of nano wire changes with increasing of RHA from 20% to 80%. It was shown that the optimum amount of RHA to grow SiC nanowires with the minimum amount of impurities, with sizes between 30 and 40 nm, and with the maximum yield, is of 40% RHA mixed with oil palm. Besides, Kantee et al. [237] have synthesized nanostructured from high silica rice husk ash in combination with Cu or $SnO_2$ powder and coconut shell charcoal. The mixtures powder and Si substrates were heated up to 1250 °C in argon atmosphere. The result confirmed the presence of SiC and $SiO_2$ nanostructures.

### *6.2. Arc plasma reactor*

Thermal plasma offers an attractive route for synthesis of fine and ultrafine powders among others methods. Ultrafine SiC has been prepared by thermal plasma processes, according to several reports [238–240]. Some of the advantages of thermal plasma are the reduction of the reaction time significantly, high operating temperature, steep temperature gradients, and high quench rates. Almost all the processes devoted to the formation of SiC from rice husk through different routes so far, involve two process steps: (i) pyrolyzing at low temperature (400–800 °C) in a controlled manner to remove volatiles, and (ii) reacting the pyrolyzed rice husk at high temperature (>1300 °C) to form SiC. In a novel approach, SiC forms from rice husk in a single step [217]. Plasma processes are not only suited for operation in a continuous manner but can be competitive with the current Acheson-produced material (commercial route that is used for producing SiC) [240]. The plasma-synthesized powder was very fine and dark green in color. Singh et al. [189] used a DC extended arc plasma reactor in order to produce β-SiC particles from a mixture of boiler-burned rice husk and graphite powder. A SiC yield as high as 72% was achieved at a 3.03:1 carbon-to-silica ratio. In another investigation, they synthesized ultrafine SiC powders through thermal plasma technique using argon as both plasma-generating gas and carrier gas. After pretreatment of rice husk at 550 °C under nitrogen atmosphere the sample was treated at very high temperature, steep temperature gradients ($10^6\,°C\,m^{-1}$) and high quench rates ($10^6\,°C\,s^{-1}$). The plasma-produced powder was then treated in air at 700 °C in a tube furnace using natural convection to remove the excess carbon. The removal of excess silica was carried out by treatment with concentrated HF. The resulted sample shows β-SiC structure.

### *6.3. Microwave heating*

Recently, the microwave heating method was developed to synthesize SiC from rice husk [241–244]. In conventional heating, heat is transferred between objects by the mechanisms of conduction, radiation and convection and both the amorphous $SiO_2$ and carbon are slowly heated to high temperature. Thus, in the final product both SiC and unreacted $SiO_2$ can be detected. In microwave heating method, it is known that the exothermic phenomenon of materials in a microwave field is derived from the effects of Joule loss, dielectric loss and magnetic hysteresis loss. In the case of the carbon and $SiO_2$ powder mixture, the Joule loss becomes important, whereas the dielectric loss and magnetic hysteresis loss can be ignored [220]. The carbon is firstly heated to high temperature in a short time and the carbothermal reduction of $SiO_2$ is rapidly achieved. Thus, the crystallization of $SiO_2$ can be ignored. Fig. 23 shows the mechanism for the formation of SiC by the carbothermal reduction reaction from $SiO_2$ and carbon black using microwave heating.

Firstly, when microwaves act upon the material, carbon black is heated due to the Joule loss effect. During this time, hot spots at which exothermic reactions occur begin to appear in some areas of the sample. The temperature around the hot spots increases to over 1500 °C, which results in the generation of SiO (g) from $SiO_2$ and subsequently, the generated SiO (g) moves to carbon black particles at high temperatures over 1500 °C where SiC is formed.

Li et al. [245] showed the carbonized rice husk (CRH) at 700 °C for 30 min in an argon atmosphere. The as-received CRH was milled for 1 h at room temperature. Rapid carbothermal reduction reactions were achieved in a 2.45 GHz microwave field in an argon atmosphere. The complete carbothermal reduction of silica was achieved at 1300 °C for 60 min or at 1500 °C for only 15 min by microwave heating, resulting in β-SiC formation. The β-SiC whiskers show diameters of 110–170 nm with a length of several to tens of micrometer. Qadri et al. [243] produced nanoparticles of β(3C)-SiC from the agricultural waste of rice husks by microwave processing in controlled conditions of temperature (1900 °C) and vacuum. Transmission electron microscopy revealed the presence of stacking faults along the [111] direction. The presence of 6H/4H stacking faults in 3C phase is explained in terms of their total energies. Fig. 24(a) shows the high density of stacking faults oriented along the (1 1 1) plane. The corresponding selected area electron diffraction pattern from one such particle close to the [0 1 1]

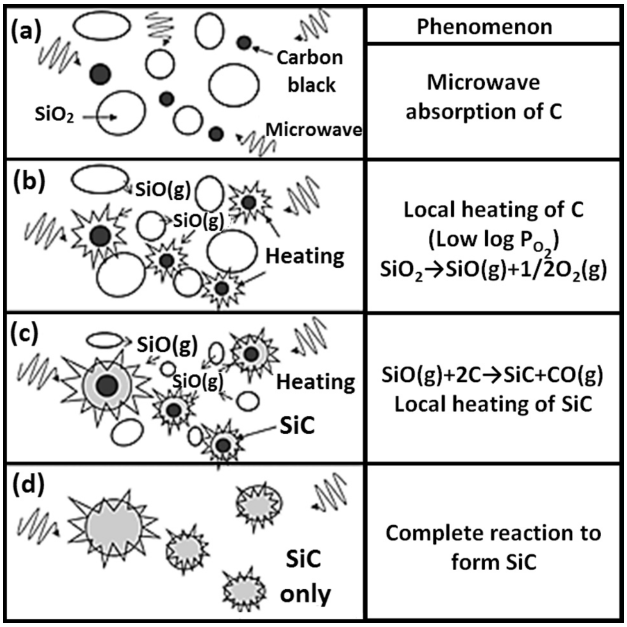

**Fig. 23.** Schematic diagram showing the mechanism for the formation of SiC by carbothermal reduction reaction from $SiO_2$ and carbon black using microwave heating [220].

zone axis is shown in Fig. 24(b). The diffraction spots, the *d*-spacing, and the angle between planes conforms β-SiC crystal. The *d*-spacing of (111) planes was observed to be around 2.52 Å. The streaks along the [111] direction in the diffraction pattern are due to thin stacking faults. In some particles, one could observe (111) twins, Fig. 24(c), as well as stacking faults.

## 7. Silicon nitride

Because of the importance of silicon nitride ($Si_3N_4$) in engineering materials, their properties and potential applications at high temperature, in microelectronics and optoelectronics, in recent years there has been a growing interest in this material from different perspectives. Silicon nitride ($Si_3N_4$) is one of the most promising structural materials for high temperature and high mechanical stress applications because of its excellent properties such as high strength retention at elevated temperature, low thermal expansion coefficient, good thermal shock resistance, and high corrosion resistance. It has a much higher creep resistance than metals and its thermal shock resistance is much better than other ceramics [246,247]. There are basically four different synthetic routes for this powder, which differ in purity, morphology and sintering activity: (i) a direct reaction of elemental silicon with nitrogen that gives relatively coarse products and have to be milled prior to further processing [248]; (ii) carbothermal reduction utilizes a fine mixture of carbon and $SiO_2$ powders in a flowing of $N_2$ at 1500 °C [249]; (iii) the so-called diimide-process is a liquid or gas-phase route to $Si_3N_4$ powders [250]; (iv) CVD techniques using volatile silicon compounds such as $SiCl_4$, $SiH_4$ or related molecular compounds yield $Si_3N_4$ powders upon gas phase reaction with ammonia [251]. Because of the high purity of fine silica and carbon and their commercial availability, the carbothermal reduction of silica is the main method for manufacturing silicon nitride powder. However, this method has a high requirement on raw materials; high reactivity and a good distribution of the silica and carbon are important for the reaction. The better the distribution, the more helpful for nitridation. Therefore, RH, which naturally contains both silica and carbon, is a potential material for producing silicon nitride [2,81].

### 7.1. $Si_3N_4$ formation through carbothermal reduction and nitridation of rice husk

Reaction for carbothermal reduction and nitridation of rice husk were suggested by several investigators [252,253]. The factors which have influence on the overall reaction are characteristics of starting materials, temperature, gas flow rate and catalysts [254,255]. The homogeneity mixture of carbon and silica, which occurs naturally in rice husk determine the level of completion of reaction. In all cases, excess carbon is required to complete the reaction in a reasonable time and temperature. The role of carbon in the formation of $Si_3N_4$ is to act as a reducing agent to promote the nitridation reaction, and also to provide a source of active sites at which the $Si_3N_4$ can nucleate. Lee and Cutler [256] have attempted to emphasize the important role played by the molar C:$SiO_2$ ratio in the formation of silicon nitride. As long as carbon is present in excess or at least in the stoichiometric ratio of the overall carbothermal reductions, the formation of silicon oxynit-

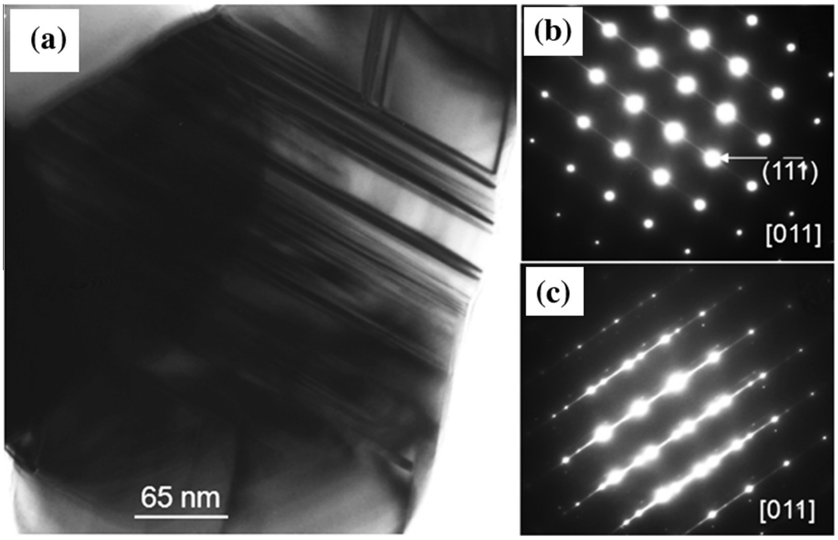

**Fig. 24.** (a) Particle showing stacking faults, (b) the corresponding diffraction pattern in the [011] zone, and (c) diffraction pattern from another particle showing twined spots close to zone [243].

ride can be eliminated [257] by effectively removing the oxygen from the system through reaction,

$$1/2O_2\ (g) + C\ (s) = CO\ (g) \tag{27}$$

In order to increase the rate of reaction, the partial pressure of produced CO during the reaction must be reduced by introducing a higher flow rate of nitrogen. Hence, a higher flow rate of nitrogen would be favorable in maintaining a low CO concentration and will also provide a more efficient reaction of silicon dioxide with nitrogen to silicon nitride.

The general idea about the carbothermal reduction and nitridation of rice husk is that SiO gas plays an important role in $Si_3N_4$ formation. SiO (g) is generated by the reaction between $SiO_2$ and C (reaction 28) [102].

$$SiO_2\ (s) + C\ (s) = SiO\ (g) + CO\ (g) \tag{28}$$

The subsequent reaction is:

$$SiO\ (g) + 2/3N_2\ (g) = 1/3Si_3N_4\ (s) + 1/2O_2\ (g) \tag{29}$$

One of the problems that is associated with this method is that the nitrogen and the powder are not in contact with each other, indeed the produced SiO cannot take out of the heated sample and reacts with nitrogen. Some alternatives proposed to use carrier gas are to diffuse into the voids of the heated powder to take out the silicon-containing vapor to react with nitrogen. Passing the mixture of nitrogen and chlorine or hydrogen through the silicon-containing material causes removal of vapor from the heated material, but delays or inhibits the reaction between the silicon component and nitrogen so that the silicon nitride does not cover the reactive material. In these two methods, the purity of $Si_3N_4$ is low; the whiskers grow on ceiling, and side walls of furnace. Tanaka and Kawabe [258] prepared the carbon–silica with thin configuration and sufficient porosities and used the moving tray for producing $Si_3N_4$. By passing the tray through a series of temperatures from 400 to 1300 °C in the presence of $N_2$, the gas passes into the porosities and provides spaces for growing whiskers.

Liou et al. [259] showed that the conversion of silicon dioxide increased with increasing gas flow rate up to 200 mL/min. A further increase of gas flow rate has no effect on the conversion. They also proposed using pellet-forming pressure for increasing the rate of nitradation due to shortening the distance between carbon and silicon dioxide and consequently increasing the contact area of the two components [259]. This method is not practical for samples without excess carbon because the naturally distance between carbon and silicon dioxide is in its minimum level.

Rahman and co-workers [146] nitrided the pyrolyzed rice husk at temperatures between 1260 and 1450 °C under 95% nitrogen-5% hydrogen and obtained $\alpha$-silicon nitride powder of high purity. It was found that hydrogen addition is beneficial in accelerating the rate of nitride formation. The addition of pre-formed silicon nitride powder to pyrolyzed rice husk powder before nitridation is noticeably beneficial in yielding a product consisting of uniform sub-micrometer (<0.5 μm), equiaxed, $\alpha$-$Si_3N_4$ crystals. In addition, they reported that milling of pyrolyzed rice husk has a great effect on the crystal size of silicon nitride due to increment in nucleation sites densities for the growth of $\alpha$-$Si_3N_4$. It has also been shown that, in addition to obtaining a high powder surface area and homogeneous particle distribution, the carbon and silica content of the husk can be controlled through a proper digestion with hot $HNO_3$ [260].

The phase transition from $\alpha$ to $\beta$ occurs via the diffusion of the vapor phase or liquid at a temperature greater than 1400 °C [261].

### *7.1.1. Effect of catalysts on $Si_3N_4$ formation*

Hashishin et al. [262] evaluated the effect of cryolite in $SiO_2$–$N_2$–$Na_3AlF_6$ system under the presence of graphite. Whiskers were synthesized when $SiO_2/Na_3AlF_6$ molar ratio ranged from 2 to 8. The maximum amount of whiskers was synthesized when the $SiO_2/Na_3AlF_6$ molar ratio was 3. In another report, the same authors [261] studied the effect of impurities on $Si_3N_4$ whiskers via a carbothermal reduction from $SiO_2$–$N_2$–$Na_3AlF_6$ system. In this process cryolite is added as flux in the molar ratio of $SiO_2/Na_3AlF_6 = 3$. The aim of their study was to investigate the effects of adding impurities which are containing $Fe_2O_3$, $Al_2O_3$, $TiO_2$, MgO, and CaO on the growth of the $Si_3N_4$ whiskers. As it can be seen in Fig. 25, $Fe_2O_3$, $Al_2O_3$, and $TiO_2$ accelerate the growth of the whiskers by the vapor–liquid–solid (VLS) mechanism, CaO and MgO by the vapor–solid (VS) and VLS mechanisms. It is clear that the shapes of the $Si_3N_4$ whiskers that were synthesized by CaO and MgO consist of columnar-like and square pole-like. The droplets were found on the top of the columnar whiskers but no droplets were observed on the top of the square pole. It has also been shown that the addition of CaO and MgO leads to a decrease in the length and an increase in the diameter of $Si_3N_4$. The effects of these impurities corresponded to the solubility of the metal in silicon. The components of the droplets were mainly the alloys of Fe–Si and Al–Si systems, and those of Ti–Si system rarely existed that it can be attributed to the solubility of Si into metal. Darken and Gurry [263] indicated that the solubility significantly depended on the atomic diameter and electronegativity. The electronegativities of Si, Fe, Al, and Ti were 1.17, 1.24, 1.43, and 1.47, respectively. There-

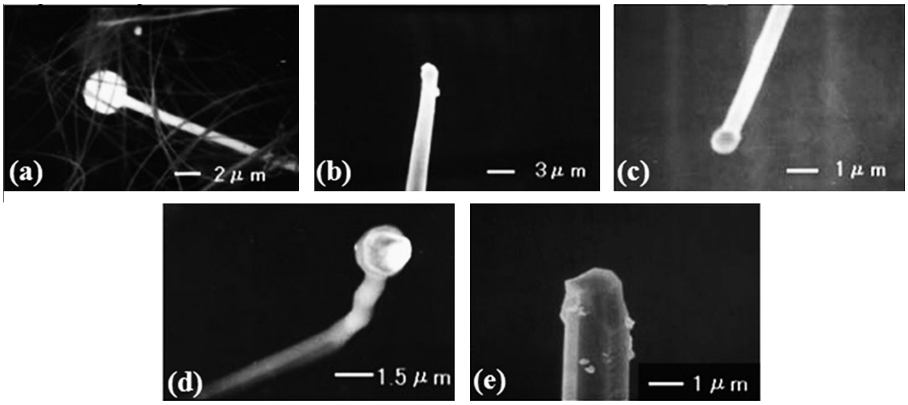

**Fig. 25.** The morphologies and the compositions of the droplets grown on the top of the $Si_3N_4$ whiskers synthesized from the mixture of the cryolite-containing silica and impurities by the carbothermal reduction and nitridation process. (a) $Fe_2O_3$ (Fe/Si = 1–2), (b) $Al_2O_3$ (Al/Si = 0.09), (c) $TiO_2$ (Ti/Si = 0.81), (d) CaO (Ca/Si = 0.04), and (e) MgO [261].

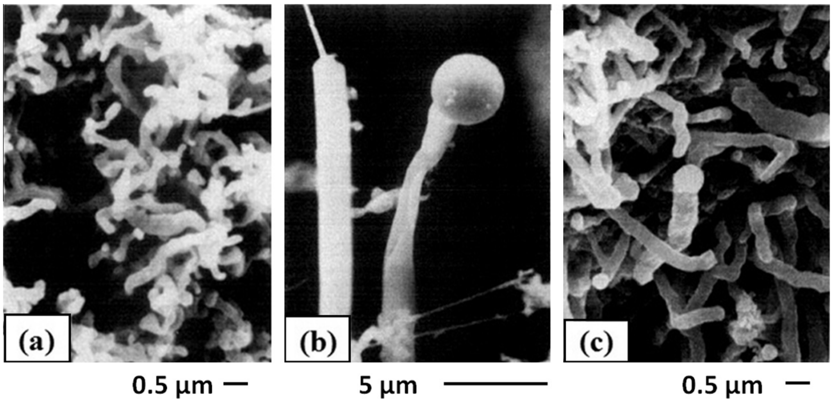

**Fig. 26.** SEM of powder obtained from nitridation of (a) PRH-$V_2O_5$ at 1400 °C, (b) PRH-2$Fe_2O_3$ and (c) PRH 2NiO at 1500 °C in 95% nitrogen 5% hydrogen [174].

fore, the solubility of silicon in Fe is higher than that in Al and Ti. These results indicated that the diameter of the whiskers is controllable. The effect of $Fe_2O_3$ addition in $SiO_2$–$N_2$–$Na_3AlF_6$ system on the growth mechanism and composition of the droplets has been studied by Hashishin et al. [262]. They showed that Al plays an important role in the synthesis of $Si_3N_4$ whiskers. It has been seen droplets of Al–Si obtained when $Fe_2O_3$: $SiO_2$ ranged from 3.0–4.0:100 and 5.0–6.25: 100. No droplets obtained for other values. The greatest Al/Si ratio obtained when $Fe_2O_3$:$SiO_2$ was 3.5:100 and 5.63:100. Interestingly, Fe was not contained in the droplets, although $Fe_2O_3$ added to the starting material. At high temperatures such as 1400 °C, both Al–Si and Fe–Si droplets can exist.

The maximum formation of whiskers has been observed from the sample of 6% Fe concentration treated at 1400 °C by Sarangi [264]. It has been shown that at 1450 °C, the amount of whiskers is gradually changed to globules.

Rahman and Riley [174] produced $Si_3N_4$ from rice husk powder at temperatures in the range of 1260–1450 °C under a flow of 95% nitrogen-5% hydrogen by utilization of different catalysts such as $Y_2O_3$, $ZrO_2$, $TiO_2$, $CeO_2$, $Fe_2O_3$, NiO and $V_2O_5$. It was found that $Y_2O_3$ and $ZrO_2$ were not significantly reduced by carbon or hydrogen under nitridation conditions and did not have any effects on the amount of fabricated silicon nitride. Both $TiO_2$ and $CeO_2$ appeared to accelerate silicon nitride formation, and led to higher overall yields. $TiO_2$ was easily reduced but $CeO_2$ was also readily reduced to $Ce_2O_3$ with a range of intermediate non-stoichiometric oxides $CeO_{2-x}$. Results by XRD also showed the presence of CeN in the silicon nitride for the higher nitrogen flow rate. $Fe_2O_3$ and NiO are easily reduced under low oxygen partial pressure to the metals, which in turn yield the liquid silicides at the nitridation temperature. Globules at whisker tips, which are shown in Fig. 26, indicative of a vapor–liquid–solid (VLS) mechanism of growth, although a significant amount of SiC was also formed.

It was reported that the amount of β-$Si_3N_4$ increased significantly with $V_2O_5$ content. It has to be mentioned that VC and VN were detected as by-products and VC was found to be the predominant phase due to its greater thermodynamic stability as compared to VN under reaction conditions [257].

$$V_2O_5\ (l) + 7C\ (s) = 2VC\ (s) + 5CO\ (g) \tag{30}$$

$$V_2O_5\ (l) + 5C\ (s) + N_2\ (g) = 2VN\ (s) + 5CO\ (g) \tag{31}$$

It was reported that growth of SiC in presence of $V_2O_5$ is not as favored as in Fe–Si liquid (iron catalyst). It shows that $V_2O_5$ liquid is not able to take into solution a significant amount of carbon or carbon monoxide and silicon monoxide through solid–liquid–vapor mechanism. However, it was observed that $Si_2ON_7$ could be obtained by utilization digested rice husk in presence of $V_2O_5$ without any excess carbon. Due to consumption of carbon by VC and VN, carbon to silica molar ratio is reduced below the stoichiometric ratio. This condition most likely caused the oxygen partial pressure to increase and increase the formation of $Si_2N_2O$ [257].

By using $Si_3N_4$ and rice husk ash with different metal oxides $Y_2O_3$, MgO and $A1_2O_3$, $Si_2N_2O$ can be produced by VLS mechanism. The conversion rate to $Si_2N_2O$ is much higher for $Y_2O_3$ and MgO additions than for $A1_2O_3$ additions and maximum amount of $Si_2N_2O$ (about 80%) with $Y_2O_3$ and MgO obtained at a temperature of about 1600 °C. The decrease in the amount of $Si_2N_2O$ corresponds well with the increase in β-$Si_3N_4$. At the higher temperatures, $Si_2N_2O$ presumably has decomposed to SiO, $N_2$, and $Si_3N_4$ [265].

### *7.2. $Si_3N_4$ formation through chemical vapor deposition*

A new method that has been used in order to prepare $Si_3N_4$, is based on chemical vapor deposition. In this method, silicon halides in atmosphere of $N_2$ can produce silicon nitride powder of very high purity and high specific surface area in a simple and economic way. This type of powder is likely to be relatively expensive. Hybrid precursor system-chemical vapor deposition (HYSYCVD) is a method recently developed at CINVESTAV[1]-Saltillo, for the production of advanced ceramics (for example, alpha and beta $Si_3N_4$) in which solid–gas reaction systems or hybrid systems are used. This method is based on the ability of some solids like sodium hexafluorosilicate ($Na_2SiF_6$) to produce highly reactive gas species ($SiF_3$, $SiF_2$, SiF and Si) which, by the reaction with other proper precursors (for instance, nitrogen precursors), allow the formation of condensed phases like $Si_3N_4$ and $Si_2N_2O$ as stable solids [266]. Sodium hexafluorosilicate ($Na_2SiF_6$, as silicon halides source, was prepared in CINVESTAV-Saltillo laboratory by means of the dissolution of $SiO_2$ (obtained from rice husks) in hydrofluoric acid (HF) and the subsequent precipitation with a solution of sodium hydroxide (NaOH). Synthesis tests were carried out in a HYSYCVD reactor at constant pressure and in the atmosphere of nitrogen precursors ($N_2$, 50% $N_2$-balance $NH_3$ and, 5% $N_2$-balance $NH_3$) [267].

## 8. High purity silicon

The conventional process of manufacturing silicon of reasonable purity involves a very high cost of production [268]. Therefore worldwide efforts are being directed to develop a low-cost, high-volume and commercially feasible process for production of high purity silicon to be used in solar cells for photovoltaic power generation [269–271]. One such process involves reduction of rice

---

[1] **CINVESTAV** is the Spanish acronym of Center for Research and Advanced Studies.

**Table 7**
Silica-metal reaction thermodynamic data [274].

| Reaction | Temp. (°C) | ΔH (kJ/mol) | ΔG° (kJ/mol) | Adiabatic Temp. (°C) |
|---|---|---|---|---|
| $SiO_2 + 2Ca = Si + 2CaO$ | 650 °C | −363 | −333 | 2348 |
| $SiO_2 + 2\,Mg = Si + 2MgO$ | 650 °C | −312 | −261 | 1906 |
| $SiO_2 + 4/3Al = Si + 2/3Al_2O_3$ | 650 °C | −210 | −180 | 1477 |
| $SiO_2 + Ti = Si + TiO_2$ | 650 °C | −34 | −33 | 407 |

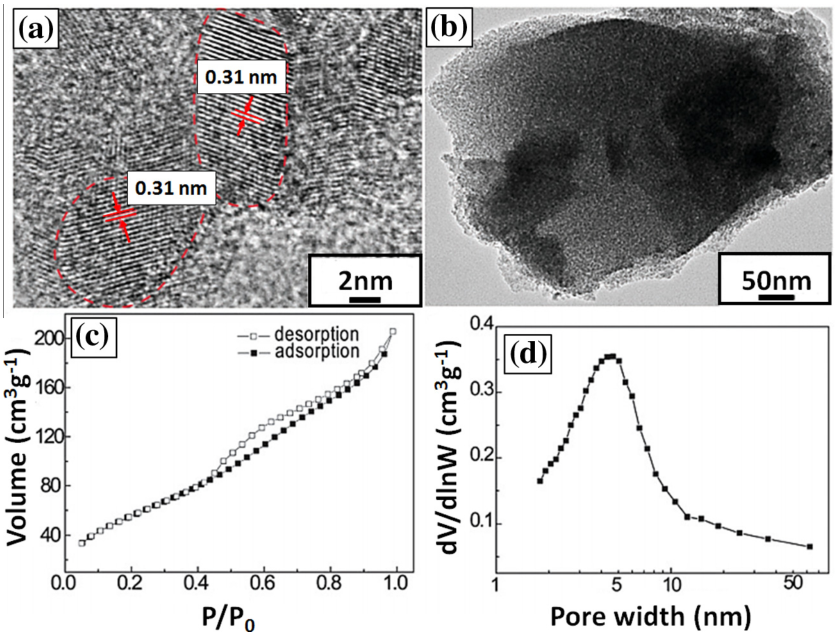

**Fig. 27.** (a and b) High and low magnification bright field TEM images, respectively, of porous Si prepared via reaction with Mg for 3 h at 300 °C and then 12 h at 500 °C, followed by acid dissolution of Mg-bearing product phases. (c) Isothermal nitrogen adsorption and desorption curves of the silicon product at −196 °C, and (d) Pore size distribution (from BJH analysis) of the porous silicon product [275].

husk ash to produce silicon. Several approaches have been developed to produce silicon from RHs. Among the various methods, reduction of amorphous silica by metallic metals has been discussed extensively. The metallic elements Mg, Ca, Al and Ti can reduce $SiO_2$ at comparatively lower temperature and forms mixtures of condensed phase products. The relevant overall reactions and their corresponding free energy change and adiabatic temperature rise per mole of silicon are shown in Table 7.

Mishra et al. [271] investigated production and purification of silicon through calcium reduction of rice-husk white ash. They mixed rice-husk ash obtained at 500 °C and commercial grade calcium thoroughly in stoichiometric proportions. Then the mixture was reduced at 720 °C. The reduced product leached with concentrated $HNO_3$ and HF to achieve high purity of 99.9% silicon. Obtaining silicon of (99.9999%) purity by reducing white rice husk ash with magnesium at temperature of 800 °C followed by several successive acid (mixtures of HF, $H_2SO_4$ and HCl) leaching treatments were reported in several works [272,273]. With acid treatment, it is possible to remove MgO, $Mg_2Si$ and unreacted Mg as by products. Larbi [274] reported that by utilization of pellet of RHA with magnesium content 5 wt.% in excess of stoichiometry requirement and heating in the temperature range of 900 °C under flowing argon, it is possible to achieve a maximum silicon yield. The presence of fine silicon nanocrystals from magnesiothermic reaction was confirmed using high resolution transmission electron microscopy (see Fig. 27a and b). The surface area and pore size distribution of the Si product were evaluated via nitrogen adsorption–desorption analyses. The isothermal adsorption–desorption curve of the silicon product (Fig. 27c) was of type IV with a H1 type hysteresis loop, indicated that the Si product was largely mesoporous. BET analyses yielded values of 218.4 $m^2\,g^{-1}$ for the specific surface area [275].

In the invention of Sung et al. [276] a method for producing high purity porous silica and silicon, which are derived from rice husk, was presented. In this method, silica was extracted from cooking liquor separated in a cooking treatment of rice husk alkali, then silicon was synthesized by performing a reduction reaction. In this method, improved metallurgical grade silicon that does not contain boron or phosphorus may be produced through an acid treatment that greatly reduces the presence of impurities. In addition, the silicon produced by using this method may be used in the manufacture of low cost solar cells. Carbon can also be utilized for reduction of silica to silicon. The required ratio of C to $SiO_2$ for the production of solar grade silicon is 2:1. However, purifying RHs allows obtaining a $C/SiO_2$ ratio of about 4:1 [16,277]. Hunt et al. [278] leached RHs in hot HCl and then coked them in inert gas to further remove impurities. The coked RHs were extruded with sucrose as a binder to produce 5-mm diameter pellets with an average bulk density of about 800 g/L. The pellets were pyrolyzed in an arc furnace to produce pure silicon.

## 9. Magnesium silicide ($Mg_2Si$)

The intermetallic compound $Mg_2Si$ exhibits a high melting temperature (1085 °C), low density ($1.99 \times 10^3$ $kg/m^3$), high hardness (4500 MN $m^{-2}$), a low coefficient of thermal expansion ($7.5 \times 10^{-6}$ $K^{-1}$) and a reasonably high elastic modulus (120 GPa)

[279,280]. Due to abundance of environment friendly Mg and Si components in the Earth's crust, magnesium silicide ($Mg_2Si$) seems to be ecologically and economically profitable material for electronics. It is a light-weight and indirect-gap narrow-band semiconductor prospective, in particular, for thermoelectric applications [281].

$SiO_2$ could be employed as industrial raw materials to synthesize magnesium silicide ($Mg_2Si$) via a deoxidization reaction of $SiO_2$ by magnesium in solid-state. $Mg_2Si$ intermetallics are suitable reinforcements for aluminum and magnesium alloys because of their superior characteristics. In particular, aluminum or magnesium composite alloys with $Mg_2Si$ dispersoids fabricated by powder metallurgy or in-situ casting process show high mechanical properties and a good wear resistance due to the uniform distribution of fine $Mg_2Si$ particles in the matrix [78,282–285].

The solid-state synthesis of $Mg_2Si$ compounds by reaction of $SiO_2$ with magnesium were suggested by Kondoh et al. [78]. They extruded the compact of mixture AZ31 alloys and rice husk wastes burned at 1000 °C. It was found that acid treatment of rice husk has a dramatic effect on the reaction between magnesium alloy powder and rice husk ash. It can be attributed to the reactivity of high purity and fine and amorphous structure of $SiO_2$.

Bose et al. [63] prepared $Mg_2Si$ by alloying technique. Appropriate amounts of prepared white ash and commercially available 99.9% pure magnesium powder were thoroughly mixed and then tightly packed in an MgO-coated (inside) selemenite crucible and then fired at about 650 °C inside a muffle furnace. The amorphous $SiO_2$ was thus reduced to form silicon according to the following reaction:

$$SiO_2 + 2Mg = Si + 2MgO + SiO_2\ (\text{unreacted}) \tag{32}$$

The resulting mass after reduction was successively leached with HC1 and HF to remove MgO and unreacted $SiO_2$, respectively, and then used for preparing $Mg_2Si$ by the alloying technique. Appropriate quantities of obtained silicon and magnesium powder (both 99.9% pure) were intimately mixed and then fired inside an alloying furnace at 500 °C for 24 h under an $H_2$ atmosphere. The alloying took place according to the reaction:

$$Si + 2Mg = Mg_2Si \tag{33}$$

Umeda and co-workers synthesized amorphous and porous silica particles originated from rice husks, which were coated with CNTs, also contained in the pores. The in situ synthesis of $Mg_2Si$ and MgO via deoxidization and oxidation reaction occurred from the elemental mixture of pure magnesium and CNT–$SiO_2$ composite particles via the spark plasma sintering process [286]. Although the reports on the preparation of $Mg_2Si$ with rice husk is scarce, it is expected that the growing interest will encourage numerous publications in this field.

## 10. Activated carbon

In addition to silicon, silica, $Si_3N_4$ and SiC, activated carbon was prepared separately from rice husk. According to different burning temperature of RH in air always silica ash varying in color from grey to black and inorganic impurities along with unburned carbon is forming. Very fine and closed pores are created during these steps. The purpose of activation is to enlarge the diameter of the pores and to create new pores. According to the International Union of Pure and Applied Chemistry (IUPAC), the pores of porous materials are classified into three groups: micropores (width $d < 2$ nm), mesopores ($2\text{ nm} < d < 50$ nm), and macropores ($d > 50$ nm) [287]. Therefore, due to extensive surface area, high degree of surface reactivity, and favorable pore size distribution, activated carbons absorb many interests. Basically, there are two main steps for the preparation and manufacture of active carbon from rice husk: (1) the carbonization of the carbonaceous raw material below 700 °C, in the absence of oxygen (char), and (2) the activation of the carbonized product (char), which is either physical or chemical. Carbonization and chemical activation can be performed in a single step.

### 10.1. Physical activation

The physical activation consists of heating at high temperature under a carbon gasification reactant ($H_2O$, $CO_2$, air). In other words, carbonization is followed by the activation of the resulting char at elevated temperature in the presence of suitable oxidizing gases. It is possible to attain any degree of conversion of carbon in the rice husk by first pyrolyzing the husk to get reactive char and subsequently reacting this char with steam and carbon dioxide at 800–900 °C. If the nitrogen atmosphere of carbonized rice husk replaces by atmospheric air, carbon dioxide and steam, at various temperatures, different results will be achieved [288]. By increasing the temperature, non-carbonaceous materials are first removed in gaseous form. Then freed atoms of elementary carbon are irregularly grouped into the elementary micro crystallites. The irregular arrangement creates free interstices that trap tarry hydrocarbonates on their way out. Therefore, the resulting carbonized material tends to have low absorption capacity due to blockage of the interstices. Such carbonized material can only be activated by removing the tray substances through heating them in a steam of suitable oxidizing gases [289]. Ganesh and Dutt Grover [290] reported that the samples pyrolyzed under 600 °C followed by carbonization under the air flow, yield carbon free as well as the samples which were subjected to steam and carbon dioxide. In this method disorganized carbon is burned-off completely and no trace of carbon is detected in the samples. By increasing the pyrolyzing temperature up to 800 °C the carbon disorganized achieve almost micro crystallite phase. In addition, by subjecting to oxidant gas, the reaction just proceeds on carbon atoms at the edge and corners of elementary of micro crystallite, sites which are very reactive [289]. It was reported that by pyrolyzing rice husk at 900 °C, carbon reacts partially with the silica of rice husk. The carbon–silica bonds are strong and stable, consequently combined carbon does not become oxidized, even under oxygen at temperatures as high as 1200 °C. In the case of the samples that were subjected in the atmosphere of steam and dioxide carbon, it was explained that the carbon–carbon dioxide and carbon–steam reactions are both endothermic and result in two moles of gaseous products for each mole of gaseous reactant (reactions (34) and (35)). The endothermic reaction restricts further increase in the local temperatures of the reactants. Further, the doubled increase in the volume of the products during these reactions exerts increasing pressure, resulting in progressive fracture of the already fragile char [290].

$$C\ (s) + CO_2\ (g) = 2CO\ (g) \quad \Delta H = +174\ \text{kJ/mol} \tag{34}$$

$$C\ (s) + H_2O\ (g) = CO\ (g) + H_2\ (g) \quad \Delta H = +131\ \text{kJ/mol} \tag{35}$$

Since the carbon–carbon dioxide reaction is slower than the carbon–steam reaction under similar conditions, the removal of carbon tends to be partial for the former reaction. Further, the carbon–steam reaction is catalyzed, owing to the presence of alkali metal oxides, especially potash, in ash and therefore is more effective in removal of carbon from char. Molina-Sabio and co-workers [291] reported that carbon dioxide activation mainly causes the creation of microporosity. However, steam activation expands the micro porosity from the early stages of the activation process, even in the case in which the removal rate of carbon atoms from the char is the same for the two activating agents. Then, the obtained char was leached with dilute hydrochloric acid at

60–100 °C for 2–3 h. During leaching, different impurities like oxides of sodium, potassium and magnesium were dissolved and then removed from the char by filtration under vacuum. The char was then washed thoroughly to remove the remaining acid and then dried.

### 10.2. Chemical activation

Chemical activation (ChA) can be accomplished in a single step by carrying out thermal decomposition of raw material with chemical reagents (dehydration agents) at low temperature. In preparing of activated carbon, base-leaching and acid-washing as the first and last stages, respectively, can be done. The base-leaching procedure can effectively remove ash and improve the surface area and pore volume of the simple. The acid-washing procedure can act as a cleaning process to remove metallic impurities and residual activating agent [292,293]. However, the pre-treatment of the rice husk with HF acid can also lead to removal of $SiO_2$ from the composition of the materials.

In comparison to physical activation, chemical activation provides three important advantages. (i) The lower temperature at which the process is performed, (ii) the global yield of chemical activation tends to be greater because burn off char is not required and (iii) obtaining activated carbon with a smaller pore size [294]. Some special factors define the quality of obtained activated carbon, such as the ratio of the activation agent to rice husks, activation temperature and time. Experimental results revealed that the BET surface area, pore volume, and average pore diameter of the resulting porous carbon generally increase with increasing activation time, activation temperature and ratio of activation agents.

The mechanism of pore development in active carbon (AC) can be summarized as two main antagonic contributions to $S_{BET}$: the formation and disappearance of micropores. Fig. 28 exhibits the scheme of the mechanism for pore development in ACs.

On the one hand, appropriate conditions like the mass ratio were beneficial to the development of pore structure. Under this condition, the formation rate of micropores was greater than the disappearance rate, hence increasing the $S_{BET}$ of AC. When the formation and deformation rates were equal, pore development reached a state of dynamic equilibrium with the maximum $S_{BET}$. On the other hand, extreme conditions accelerated the widening of micropores. Many micropores were destroyed by collapsing or merging into mesopores and macropores, leading to reduction of $S_{BET}$ [295]. The most widely used chemical agents include $ZnCl_2$, $H_3PO_4$, $H_2SO_4$, KOH and $K_2CO_3$ [82, 296–299]. $ZnCl_2$ and $H_3PO_4$ are usually used for activating biomasses which are rich in cellulose, hemicellulose and lignin such as wood and nut shell [300,301]. KOH, $K_2CO_3$ and $Na_2CO_3$ are usually used for activating residue, which is rich in ash. Nevertheless, compared with alkali hydroxide, the carbonate has lower cost, and the green recycling route is achieved easily. However, $Na_2CO_3$ has poor activation effect and $K_2CO_3$ is the optimum activated agent. Different pore size was found to be linked to the nature of the alkali cation of the carbonate in the following order: Li < Na < K < Rb < Cs [302–304]. The effect of alkali carbonate in the activation process can be related to formation of porosity due to $SiO_2$ interaction with the carbonates, which proceeds with formation of potassium and sodium silicates and $CO_2$. $CO_2$ reacts with the carbon phase with formation of CO, according to reactions (36) and (37):

$$M_2CO_3 + SiO_2 = M_2SiO_3 + CO_2 \tag{36}$$

$$CO_2 + C = 2CO \tag{37}$$

where M = Na, K. In addition, carbonates can interact with the carbon phase from 700 °C to 950 °C; the process completes in accordance with reaction (38):

$$K_2CO_3 + 2C = 2K + 3CO \tag{38}$$

Activation reaction between alkali hydroxide and rice husk is complicated. Ordinarily, the reaction may be as follows [305,306]:

$$4KOH + C = K_2CO_3 + K_2O + 2H_2 \tag{39}$$

Considering the decomposition of potassium hydroxide and the reduction of carbon, some reactions given below may also be followed simultaneously.

$$2KOH = K_2O + H_2O \tag{40}$$

$$C + H_2O = H_2 + CO \tag{41}$$

$$CO + H_2O = H_2 + CO_2 \tag{42}$$

$$K_2O + CO_2 = K_2CO_3 \tag{43}$$

$$K_2O + H_2 = 2K + H_2O \tag{44}$$

$$K_2O + C = 2K + CO \tag{45}$$

$$K_2CO_3 + 2C = 2K + 3CO \tag{46}$$

$$K_2O + SiO_2 = K_2SiO_3 \tag{47}$$

The reaction (39), is the special characteristic of this method. It is important in the activation process, amorphous carbon and silica in the rice husk disappear through the above reactions and pore structure is formed.

From both economical and environmental perspectives, phosphoric acid activation can be another appropriate alternative because in this case the activation temperature is much lower (usually around 400–500 °C) than that of physical and alkali hydroxides activations (>650 °C). In addition, phosphoric acid can be recovered and it can be removed easily after activation of the

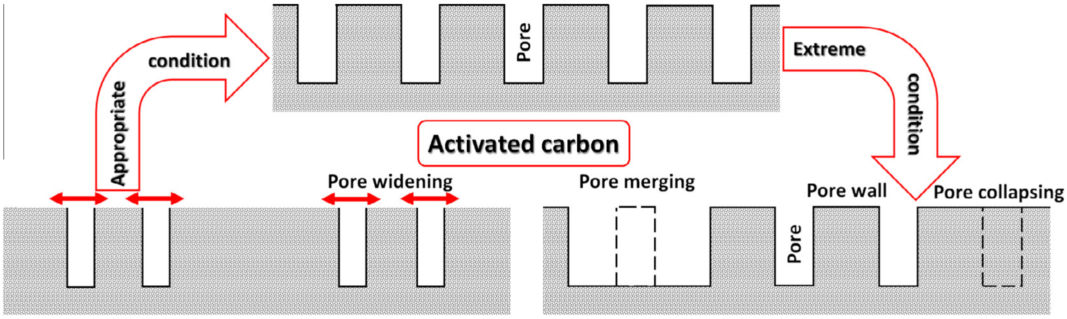

**Fig. 28.** The schemic of the mechanism for pore development in ACs [294].

carbon by washing with hot and cold water. The percent of $H_3PO_4$ recovery was calculated with Eq. (48) [307]:

$$\text{Recovery} = \frac{\text{product weight before washing} - \text{product weight after washing}}{H_3PO_4\ \text{weight for impregnation}} \times 100 \tag{48}$$

Nevertheless, the pore size due to using $H_3PO_4$ is lower in comparison to other activation agents. The lower surface areas of obtained carbon may be due to high retention of phosphates in the carbon structure. Reaction of $H_3PO_4$ with the precursor matrix can create phosphate esters and other polymerization by-products that bind strongly to the solid matrix [308].

Another activated agent was proposed by Uzunova et al. [17]. Rice husks were activated with carbamide. The probable mechanism of activation is associated with the interaction of carbamide with the OH and COOH groups, whereupon the $-NHCONH_2$ and the $-CONHCONH_2$ groups are obtained. The latter groups at a temperature of 700 °C and in the absence of air decomposed into $NH_3$ and $CO_2$. Thereupon part of the nitrogen of the carbamide can be included in the structure of the carbon, forming the so called diazo groups ($-N{=}N-$).

In order to obtain activated carbon, in all those mentioned procedures, the rice husk was exposed to single step of chemical activation. However, it has been found pre-calcination in absence of air before chemical activation has a great effect on the porosity of the porous carbons [309]. Comparison of all resulting porous carbons indicates that an activation process can produce carbons with micro-porosity and meso-porosity. Microporous carbons are produced with higher pre-calcination times. Increment in porosity due to pre-calcination can help the activating agents to penetrate the interior or disperse well. The effect of carbonization temperature should also be considered. The carbonization at temperature higher than 700 °C leads to formation of less stable and inactive carbon structure, which is connected with the presence of small quantities of oxygen containing groups, that diminishes the porosity content of the material [310]. It was also reported that rice husk pyrolysis at 450 °C followed by silica removal with HF and a final and subsequent chemical activation, produces lower specific area than the process where the HF treatment is applied before pyrolysis at the same temperature. This outcome on the specific surface area has been observed particularly when $ZnCl_2$ was used as activating agent [17]. Several authors showed that pre-calcination under $N_2$ has a dramatic influence on the porosity of final active carbon activated by agents like NaOH, KOH, $K_2CO_3$. However, it was shown pre-calcination under the atmosphere of $N_2$ does not have any influence on the pores of active carbon activated by phosphoric acid [304,306,311,312]. The change in the value of the specific surface area and the pore volume in the process of treatment and activation of the rice husks are represented in Table 8.

### 10.3. Microwave heating technology

Recently, microwave heating technology has been applied instead of conventional heating in chemical activation processes. A comparison of the results of ChA using conventional heating and microwave heating processes for the same precursors revealed that impregnation with the microwave method leads to the development of relatively higher surface areas and more economically competitive than those obtained in impregnation via conventional heating. Combination of microwave heating with other activation agents like KOH, NaOH and $ZnCl_2$ have been proposed by some authors [313–315]. This results in a reduction in the processing time, energy consumption and the number of steps involved in the overall process, which eliminates the need for other reagents and devices.

## 11. Summary and conclusions

In recent years – as a source of silicon and carbon based materials –, rice husk has been strategically considered and utilized for synthesis of high purity ceramic phases like $Si_3N_4$, SiC, silica and nano silica, $Mg_2Si$, porous silicon and carbon materials. Conversion of rice husk into value-added engineering materials may have a threefold impact: (i) increase in the availability of inexpensive silicon based resources, (ii) contribution as part of the solution to the waste disposal issue, and (iii) knowledge generation through the

**Table 8**
The pore volume and specific area of activated carbons derived from rice husk under different activation chemical processes.

| Activation agent | Process | Final temp. (°C) | Impregnation ratio | Pore volume ($cm^3/g$) | Specific area ($m^2\ g^{-1}$) | Refs. |
|---|---|---|---|---|---|---|
| $ZnCl_2$ | ChA | 600 | 1 | 0.380 | 750 | [308] |
| | ChA | 600 | 10 wt.% | 1.365 | 480 | [327] |
| | ChA | 500 | 2 | 1.344 | 2434 | [292] |
| | ChA | 300 | 1 | 0.463 | 578 | [294] |
| NaOH | ChA & Pre-Cal | 800 | 3 | 0.9–1.9 | >2500 | [306] |
| | Dry ChA & Pre-Cal | 800 | 3 | 1.517 | 2841 | [328] |
| | ChA | 800 | – | 0.346 | 933 | [82] |
| $H_3PO_4$ | ChA & Pre-Cal | 900 | 4.2 | 0.4 | 438 | [304] |
| | ChA & Pre-Cal | 800 | 4.2 | 0.373 | 379 | [304] |
| | ChA | 500 | 75% | 0.43 | 376 | [329] |
| | ChA | 400 | – | – | 649 | [307] |
| | ChA | 450 | 1.5 | 0.735 | 1295 | [330] |
| | ChA | 500 | 2 | 1.315 | 1741 | [292] |
| KOH | ChA | 450 | 1.5 | 0.97 | 1930 | [330] |
| | ChA & Pre-Cal | 900 | 4 | 1.39 | 2410 | [312] |
| | ChA | 800 | 4 | 0.46 | 900 | [312] |
| | ChA & Pre-Cal | 800 | 4 | 0.94 | 1917 | [331] |
| | ChA & Pre-Cal | 800 | 4 | 1.9 | 3202 | [332] |
| | ChA | 850 | 2 | 1.22 | 1936 | [333] |
| $H_2SO_4$ | ChA Under vacuum | 100 | – | 0.529 | 704 | [334] |
| $K_2CO_3$ | ChA & Pre-Cal | 900 | 4 | 1.54 | 1676 | [311] |
| $FeSO_4{\cdot}7H_2O$ | ChA | 600 | 30% | – | 110 | [327] |
| $FeCl_3{\cdot}6H_2O$ | ChA | 600 | 30% | – | 13 | [327] |
| $CaCl_2{\cdot}2H_2O$ | ChA | 600 | 30% | – | 53 | [327] |
| KCl | ChA | 600 | 30% | – | 64 | [327] |
| Urea | ChA & Pre-Cal | 700 | 5 | 0.81 | 1259 | [17] |

ChA: chemical activation.
ChA & Pre-Cal: chemical activation and pre-calcination.

scientific/technological research conducted. The present critical review substantiates that numerous investigations have focused on the synthesis of $Si_3N_4$, SiC, silica and active carbon, and that a promising future can be envisioned. Within the framework of the objectives established for this review, the following most relevant conclusions can be drawn:

- The structure, properties and purity of obtained silica from rice husk are quite sensitive to the chosen extraction methods. Depending on the selected temperature or chemical treatments, the products can range from amorphous to different crystalline phases.
- By properly controlling both nucleation and growth of SiC whiskers, the amount of SiC obtained can be increased. The temperature, gas flow rates, availability and concentration of growth species, Si/C ratio and a free space to grow, are some of the important parameters that must be taken into account. It has been recognized that final purity, morphology, structure, and size of SiC ceramic phases depend largely on the chosen processing conditions and additives.
- Carbothermal reduction of silica is the main method for manufacturing silicon nitride powders. Specific characteristics of the raw materials such as high reactivity and a good distribution of the silica and carbon are of considerable importance for the reaction. The better the distribution, the more beneficial is for nitridation. Therefore, as RH naturally contains both, silica and carbon, it is a potential material for producing silicon nitride. In the case of formation of $Si_3N_4$ whiskers via a carbothermal reduction, it has been found that the impurities play a key role.
- Amongst the various methods, the reduction of amorphous silica by metallic metals to silicon has been discussed extensively. The metallic elements Mg, Ca, Al and Ti can reduce $SiO_2$ at comparatively lower temperatures and form mixtures of condensed phase products.
- The reports on the preparation of $Mg_2Si$ starting from rice husk are quite scarce. In general, $Mg_2Si$ can be prepared by a mixture of pure magnesium and CNT–$SiO_2$ composite particles (i) via the spark plasma sintering process, (ii) alloying of white ash and commercially pure magnesium powder, and (iii) extrusion the compact of mixture AZ31 alloys and rice husk.
- There are two main steps for the preparation and manufacture of active carbon from rice husk: (1) carbonization of the carbonaceous raw material below 700 °C in the absence of oxygen (char), and (2) activation of the carbonized product (char), which can be either physical or chemical. Carbonization and chemical activation can be carried out in a single step. In comparison to physical activation, chemical activation provides three important advantages: (i) lower temperature at which the process is conducted, (ii) the global yield of chemical activation tends to be greater because burn off char is not required and (iii) the product has a smaller pore size.

## Acknowledgments

Ms. Niloofar Soltani and Mr. Amin Bahrami gratefully acknowledge CONACYT (National Council of Science and Technology, in Mexico) for granting a doctoral scholarship. The authors are also thankful to Cinvestav IPN-Saltillo for support in the research activities in the field of advanced materials.

## References

[1] S.V. Joshi, L. Drzal, A. Mohanty, S. Arora, Are natural fiber composites environmentally superior to glass fiber reinforced composites?, Compos Part A: Appl. Sci. Manuf. 35 (2004) 371–376.
[2] L. Sun, K. Gong, Silicon-based materials from rice husks and their applications, Ind. Eng. Chem. Res. 40 (2001) 5861–5877.
[3] H.S. Song, D. Ramkrishna, Issues with increasing bioethanol productivity: a model directed study, Korean J. Chem. Eng. 27 (2010) 576–586.
[4] M.P. Westman, L.S. Fifield, K.L. Simmons, S. Laddha, T.A. Kafentzis, Natural Fiber Composites: A Review, Pacific Northwest National Laboratory, Oak Ridge, 2010.
[5] P. Lodha, A.N. Netravali, Characterization of interfacial and mechanical properties of "green" composites with soy protein isolate and ramie fiber, J. Mater. Sci. 37 (2002) 3657–3665.
[6] R.M. Rowell, A.R. Sanadi, D.F. Caulfield, R.E. Jacobson, Utilization of natural fibers in plastic composites: problems and opportunities, Lignocellulosic-Plast. Compos. (1997) 23–51.
[7] M. Jawaid, H. Abdul Khalil, Cellulosic/synthetic fibre reinforced polymer hybrid composites: a review, Carbohydr. Polym. 86 (2011) 1–18.
[8] D. Chandramohan, K. Marimuthu, A review on natural fibers, Int. J. Res. Rev. Appl. Sci. 8 (2011) 194–206.
[9] S.N. Monteiro, F.P.D. Lopes, A.P. Barbosa, A.B. Bevitori, I.L.A.D. Silva, L.L.D. Costa, Natural lignocellulosic fibers as engineering materials—an overview, Metall. Mater. Trans. A 42 (2011) 2963–2974.
[10] K. Joseph, R. Toledo, B. James, S. Thomas, L.H. Carvalho, A review on sisal fiber reinforced polymer composites, Revista Brasileira de Engenharia Agrícola e Ambiental 3 (1999) 367–379.
[11] J. Guimarães, E. Frollini, C. Da Silva, F. Wypych, K. Satyanarayana, Characterization of banana, sugarcane bagasse and sponge gourd fibers of Brazil, Ind. Crops Prod. 30 (2009) 407–415.
[12] L. Vlaev, I. Markovska, L. Lyubchev, Non-isothermal kinetics of pyrolysis of rice husk, Thermochim. Acta 406 (2003) 1–7.
[13] V.S. Mane, I. Deo, Kinetic and equilibrium isotherm studies for the adsorptive removal of Brilliant Green dye from aqueous solution by rice husk ash, J. Environ. Manage. 84 (2007) 390–400.
[14] K. Foo, B. Hameed, Utilization of rice husk ash as novel adsorbent: a judicious recycling of the colloidal agricultural waste, Adv. Colloid Interface Sci. 152 (2009) 39–47.
[15] D. Hall, J. Scrase, Will biomass be the environmentally friendly fuel of the future?, Biomass Bioenergy 15 (1998) 357–367
[16] M. Patel, A. Karera, P. Prasanna, Effect of thermal and chemical treatments on carbon and silica contents in rice husk, J. Mater. Sci. 22 (1987) 2457–2464.
[17] S. Uzunova, I. Uzunov, S. Vassilev, A. Alexandrova, S. Staykov, D. Angelova, Preparation of low-ash-content porous carbonaceous material from rice husks, Bul. Chem. Commun. 42 (2010) 130–137.
[18] A. Pande, S. Makarande, Effect of rice husk ash on concrete, Int. J. Eng. Res. Appl. 3 (2013) 1718–1723.
[19] N. Johar, I. Ahmad, A. Dufresne, Extraction, preparation and characterization of cellulose fibres and nanocrystals from rice husk, Ind. Crops Prod. 37 (2012) 93–99.
[20] V.C. Srivastava, I.D. Mall, I.M. Mishra, Adsorption thermodynamics and isosteric heat of adsorption of toxic metal ions onto bagasse fly ash (BFA) and rice husk ash (RHA, Chem. Eng. J. 132 (2007) 267–278.
[21] S. Abo-El-Enein, M. Eissa, A. Diafullah, M. Rizk, F. Mohamed, Removal of some heavy metals ions from wastewater by copolymer of iron and aluminum impregnated with active silica derived from rice husk ash, J. Hazard. Mater. 172 (2009) 574–579.
[22] M. Ajmal, R. Ali Khan Rao, S. Anwar, J. Ahmad, R. Ahmad, Adsorption studies on rice husk: removal and recovery of Cd (II) from wastewater, Bioresour. Technol. 86 (2003) 147–149.
[23] C.G. Rocha, D.A.M. Zaia, R.V.S. Alfaya, A.A.S. Alfaya, Use of rice straw as biosorbent for removal of Cu (II), Zn (II), Cd (II) and Hg (II) ions in industrial effluents, J. Hazard. Mater. 166 (2009) 383–388.
[24] M.N. Amin, S. Kaneco, T. Kitagawa, A. Begum, H. Katsumata, T. Suzuki, K. Ohta, Removal of arsenic in aqueous solutions by adsorption onto waste rice husk, Ind. Eng. Chem. Res. 45 (2006) 8105–8110.
[25] T. Khan, S.A.B. Ab Wahap, M. Chaudhuri, Adsorption of arsenite from water by rice husk silica, Nat. Environ. Pollut. Technol. 11 (2012) 229–233.
[26] L.H. Wang, C.I. Lin, Adsorption of chromium (III) ion from aqueous solution using rice hull ash, J. Chin. Inst. Chem. Eng, 39 (2008) 367–373.
[27] W. Nakbanpote, P. Thiravetyan, C. Kalambaheti, Comparison of gold adsorption by *Chlorella vulgaris*, rice husk and activated carbon, Miner. Eng. 15 (2002) 549–552.
[28] R. Han, D. Ding, Y. Xu, W. Zou, Y. Wang, Y. Li, L. Zou, Use of rice husk for the adsorption of congo red from aqueous solution in column mode, Bioresour. Technol. 99 (2008) 2938–2946.
[29] O. Abdelwahab, A. El Nemr, A. El Sikaily, A. Khaled, Use of rice husk for adsorption of direct dyes from aqueous solution: a case study of Direct F. Scarlet, Egypt. J. Aquat. Res. 31 (2005) 1–11.
[30] V. Ganvir, K. Das, Removal of fluoride from drinking water using aluminum hydroxide coated rice husk ash, J. Hazard. Mater. 185 (2011) 1287–1294.
[31] A. Proctor, S. Palaniappan, Soy oil lutein adsorption by rice hull ash, J. Am. Oil. Chem. Soc. 66 (1989) 1618–1621.
[32] K.T. Lee, A. Matlina Mohtar, N.F. Zainudin, S. Bhatia, A.R. Mohamed, Optimum conditions for preparation of flue gas desulfurization absorbent from rice husk ash, Fuel 84 (2005) 143–151.
[33] I. Dahlan, K.T. Lee, A.H. Kamaruddin, A.R. Mohamed, Sorption of $SO_2$ and NO from simulated flue gas over rice husk ash (RHA)/CaO/$CeO_2$ sorbent: evaluation of deactivation kinetic parameters, J. Hazard. Mater. 185 (2011) 1609–1613.

[34] I. Dahlan, K.T. Lee, A.H. Kamaruddin, A.R. Mohamed, Evaluation of various additives on the preparation of rice husk ash (RHA)/CaO-based sorbent for flue gas desulfurization (FGD) at low temperature, J. Hazard. Mater. 161 (2009) 570–574.
[35] L.C. Lau, K.T. Lee, A.R. Mohamed, Rice husk ash sorbent doped with copper for simultaneous removal of $SO_2$ and NO: optimization study, J. Hazard. Mater. 183 (2010) 738–745.
[36] I. Dahlan, K.T. Lee, A.H. Kamaruddin, A.R. Mohamed, Selection of metal oxides in the preparation of rice husk ash (RHA)/CaO sorbent for simultaneous $SO_2$ and NO removal, J. Hazard. Mater. 166 (2009) 1556–1559.
[37] T. Witoon, Polyethyleneimine-loaded bimodal porous silica as low-cost and high-capacity sorbent for $CO_2$ capture, Mater. Chem. Phys. 137 (2012) 235–245.
[38] W. Zeng, H. Bai, Swelling-agent-free synthesis of rice husk derived silica materials with large mesopores for efficient $CO_2$ capture, Chem. Eng. J. 251 (2014) 1–9.
[39] M. Azadi, M.E. Bahrololoom, F. Heidari, Enhancing the mechanical properties of an epoxy coating with rice husk ash, a green product, J. Coat. Technol. Res. 8 (2011) 117–123.
[40] N. Tipsotnaiyana, L. Jarupan, C. Pechyen, Synthesized silica powder from rice husk for printing raw materials application, Adv. Mater. Res. 506 (2012) 218–221.
[41] F. Bondioli, F. Andreola, L. Barbieri, T. Manfredini, A.M. Ferrari, Effect of rice husk ash (RHA) in the synthesis of (Pr, Zr) $SiO_4$ ceramic pigment, J. Eur. Ceram. Soc. 27 (2007) 3483–3488.
[42] F. Andreola, L. Barbieri, F. Bondioli, Agricultural waste in the synthesis of coral ceramic pigment, Dyes Pigm. 94 (2012) 207–211.
[43] D.G. Nair, A. Fraaij, A.A.K. Klaassen, A.P.M. Kentgens, A structural investigation relating to the pozzolanic activity of rice husk ashes, Cem. Concr. Res. 38 (2008) 861–869.
[44] V. Papadakis, S. Tsimas, Supplementary cementing materials in concrete: Part I: efficiency and design, Cem. Concr. Res. 32 (2002) 1525–1532.
[45] S. Chandrasekhar, P. Pramada, J. Majeed, Effect of calcination temperature and heating rate on the optical properties and reactivity of rice husk ash, J. Mater. Sci. 41 (2006) 7926–7933.
[46] V. Saraswathy, H.W. Song, Corrosion performance of rice husk ash blended concrete, Constr. Build. Mater. 21 (2007) 1779–1784.
[47] M. Gonçalves, C. Bergmann, Thermal insulators made with rice husk ashes: production and correlation between properties and microstructure, Constr. Build. Mater. 21 (2007) 2059–2065.
[48] B.I. Ugheoke, E.O. Onche, O.N. Namessan, G.A. Asikpo, Property optimization of kaolin-rice husk insulating fire-bricks, Leonardo Electron. J. Pract. Technol. 5 (2006) 167–178.
[49] H. Haxo Jr, P. Mehta, Ground rice-hull ash as a filler for rubber, Rubber Chem. Technol. 48 (1975) 271–288.
[50] P. Sae-Oui, C. Rakdee, P. Thanmathorn, Use of rice husk ash as filler in natural rubber vulcanizates: in comparison with other commercial fillers, J. Appl. Polym. Sci. 83 (2002) 2485–2493.
[51] M.Y.A. Fuad, Z. Ismail, Z.A.M. Ishak, A.K.M. Omar, Application of rice husk ash as fillers in polypropylene: effect of titanate, zirconate and silane coupling agents, Eur. Polymer J. 31 (1995) 885–893.
[52] S. Siriwardena, H. Ismail, U. Ishiaku, White rice husk ash filled ethylene–propylene–diene terpolymer/polypropylene blends: effect of dynamic vulcanization and filler loading, Polym. Plast. Technol. Eng. 40 (2001) 519–538.
[53] S. Siriwardena, H. Ismail, U. Ishiaku, M. Perera, Mechanical and morphological properties of white rice husk ash filled polypropylene/ethylene–propylene–diene terpolymer thermoplastic elastomer composites, J. Appl. Polym. Sci. 85 (2002) 438–453.
[54] S. Siriwardena, H. Ismail, U. Ishiaku, Water absorption behavior and its effect on tensile properties of ethylene–propylene–diene–terpolymer/polypropylene/filler ternary composites: a preliminary study, Polym. Plast. Technol. Eng. 41 (2002) 419–433.
[55] M.J. John, B. Francis, K. Varughese, S. Thomas, Effect of chemical modification on properties of hybrid fiber biocomposites, Compos. A Appl. Sci. Manuf. 39 (2008) 352–363.
[56] S. Kalia, B. Kaith, I. Kaur, Pretreatments of natural fibers and their application as reinforcing material in polymer composites—a review, Polym. Eng. Sci. 49 (2009) 1253–1272.
[57] G. Cristaldi, A. Latteri, G. Recca, G. Cicala, Composites based on natural fibre fabrics, Woven Fabric Eng. (2010) 317–342.
[58] D. Chaudhary, M. Jollands, F. Cser, Understanding rice hull ash as fillers in polymers: a review, Silicon Chem. 1 (2002) 281–289.
[59] C. Wu, Rice hulls could nourish Silicon Valley, Sci. News 157 (2000) 164.
[60] F. Adam, J. Andas, I. Rahman, The synthesis and characterization of cobalt-rice husk silica nanoparticles, Open Colloid Sci. J. 4 (2011) 12–18.
[61] H. Ismail, L. Mega, H.P.S.A. Khalil, Effect of a silane coupling agent on the properties of white rice husk ash–polypropylene/natural rubber composites, Polym. Int. 50 (2001) 606–611.
[62] K. Omatola, A. Onojah, Elemental analysis of rice husk ash using X-ray fluorescence technique, Int. J. Phys. Sci. 4 (2009) 189–193.
[63] S. Bose, H. Acharya, H. Banerjee, Electrocal, thermal, thermoelectric and related properties of magnesium silicide semiconductor prepared from rice husk, J. Mater. Sci. 28 (1993) 5461–5468.
[64] E. Natarajan, A. Nordin, A. Rao, Overview of combustion and gasification of rice husk in fluidized bed reactors, Biomass Bioenergy 14 (1998) 533–546.
[65] S.R. Decker, J. Sheehan, D.C. Dayton, J.J. Bozell, W.S. Adney, B. Hames, S.R. Thomas, R.L. Bain, S. Czernik, M. Zhang, Biomass Conversion, Kent and Riegel's Handbook of Industrial Chemistry and Biotechnology, Springer, 2007. pp. 1449–1548.
[66] A. Faaij, Modern biomass conversion technologies, Mitig. Adapt. Strat. Glob. Change 11 (2006) 335–367.
[67] M. Kaltschmitt, G. Reinhardt, T. Stelzer, Life cycle analysis of biofuels under different environmental aspects, Biomass Bioenergy 12 (1997) 121–134.
[68] T. Chungsangunsit, S.H. Gheewala, S. Patumsawad, Environmental assessment of electricity production from rice husk: a case study in Thailand, Int. Energy J. 6 (2005) 347–356.
[69] M.R. Taib, A. Johari, S. Ngo, A. Salema, K. Tan, Utilisation of rice husk waste and its ash (Part 2), Ingineur 42 (2009) 37–41.
[70] A. Ghaly, A. Al-Taweel, G. Mackay, Project Report Renewable Energy Division, Energy Mines and Resources, Canada, Ottawa, Ontario, 1986.
[71] H. Jiang, X. Zhu, Q. Guo, Q. Zhu, Gasification of rice husk in a fluidized-bed gasifier without inert additives, Ind. Eng. Chem. Res. 42 (2003) 5745–5750.
[72] C. Loha, H. Chattopadhyay, P.K. Chatterjee, Energy generation from fluidized bed gasification of rice husk, J. Renewable Sustainable Energy 5 (2013) 043111.
[73] M. Fang, L. Yang, G. Chen, Z. Shi, Z. Luo, K. Cen, Experimental study on rice husk combustion in a circulating fluidized bed, Fuel Process. Technol. 85 (2004) 1273–1282.
[74] V. Skoulou, G. Koufodimos, Z. Samaras, A. Zabaniotou, Low temperature gasification of olive kernels in a 5-kW fluidized bed reactor for $H_2$-rich producer gas, Int. J. Hydrogen Energy 33 (2008) 6515–6524.
[75] C.-z. Wu, X.-l. Yin, L.-l. Ma, Z.-q. Zhou, H.-p. Chen, Operational characteristics of a 1.2-MW biomass gasification and power generation plant, Biotechnol. Adv. 27 (2009) 588–592.
[76] I. Narvaez, A. Orio, M.P. Aznar, J. Corella, Biomass gasification with air in an atmospheric bubbling fluidized bed. Effect of six operational variables on the quality of the produced raw gas, Ind. Eng. Chem. Res. 35 (1996) 2110–2120.
[77] P. Lv, Z. Xiong, J. Chang, C. Wu, Y. Chen, J. Zhu, An experimental study on biomass air–steam gasification in a fluidized bed, Bioresour. Technol. 95 (2004) 95–101.
[78] K. Kondoh, H. Oginuma, J. Umeda, T. Umeda, Innovative reuse of agricultural wastes as industrial raw materials to form magnesium composites, Mater. Trans. 46 (2005) 2586.
[79] I. Valchev, V. Lasheva, T. Tzolov, N. Josifov, Silica products from rice hulls, J. Univ. Chem. Technol. Metall. 44 (2009) 257–261.
[80] E. Mizuki, S. Okumura, H. Saito, S. Murao, Formation of silicon carbide from rice husks using enzymatic methods for carbon control, Bioresour. Technol. 44 (1993) 47–51.
[81] W. Hua, D. Yowian, The character of reaction kinetics for producing ultra fine Si3N4 powder with rice husks, Naihuo Cailiao (1996) 02.
[82] Y. Liu, Y. Guo, W. Gao, Z. Wang, Y. Ma, Z. Wang, Simultaneous preparation of silica and activated carbon from rice husk ash, J. Cleaner Prod. 32 (2012) 204–209.
[83] S. Das, T. Dan, S. Prasad, P. Rohatgi, Aluminium alloy-rice husk ash particle composites, J. Mater. Sci. Lett. 5 (1986) 562–564.
[84] D. Zhu, M. Gao, S. Zhang, H. Wu, Y. Pan, Y. Liu, H. Pan, F.J. Oliveira, J.M. Vieira, A high-strength $SiC_w$/SiC–Si composite derived from pyrolyzed rice husks by liquid silicon infiltration, J. Mater. Sci. 47 (2012) 4921–4927.
[85] D. Zhu, M. Gao, H. Pan, Z. Hong, B. Zhao, S. Li, H. Ge, Y. Liu, Y. Pan, Fabrication and mechanical properties of $SiC_w/MoSi_2$–SiC composites by liquid Si infiltration of pyrolyzed rice husk preforms with Mo additions, Int. J. Refract Metal Hard Mater. 35 (2012) 152–158.
[86] O. Chakrabarti, P.K. Das, Reactive infiltration of Si–Mo alloyed melt into carbonaceous preforms of silicon carbide, J. Am. Ceram. Soc. 83 (2000) 1548–1550.
[87] R. Mitra, Y. Mahajan, N.E. Prasad, W. Chiou, Processing—microstructure—property relationships in reaction hot-pressed $MoSi_2$ and $MoSi_2/SiC_p$, Mater. Sci. Eng., A 225 (1997) 105–117.
[88] H. Wu, M. Gao, D. Zhu, S. Zhang, Y. Pan, H. Pan, Y. Liu, F.J. Oliveira, J.M. Vieira, SiC whisker reinforced multi-carbides composites prepared from $B_4C$ and pyrolyzed rice husks via reactive infiltration, Ceram. Int. 38 (2012) 3519–3527.
[89] S. Niyomwas, Synthesis and characterization of silicon–silicon carbide composites from rice husk ash via self-propagating high temperature synthesis, J. Metals Mater. Miner. 19 (2009) 21–25.
[90] X.G. Chen, S.S. Lv, Y. Ye, J.P. Cheng, S.H. Yin, Preparation and characterization of rice husk/ferrite composites, Chin. Chem. Lett. 21 (2010) 122–126.
[91] D.S. Prasad, A.R. Krishna, Fabrication and characterization of A356. 2-rice husk ash composite using stir casting technique, Int. J. Eng. Sci. Technol. 2 (2010) 7603–7608.
[92] D.S. Prasad, A.R. Krishna, Production and mechanical properties of A356. 2/RHA composites, Int. J. Adv. Sci. Technol. 33 (2011) 51–58.
[93] U. Rattanasak, P. Chindaprasirt, P. Suwanvitaya, Development of high volume rice husk ash alumino silicate composites, Int. J. Miner. Metall. Mater. 17 (2010) 654–659.
[94] T. Luangvaranunt, C. Dhadsanadhep, J. Umeda, E. Nisaratanaporn, K. Kondoh, Aluminum-4 mass% copper/alumina composites produced from aluminum copper and rice husk ash silica powders by powder forging, Mater. Trans. 51 (2010) 756–761.

[95] V.S. Aigbodion, Development of Al–Si–Fe/rice husk ash particulate composites synthesis by double stir casting method, Usak Univ. J. Mater. Sci. 2 (2012) 187–197.

[96] S. Niyomwas, Effect of silica sources on synthesis of alumina-mullite-silicon carbide composite, Adv. Mater. Res. 488 (2012) 607–611.

[97] J. Umeda, K. Kondoh, M. Kawakami, H. Imai, Powder metallurgy magnesium composite with magnesium silicide in using rice husk silica particles, Powder Technol. 189 (2009) 399–403.

[98] S. Kumagai, J. Sasaki, Carbon/silica composite fabricated from rice husk by means of binderless hot-pressing, Bioresour. Technol. 100 (2009) 3308–3315.

[99] V.M. Sreekumar, R.M. Pillai, B.C. Pai, M. Chakraborty, Microstructural development in Al/MgAl$_2$O$_4$ in situ metal matrix composite using value-added silica sources, Sci. Technol. Adv. Mater. 9 (2008) 1–9.

[100] D. Zhu, M. Gao, H. Pan, Y. Liu, X. Wang, Y. Pan, F.J. Oliveira, J.M. Vieira, Reactive infiltration processing of SiC/Fe–Si composites using preforms made of coked rice husks and SiC powder, Ceram. Int. 39 (2013) 3831–3842.

[101] F. Adam, J.N. Appaturi, Z. Khanam, R. Thankappan, M.A.M. Nawi, Utilization of tin and titanium incorporated rice husk silica nanocomposite as photocatalyst and adsorbent for the removal of methylene blue in aqueous medium, Appl. Surf. Sci. 264 (2013) 718–726.

[102] M. Zawrah, M. Zayed, M.R. Ali, Synthesis and characterization of SiC and SiC/Si$_3$N$_4$ composite nano powders from waste material, J. Hazard. Mater. 227 (2012) 250–256.

[103] A. Jaroenworaluck, N. Pijarn, N. Kosachan, R. Stevens, Nanocomposite TiO$_2$–SiO$_2$ gel for UV absorption, Chem. Eng. J. 181 (2012) 45–55.

[104] K. Kondoh, H. Oginuma, R. Tuzuki, T. Aizawa, Magnesium matrix composite with solid-state synthesized Mg$_2$Si dispersoids, Mater. Trans. 44 (2003) 611–618.

[105] S. Saravanan, M. Senthilkumar, S. Shankar, Effect of particle size on tribological behavior of rice husk ash–reinforced aluminum alloy (AlSi10Mg) matrix composites, Tribol. Trans. 56 (2013) 1156–1167.

[106] R. Escalera-Lozano, C. Gutiérrez, M.I. Pech-Canul, M.A. Pech-Canul, Degradation of Al/SiC$_p$ composites produced with rice-hull ash and aluminum cans, Waste Manage. 28 (2008) 389–395.

[107] X. Wu, S. Tong, X. Liu, X. Bao, S. Jiang, D. Feng, G. Siu, X-ray diffraction study of alternating nanocrystalline silicon/amorphous silicon multilayers, Appl. Phys. Lett. 70 (1997) 838–840.

[108] N. Awaji, S. Ohkubo, T. Nakanishi, T. Aoyama, Y. Sugita, K. Takasaki, S. Komiya, Thermal oxide growth at chemical vapor deposited SiO$_2$/Si interface during annealing evaluated by difference X-ray reflectivity, Appl. Phys. Lett. 71 (1997) 1954–1956.

[109] P.R. Pinto, L.C. Mendes, M.L. Dias, C. Azuma, Synthesis of acrylic-modified sol–gel silica, Colloid Polym. Sci. 284 (2006) 529–535.

[110] W. Wang, X. Fu, J. Tang, L. Jiang, Preparation of submicron spherical particles of silica by the water-in-oil microemulsion method, Colloids Surf., A 81 (1993) 177–180.

[111] H.D. Jang, Experimental study of synthesis of silica nanoparticles by a bench-scale diffusion flame reactor, Powder Technol. 119 (2001) 102–108.

[112] S. Komarneni, V. Menon, Hydrothermal and microwave-hydrothermal preparation of silica gels, Mater. Lett. 27 (1996) 313–315.

[113] X. Cai, R. Hong, L. Wang, X. Wang, H. Li, Y. Zheng, D. Wei, Synthesis of silica powders by pressured carbonation, Chem. Eng. J. 151 (2009) 380–386.

[114] S.R. Kamath, A. Proctor, Silica gel from rice hull ash: preparation and characterization, Cereal Chem. 75 (1998) 484–487.

[115] A. Proctor, X-ray diffraction and scanning electron microscope studies of processed rice hull silica, J. Am. Oil. Chem. Soc. 67 (1990) 576–584.

[116] C.J. Brinker, G.W. Scherer, Sol–Gel Science: The Physics and Chemistry of Sol–Gel Processing, Academic Press, 1990.

[117] J.D. Bapat, Mineral Admixtures in Cement and Concrete, CRC Press, 2012.

[118] S. Sugita, Method of producing active rice husk ash, US Patent No. 5329867 A, 1994.

[119] C.G. Sanchez, E.S. Lora, Biomass fluidized bed gasification research in the State University of Campinas, Energy Sustainable Dev. 1 (1994) 31–34.

[120] M. Rozainee, S. Ngo, A.A. Salema, K. Tan, Fluidized bed combustion of rice husk to produce amorphous siliceous ash, Energy Sustainable Dev. 12 (2008) 33–42.

[121] A. Khan, W. De Jong, P. Jansens, H. Spliethoff, Biomass combustion in fluidized bed boilers: potential problems and remedies, Fuel Process. Technol. 90 (2009) 21–50.

[122] E. Bautista, R. Aldas, E. Gagelonia, Rice hull furnaces for paddy drying: the Philippine rice research institute's experience, ACIAR Proc. (1996) 253–260.

[123] R. Singh, R. Maheshwari, T. Ojha, Development of a husk fired furnace, J. Agric. Eng. Res. 25 (1980) 109–120.

[124] N. Yalcin, V. Sevinc, Studies on silica obtained from rice husk, Ceram. Int. 27 (2001) 219–224.

[125] A. Proctor, S. Palaniappan, Adsorption of soy oil free fatty acids by rice hull ash, J. Am. Oil. Chem. Soc. 67 (1990) 15–17.

[126] R. Krishnarao, J. Subrahmanyam, T. Jagadish Kumar, Studies on the formation of black particles in rice husk silica ash, J. Eur. Ceram. Soc. 21 (2001) 99–104.

[127] M. Haslinawati, K. Matori, Z. Wahab, H. Sidek, A. Zainal, Effect of temperature on ceramic from rice husk ash, Int. J. Basic Appl. Sci. 9 (2009) 111–117.

[128] A. Zakharov, A. Belyakov, A. Tsvigunov, Forms of extraction of silicon compounds in rice husks, Glass Ceram. 50 (1993) 420–425.

[129] K. Kordatos, S. Gavela, A. Ntziouni, K. Pistiolas, A. Kyritsi, V. Kasselouri-Rigopoulou, Synthesis of highly siliceous ZSM-5 zeolite using silica from rice husk ash, Microporous Mesoporous Mater. 115 (2008) 189–196.

[130] C. Real, M.D. Alcala, J.M. Criado, Preparation of silica from rice husks, J. Am. Ceram. Soc. 79 (1996) 2012–2016.

[131] R. Withers, J. Thompson, Y. Xiao, R. Kirkpatrick, An electron diffraction study of the polymorphs of SiO$_2$-tridymite, Phys. Chem. Miner. 21 (1994) 421–433.

[132] M.A. Carpenter, M. Wennemer, Characterization of synthetic tridymites by transmission electron microscopy, Am. Mineral. 70 (1985) 517.

[133] D. Roy, R. Roy, Tridymite–cristobalite relations and stable solid solutions, Am. Mineral. 49 (1964) 952–962.

[134] M. Sarangi, S. Bhattacharyya, R. Behera, Effect of temperature on morphology and phase transformations of nano-crystalline silica obtained from rice husk, Phase Transitions 82 (2009) 377–386.

[135] A. Chakraverty, P. Mishra, H. Banerjee, Investigation of combustion of raw and acid-leached rice husk for production of pure amorphous white silica, J. Mater. Sci. 23 (1988) 21–24.

[136] A. Ghosh, S. Ahmed, M. Mollah, Synthesis and characterization of zeolite NaY using local rice husk as a source of silica and removal of Cr (VI) from wastewater by zeolite, Bangladesh J. Sci. Ind. Res. 48 (2013) 81–88.

[137] V. Carmona, R. Oliveira, W. Silva, L. Mattoso, J. Marconcini, Nanosilica from rice husk: extraction and characterization, Ind. Crops Prod. 43 (2013) 291–296.

[138] K. Kumproa, S. Singhykaew, A. Nuntiya, Effects of reaction time and hydrochloric acid concentration on acid hydrolysis of rice Husk by reflux method, Adv. Mater. Res. 550 (2012) 592–597.

[139] T.N. Ang, G.C. Ngoh, A.S.M. Chua, Comparative study of various pretreatment reagents on rice husk and structural changes assessment of the optimised pretreated rice husk, Bioresour. Technol. 135 (2013) 116–119.

[140] L. Xiong, E.H. Sekia, P. Sujaridworakun, S. Wada, K. Saito, Burning temperature dependence of rice husk ashes in structure and property, J. Metals Mater. Miner. 19 (2009) 95–99.

[141] J. Umeda, K. Kondoh, Y. Michiura, Process parameters optimization in preparing high-purity amorphous silica originated from rice husks, Mater. Trans. 48 (2007) 3095–3100.

[142] A. Chakraverty, P. Mishra, H. Banerjee, Investigation of thermal decomposition of rice husk, Thermochim. Acta 94 (1985) 267–275.

[143] T. Sonobe, N. Worasuwannarak, Kinetic analyses of biomass pyrolysis using the distributed activation energy model, Fuel 87 (2008) 414–421.

[144] T.-H. Liou, Evolution of chemistry and morphology during the carbonization and combustion of rice husk, Carbon 42 (2004) 785–794.

[145] E. Gorzkowski, S. Qadri, B. Rath, R. Goswami, J. Caldwell, Formation of nanodimensional 3C-SiC structures from rice husks, J. Electron. Mater. 42 (2013) 799–804.

[146] J. Umeda, K. Kondoh, High-purity amorphous silica originated in rice husks via carboxylic acid leaching process, J. Mater. Sci. 43 (2008) 7084–7090.

[147] J. Umeda, K. Kondoh, Process optimization to prepare high-purity amorphous silica from rice husks via citric acid leaching treatment, Trans. Joining Weld. Res. Inst. 37 (2008) 13–17.

[148] Y. Ding, D. Su, Purifying native in-situ mastoid SiO$_2$ from rice husk, Energy Proc. 16 (2012) 1269–1274.

[149] S. Javed, S. Naveed, N. Feroze, M. Zafar, M. Shafaq, Crystal and amorphous silica from KMnO$_4$ treated and untreated rice husk, J. Qual. Technol. Manage. 6 (2010) 81–90.

[150] J. Shen, X. Liu, S. Zhu, H. Zhang, J. Tan, Effects of calcination parameters on the silica phase of original and leached rice husk ash, Mater. Lett. 65 (2011) 1179–1183.

[151] U. Kalapathy, A. Proctor, J. Shultz, An improved method for production of silica from rice hull ash, Bioresour. Technol. 85 (2002) 285–289.

[152] T.-H. Liou, C.-C. Yang, Synthesis and surface characteristics of nanosilica produced from alkali-extracted rice husk ash, Mater. Sci. Eng., B 176 (2011) 521–529.

[153] M.-J. Muñoz-Aguado, M. Gregorkiewitz, Sol–gel synthesis of microporous amorphous silica from purely inorganic precursors, J. Colloid Interface Sci. 185 (1997) 459–465.

[154] J. Schlomach, M. Kind, Investigations on the semi-batch precipitation of silica, J. Colloid Interface Sci. 277 (2004) 316–326.

[155] D. Li, X. Zhu, Short-period synthesis of high specific surface area silica from rice husk char, Mater. Lett. 65 (2011) 1528–1530.

[156] D. Li, D. Chen, X. Zhu, Reduction in time required for synthesis of high specific surface area silica from pyrolyzed rice husk by precipitation at low pH, Bioresour. Technol. 102 (2011) 7001–7003.

[157] K.C.S. D.N. Subbukrishna, P.J. Paul, S. Dasappa, N.K.S. Rajan, Precipitated silica from rice husk ash by IPSIT process, in: 15th European Biomass Conference and Exhibition Berlin, Germany, 2007.

[158] R.B. Heimann, Classic and Advanced Ceramics, Wiley.com, 2010.

[159] X. Ma, B. Zhou, W. Gao, Y. Qu, L. Wang, Z. Wang, Y. Zhu, A recyclable method for production of pure silica from rice hull ash, Powder Technol. 217 (2011) 497–501.

[160] A. Rabenau, The role of hydrothermal synthesis in preparative chemistry, Angew. Chem., Int. Ed. Engl. 24 (1985) 1026–1040.

[161] K. Byrappa, M. Yoshimura, Hydrothermal Technology-Principals and Applications in ''Handbook of Hydrothermal Technology'', William Andrew Publishing, 2000.

[162] J.D. Corbett, Polyatomic Zintl anions of the post-transition elements, Chem. Rev. 85 (1985) 383–397.

[163] H. Schäfer, On the problem of polar intermetallic compounds: the stimulation of E. Zintl's work for the modern chemistry of intermetallics, Annu. Rev. Mater. Sci. 15 (1985) 1–42.

[164] G.R. Patzke, F. Krumeich, R. Nesper, Oxidic nanotubes and nanorods—anisotropic modules for a future nanotechnology, Angew. Chem. Int. Ed. 41 (2002) 2446–2461.

[165] U. Benjamin Iyenagbe, O. Mamat, Hydro thermo-baric processing and properties of nano silica from rice husk, Appl. Mech. Mater. 152 (2012) 177–182.

[166] B.I. Ugheoke, O. Mamat, B. Ari-Wahjoedi, A direct comparison of processing methods of high purity rice husk silica, Asian J. Sci. Res. 6 (2013) 573–580.

[167] K. Mochidzuki, A. Sakoda, M. Suzuki, J. Izumi, N. Tomonaga, Structural behavior of rice husk silica in pressurized hot-water treatment processes, Ind. Eng. Chem. Res. 40 (2001) 5705–5709.

[168] K. Rohatgi, S.V. Prasad, P.K. Rohatgi, Release of silica-rich particles from rice husk by microbial fermentation, J. Mater. Sci. Lett. 6 (1987) 829–831.

[169] M. Estevez, S. Vargas, V. Castano, R. Rodriguez, Silica nano-particles produced by worms through a bio-digestion process of rice husk, J. Non-Cryst. Solids 355 (2009) 844–850.

[170] R. Krishnarao, M. Godkhindi, Effect of $Si_3N_4$ additions on the formation of SiC whiskers from rice husks, Ceram. Int. 18 (1992) 185–191.

[171] A. Davidson, D. Regener, A comparison of aluminium-based metal-matrix composites reinforced with coated and uncoated particulate silicon carbide, Compos. Sci. Technol. 60 (2000) 865–869.

[172] M. Mukherjee, Silicon Carbide-Materials, Processing and Applications in Electronics Devices, 1st ed., Intech Publications, Croatia, 2011. pp. 337–368.

[173] F. Narciso-Romero, F. Rodriguez-Reinoso, Synthesis of SiC from rice husks catalysed by iron, cobalt or nickel, J. Mater. Sci. 31 (1996) 779–784.

[174] I. Rahman, F. Riley, The control of morphology in silicon nitride powder prepared from rice husk, J. Eur. Ceram. Soc. 5 (1989) 11–22.

[175] B.K. Parekh, W.M. Goldberger, Recovery of silicon carbide whiskers from coked, converted rice hulls by liquid–liquid separation, US Patent No. 4249700, 1981.

[176] P. Somasundaran, K.P. Ananthapadmanabhan, Recovery of silicon carbide whiskers from coked, converted rice hulls by selective flocculation-liquid extraction, US Patent No. 4256571, 1981.

[177] S. Pickard, B. Derby, E. Feest, TEM study of silicon carbide whisker microstructures, J. Mater. Sci. 26 (1991) 6207–6217.

[178] N. Parratt, Whisker reinforced plastics and metals (reinforcement with whiskers of high temperature metals such as nickel, cobalt and nickel-chrome alloys), Chem. Eng. Prog. 62 (1966) 61–67.

[179] B. Radhakrishna Bhat, G. Sanghi, Increase in the yield of silicon carbide whiskers from rice husk, Bull. Mater. Sci. 9 (1987) 295–303.

[180] B.R. Bhat, G. Sanghi, Increase in the yield of silicon carbide whiskers from rice husk, Bull. Mater. Sci. 9 (1987) 295–303.

[181] J.V. Milewski, F.D. Gac, J.J. Petrovic, S. Skaggs, Growth of beta-silicon carbide whiskers by the VLS process, J. Mater. Sci. 20 (1985) 1160–1166.

[182] J.J. Petrovic, G.F. Hurley, Vapor–liquid–solid (VLS) SiC whiskers: synthesis and mechanical properties, in: Fiber Reinforced Ceramic Composites: Materials, Processing and Technology, Noyes Publications, 1990, pp. 93–121.

[183] S. Nutt, Defects in silicon carbide whiskers, J. Am. Ceram. Soc. 67 (2006) 428–431.

[184] G. McMahon, G. Carpenter, T. Malis, On the growth mechanism of silicon carbide whiskers, J. Mater. Sci. 26 (1991) 5655–5663.

[185] N.A.L. Mansour, S. Hanna, Silicon carbide and nitride from rice hulls: II, Effect of iron on the formation of silicon carbide, Trans. J. Br. Ceram. Soc. 78 (1979) 132–136.

[186] S.R. Nutt, Microstructure and growth model for rice-hull-derived SiC whiskers, J. Am. Ceram. Soc. 71 (1988) 149–156.

[187] M. Patel, A. Karera, SiC whisker from rice husk: microscopic study, Powder Metall. Int. 23 (1991) 30–32.

[188] A.K. Ray, G. Mahanty, A. Ghose, Effect of catalysts and temperature on silicon carbide whiskers formation from rice husk, J. Mater. Sci. Lett. 10 (1991) 227–229.

[189] S. Singh, L. Stachowicz, S. Girshick, E. Pfender, Thermal plasma synthesis of SiC from rice hull (husk), J. Mater. Sci. Lett. 12 (1993) 659–660.

[190] S. Moustafa, M. Morsi, A.A. El-Din, Formation of silicon carbide from rice hulls, Can. Metall. Q. 36 (1997) 355–358.

[191] R.V. Krishnarao, Y.R. Mahajan, T.J. Kumar, Conversion of raw rice husks to SiC by pyrolysis in nitrogen atmosphere, J. Eur. Ceram. Soc. 18 (1998) 147–152.

[192] K. Janghorban, H. Tazesh, Effect of catalyst and process parameters on the production of silicon carbide from rice hulls, Ceram. Int. 25 (1999) 7–12.

[193] B. Panigrahi, G. Roy, M. Godkhindi, Kinetic studies on production of silicon carbide from rice husks, Br. Ceram. Trans. 100 (2001) 29–34.

[194] S. Lakiza, Y.P. Dyban', Preparation of silicon carbide from rice husks, Powder Metall. Met. Ceram. 21 (1982) 117–121.

[195] R. Krishnarao, M. Godkhindi, M. Chakraborty, P. Mukunda, Formation of SiC whiskers from compacts of raw rice husks, J. Mater. Sci. 29 (1994) 2741–2744.

[196] W.-H. Chen, P.-C. Kuo, A study on torrefaction of various biomass materials and its impact on lignocellulosic structure simulated by a thermogravimetry, Energy 35 (2010) 2580–2586.

[197] T.-H. Liou, F.-W. Chang, J.-J. Lo, Pyrolysis kinetics of acid-leached rice husk, Ind. Eng. Chem. Res. 36 (1997) 568–573.

[198] S. Genieva, S.C. Turmanova, A. Dimitrova, L. Vlaev, Characterization of rice husks and the products of its thermal degradation in air or nitrogen atmosphere, J. Therm. Anal. Calorim. 93 (2008) 387–396.

[199] R. Krishnarao, Y. Mahajan, Formation of SiC whiskers from raw rice husks in argon atmosphere, Ceram. Int. 22 (1996) 353–358.

[200] I. Pastorova, R.E. Botto, P.W. Arisz, J.J. Boon, Cellulose char structure: a combined analytical Py-GC-MS, FTIR, and NMR study, Carbohydr. Res. 262 (1994) 27–47.

[201] D. Wolfe, B. Hinds, F. Wang, G. Lucovsky, B. Ward, M. Xu, R. Nemanich, D. Maher, Thermochemical stability of silicon–oxygen–carbon alloy thin films: a model system for chemical and structural relaxation at SiC–$SiO_2$ interfaces, J. Vac. Sci. Technol. A: Vac. Surf. Films 17 (1999) 2170–2177.

[202] K. Sujirote, P. Leangsuwan, Silicon carbide formation from pretreated rice husks, J. Mater. Sci. 38 (2003) 4739–4744.

[203] S. Niyomwas, In Situ synthesis of silicon–silicon carbide composites from $SiO_2$-C-Mg system via self-propagating high-temperature synthesis, EPD Congress (2009) 777–784.

[204] B.-D. Park, S.G. Wi, K.H. Lee, A.P. Singh, T.-H. Yoon, Y.S. Kim, Characterization of anatomical features and silica distribution in rice husk using microscopic and micro-analytical techniques, Biomass Bioenergy 25 (2003) 319–327.

[205] R. Krishnarao, M. Godkhindi, Distribution of silica in rice husks and its effect on the formation of silicon carbide, Ceram. Int. 18 (1992) 243–249.

[206] V. Martinez, M. Valencia, J. Cruz, J. Mejia, F. Chejne, Production of β-SiC by pyrolysis of rice husk in gas furnaces, Ceram. Int. 32 (2006) 891–897.

[207] R.V. Krishnarao, M.M. Godkhindi, Studies on the formation of SiC whiskers from pulverized rice husk ashes, Ceram. Int. 18 (1992) 35–42.

[208] J. Sterte, J.E. Otterstedt, H. Thulin, F. Massoth, Characterization of alumina—montmorillonite complexes, Appl. Catal. 38 (1988) 119–129.

[209] M. Patel, A. Karera, SiC whiskers from rice husk: role of catalysts, J. Mater. Sci. Lett. 8 (1989) 955–956.

[210] R. Krishnarao, Effect of cobalt catalyst on the formation of SiC from rice husk silica–carbon black mixture, J. Mater. Sci. 30 (1995) 3645–3651.

[211] N.A. Mansour, S. Hanna, Silicon carbide and nitride from rice hulls: II, Effect of iron on the formation of silicon carbide, Trans. J. Br. Ceram. Soc. 78 (1979) 132–136.

[212] S. Singh, K. Parida, B. Mohanty, S. Rao, High surface area silicon carbide from rice husk: a support material for catalysts, React. Kinet. Catal. Lett. 54 (1995) 29–34.

[213] M. Kermarec, M. Patel, P. Rabette, H. Pezerat, D. Delafosse, Reactivity and structure of nickel-exchanged Prayssac vermiculite, J. Chem. Soc., Faraday Trans. 179 (1983) 599–606.

[214] V. Raman, V. Parashar, O. Bahl, Influence of boric acid on the synthesis of silicon carbide whiskers from rice husks and polyacrylonitrile, J. Mater. Sci. Lett. 16 (1997) 1252–1254.

[215] R. Krishnarao, J. Subrahmanyam, Formation of SiC from rice husk silica-carbon black mixture: effect of rapid heating, Ceram. Int. 22 (1996) 489–492.

[216] M. Zawrah, M. Zayed, M.R.K. Ali, Synthesis and characterization of SiC and SiC/$Si_3N_4$ composite nano powders from waste material, J. Hazard. Mater. 227–228 (2012) 550–556.

[217] S. Singh, B. Mohanty, S. Basu, Synthesis of SiC from rice husk in a plasma reactor, Bull. Mater. Sci. 25 (2002) 561–563.

[218] H.-P. Martin, R. Ecke, E. Müller, Synthesis of nanocrystalline silicon carbide powder by carbothermal reduction, J. Eur. Ceram. Soc. 18 (1998) 1737–1742.

[219] M. Sarangi, B. Mallick, S. Mishra, T. Tiwari, P. Nayak, High-vacuum synthesis of SiC from rice husk: a novel method, J. Phys. D Appl. Phys. 46 (2013) 1–6.

[220] S. Hashimoto, S. Ohashi, K. Hirao, Y. Zhou, H. Hyuga, S. Honda, Y. Iwamoto, Mechanism for the formation of SiC by carbothermal reduction reaction using a microwave heating technique, J. Ceram. Soc. Jpn. 119 (2011) 740–744.

[221] M. Ekelund, B. Forslund, Reactions within quartz-carbon mixtures in a nitrogen atmosphere, J. Eur. Ceram. Soc. 9 (1992) 107–119.

[222] R.V. Krishnarao, Y.R. Mahajan, Effect of acid treatment on the formation of SiC whiskers from raw rice husks, J. Eur. Ceram. Soc. 15 (1995) 1229–1234.

[223] M. Patel, P. Prasanna, Formation of SiC and $Si_2N_2O$ from acid-treated rice husk with catalysts, Trans. Indian Ceram. Soc. 52 (1993) 172–175.

[224] R.V. Krishnarao, Effect of cobalt chloride treatment on the formation of SiC from burnt rice husks, J. Eur. Ceram. Soc. 12 (1993) 395–401.

[225] S.H. Komatsu, R. Nakamizo, Porous ceramics from rice hulls. 1. Enrichment of $SiO_2$ by sieving ground rice hulls for syntheses of SiC and $Si_3N_4$ powder, Kyushu Industrial Technology Laboratory, 1990. pp. 2865–2875.

[226] Z. Ban, L. Shaw, On the reaction sequence of WC–Co formation using an integrated mechanical and thermal activation process, Acta Mater. 49 (2001) 2933–2939.

[227] R. Ren, Z. Yang, L.L. Shaw, Synthesis of nanostructured silicon carbide through an integrated mechanical and thermal activation process, J. Am. Ceram. Soc. 85 (2002) 819–827.

[228] A. Mohanty, M. Misra, L. Drzal, Sustainable bio-composites from renewable resources: opportunities and challenges in the green materials world, J. Polym. Environ. 10 (2002) 19–26.

[229] W. Shi, Y. Zheng, H. Peng, N. Wang, C.S. Lee, S.T. Lee, Laser ablation synthesis and optical characterization of silicon carbide nanowires, J. Am. Ceram. Soc. 83 (2000) 3228–3230.

[230] L.-D. Zhao, B.-P. Zhang, J.-F. Li, M. Zhou, W.-S. Liu, J. Liu, Thermoelectric and mechanical properties of nano-SiC-dispersed $Bi_2Te_3$ fabricated by mechanical alloying and spark plasma sintering, J. Alloy. Compd. 455 (2008) 259–264.

[231] Z. Li, W. Zhou, T. Lei, F. Luo, Y. Huang, Q. Cao, Microwave dielectric properties of SiC (β) solid solution powder prepared by sol–gel, J. Alloy. Compd. 475 (2009) 506–509.

[232] C.M. Lieber, One-dimensional nanostructures: chemistry, physics & applications, Solid State Commun. 107 (1998) 607–616.

[233] S. Agathopoulos, Influence of synthesis process on the dielectric properties of B-doped SiC powders, Ceram. Int. 38 (2012) 3309–3315.

[234] E. Gorzkowski, S. Qadri, B. Rath, S. Singh, Nano-dimensional structures of 3C-SiC formed from rice husk, Semiconductor Device Research Symposium (ISDRS), 2011 International, IEEE, 2011, pp. 1-1.
[235] D.D. Radev, I. Uzunov, Nanosized silicon carbide obtained from rice husks, Solid State Phenom. 159 (2010) 153–156.
[236] Y. Chiew, K. Cheong, Growth of SiC nanowires and nanocones using mixture of oil palm fibres and rice husk ash, J. Mater. Sci. (2012) 1–11.
[237] S. Kantee, P. Mahachai, S. Pukird, Growth of SiC and $SiO_2$ nanostructures prepared from rice husk ash using carbon-metal assisted, Adv. Mater. Res. 236 (2011) 1807–1810.
[238] A. Donaldson, R. Apa, T. Eddy, J. Flinn, Heat transfer in thermal plasma processing ASME 1991, in: 28th National Heat Transfer Conference (Minneapolis, USA), 1991, pp. 41–51.
[239] P. Kong, E. Pfender, Heat Transfer in Thermal Plasma Processing, ASME, New York, 1991.
[240] L. Stachowicz, S. Singh, E. Wender, S. Girshick, Synthesis of ultrafine SiC from rice hulls (husks): a plasma process, Plasma Chem. Plasma Process. 13 (1993) 447–461.
[241] D. Changhong, Z. Xianpeng, Z. Jinsong, Y. Yongjin, C. Lihua, X. Fei, The synthesis of ultrafine SiC powder by the microwave heating technique, J. Mater. Sci. 32 (1997) 2469–2472.
[242] C. Dai, X. Zhang, J. Zhang, Y. Yang, L. Cao, F. Xia, Microwave synthesis of ultrafine silicon carbide whiskers, J. Am. Ceram. Soc. 80 (1997) 1274–1276.
[243] S. Qadri, M. Imam, A. Fliflet, B. Rath, R. Goswami, J. Caldwell, Microwave-induced transformation of rice husks to SiC, J. Appl. Phys. 111 (2012) 073523–073525.
[244] C. Rambo, J. Martinelli, A.H.A. Bressiani, Synthesis of SiC and cristobalite from rice husk by microwave heating, Mater. Sci. Forum 299–300 (1999) 63–69.
[245] J. Li, T. Shirai, M. Fuji, Rapid carbothermal synthesis of nanostructured silicon carbide particles and whiskers from rice husk by microwave heating method, Adv. Powder Technol. 24 (2013) 838–843.
[246] M. Wang, M. Xie, L. Ferraioli, Z. Yuan, D. Li, D. Yang, L. Pavesi, Light emission properties and mechanism of low-temperature prepared amorphous SiN films. I. Room-temperature band tail states photoluminescence, J. Appl. Phys. 104 (2008) 083504.
[247] M. Herrmann, H. Klemm, C. Schubert, Silicon nitride based hard materials, Handb. Ceram. Hard Mater. (2000) 749–801.
[248] H.M. Jennings, B.J. Dalgleish, P. Pratt, Reactions between silicon and nitrogen, J. Mater. Sci. 23 (1988) 2573–2583.
[249] S.J. Durham, K. Shanker, R.A. Drew, Carbothermal synthesis of silicon nitride: effect of reaction conditions, J. Am. Ceram. Soc. 74 (1991) 31–37.
[250] G. Ziegenbalg, U. Breuel, E. Ebrecht, H. Holldorf, R. Brink, Synthesis of $\alpha$-silicon nitride powder by gas-phase ammonolysis of $CH_3SiCl_3$, J. Eur. Ceram. Soc. 21 (2001) 947–958.
[251] E. Kroke, M. Schwarz, Novel group 14 nitrides, Coord. Chem. Rev. 248 (2004) 493–532.
[252] S. Siddiqi, A. Hendry, The influence of iron on the preparation of silicon nitride from silica, J. Mater. Sci. 20 (1985) 3230–3238.
[253] T. Ličko, V. Figusch, J. Puchyova, Synthesis of silicon nitride by carbothermal reduction and nitriding of silica: control of kinetics and morphology, J. Eur. Ceram. Soc. 9 (1992) 219–230.
[254] S. Bandyopadhyay, J. Mukerji, Reaction sequences in the synthesis of silicon nitride from quartz, Ceram. Int. 17 (1991) 171–179.
[255] D. Perera, Conversion of precipitated silica from geothermal water to silicon nitride, J. Mater. Sci. 22 (1987) 2411–2415.
[256] J.-G. Lee, I.B. Cutler, Formation of SiC from rice hulls, Am. Ceram. Soc. Bull. 54 (1975) 195–198.
[257] I. Rahman, The formation of different $Si_3N_4$ phases in the presence of $V_2O_5$ during carbothermal reduction of untreated and acid treated rice husk, Ceram. Int. 24 (1998) 293–297.
[258] M. Tanaka, T. Kawabe, Method of manufacturing crystalline silicon nitride and method of separation thereof, US Patent No. 4504453 A, 1985.
[259] T.-H. Liou, F.-W. Chang, The nitridation kinetics of pyrolyzed rice husk, Ind. Eng. Chem. Res. 35 (1996) 3375–3383.
[260] I. Rahman, Preparation of $Si_3N_4$ by carbothermal reduction of digested rice husk, Ceram. Int. 20 (1994) 195–199.
[261] T. Hashishin, H. Iwanaga, Y. Yamamoto, Effect of impurities on silicon nitride whiskers synthesized from silica-containing natural substances, J. Mater. Res. 18 (2003) 2760–2764.
[262] T. Hashishin, Y. Kaneko, H. Iwanaga, Y. Yamamoto, The synthesis of silicon nitride whiskers from $SiO_2$–$N_2$–$Na_3AlF_6$ system, J. Mater. Sci. 34 (1999) 2193–2197.
[263] L. Darken, R. Gurry, Physical Chemistry of Metals, McGraw-Hill Book Co., New York, 1953. 18 445.
[264] M. Sarangi, Effect of an iron catalyst and process parameters on Si-based ceramic materials synthesized from rice husks, Silicon 1 (2009) 103–109.
[265] B. Bergman, H. Heping, The influence of different oxides on the formation of $Si_2N_2O$ from $SiO_2$ and $Si_3N_4$, J. Eur. Ceram. Soc. 6 (1990) 3–8.
[266] A. Leal-Cruz, Synthesis and characterization of silicon nitride reinforcements by the thermal decomposition of $Na_2SiF_6$ in nitrogen containing atmosphere, MSc Thesis, Department of Ceramic Engineering, CINVESTAV-Saltillo, Mexico, 2004.
[267] A. Leal-Cruz, M.I. Pech-Canul, E. Lara-Curzio, R. Trejo, R. Peascoe, Selective synthesis and characterization of HYSYCVD-$Si_2N_2O$, Mater. Chem. Phys. 114 (2009) 376–381.
[268] H.C. Freyhardt, Crystals–Growth, Properties, and Applications: Vol. 2, Growth and Properties, 1979.
[269] H. Acharya, S. Datta, H. Banerjee, S. Basu, Low-temperature preparation of polycrystalline silicon from silicon tetrachloride, Mater. Lett. 1 (1982) 64–66.
[270] H. Acharya, S.K. Dutta, H. Banerjee, Production of magnesium silicide and silane from rice husk ash, Sol. Energy Mater. 3 (1980) 441–445.
[271] P. Mishra, A. Chakraverty, H. Banerjee, Production and purification of silicon by calcium reduction of rice-husk white ash, J. Mater. Sci. 20 (1985) 4387–4391.
[272] R.S.a.B.K. Dhindaw, Production of high purity silicon for use in solar cells, sun: mankind's future source of energy, in: F.d.W.a.M. Cox (Ed.), Proc. Int. Solar Energy Cong., Pergamon Press, Oxford, New York, 1978, pp. 776–781.
[273] H. Banerjee, S. Sen, H. Acharya, Investigations on the production of silicon from rice husks by the magnesium method, Mater. Sci. Eng. 52 (1982) 173–179.
[274] K.K. Larbi, Synthesis of High Purity Silicon from Rice Husks, University of Toronto, 2010.
[275] A. Xing, J. Zhang, Z. Bao, Y. Mei, A.S. Gordin, K.H. Sandhage, A magnesiothermic reaction process for the scalable production of mesoporous silicon for rechargeable lithium batteries, Chem. Commun. 49 (2013) 6743–6745.
[276] Y.J. Sung, D.S. Jung, S.B. Park, D.S. Song, Method for producing high-purity porous silica and silicon derived from rice husks, WO Patent 2,012,153,897, 2012.
[277] J.A. Amick, Purification of rice hulls as a source of solar grade silicon for solar cells, J. Electrochem. Soc. 129 (1982) 864–866.
[278] L. Hunt, J. Dismukes, J. Amick, A. Schei, K. Larsen, Rice hulls as a raw material for producing silicon, J. Electrochem. Soc. 131 (1984) 1683–1686.
[279] A. Razaghian, A. Bahrami, M. Emamy, The influence of Li on the tensile properties of extruded in-situ Al–15% $Mg_2Si$ composite, Mater. Sci. Eng., A 532 (2012) 346–353.
[280] N. Soltani, A. Bahrami, M.I. Pech-Canul, The effect of Ti on mechanical properties of extruded in-Situ Al-15 pct $Mg_2Si$ composite, Metall. Mater. Trans. A 44 (2013) 4366–4373.
[281] I. Kogut, M.C. Record, Growth of magnesium silicide thin films on Si (100), Si (111) and SOI substrates during rapid thermal processing, Intermetallics 32 (2013) 184–193.
[282] A. Bahrami, A. Razaghian, M. Emamy, R. Khorshidi, The effect of Zr on the microstructure and tensile properties of hot-extruded Al–$Mg_2Si$ composite, Mater. Des. 36 (2012) 323–330.
[283] A. Bahrami, A. Razaghian, M. Emamy, H. Jafari Nodooshan, G. Mousavi, Microstructure and tensile properties of Al-15wt% $Mg_2Si$ composite after hot extrusion and heat treatment, Key Eng. Mater. 471 (2011) 1171–1176.
[284] N. Soltani, A. Bahrami, F. Moghimi, M.I. Pech-Canul, A. Hajaghasi, Der effekt von strangpressen und T6-behandlung auf die mechanischen eigenschaften eines Al-15Ma.-% $Mg_2Si$-verbundwerkstoffs, HTM J. Heat Treat. Mater. 67 (2012) 378.
[285] N. Soltani, H. Jafari Nodooshan, A. Bahrami, M.I. Pech-Canul, W. Liu, G. Wu, Effect of hot extrusion on wear properties of Al–15wt.% $Mg_2Si$ in situ metal matrix composites, Mater. Des. 53 (2014) 774–781.
[286] J. Umeda, K. Kondoh, H. Imai, Friction and wear behavior of sintered magnesium composite reinforced with CNT-$Mg_2Si$/MgO, Mater. Sci. Eng., A 504 (2009) 157–162.
[287] K. Sing, D. Everett, R. Haul, L. Moscou, R. Pierotti, J. Rouqué rol, T. Siemieniewska, Pure Appl. Chem. 57 (1985) 603.
[288] A. Jain, T. Rajeswara Rao, S. Sambi, P. Grover, Energy and chemicals from rice husk, Biomass Bioenergy 7 (1994) 285–289.
[289] J. Mdoe, L. Mkayula, Preparation and characterization of activated carbons from rice husks and shells of palm fruits, Tanzania J. Sci. 28 (2004) 131–142.
[290] A. Ganesh, P. Dutt Grover, Combustion and gasification characteristics of rice husk, Fuel 71 (1992) 889–894.
[291] M. Molina-Sabio, M. Gonzalez, F. Rodriguez-Reinoso, A. Sepulveda-Escribano, Effect of steam and carbon dioxide activation in the micropore size distribution of activated carbon, Carbon 34 (1996) 505–509.
[292] T.-H. Liou, S.-J. Wu, Characteristics of microporous/mesoporous carbons prepared from rice husk under base-and acid-treated conditions, J. Hazard. Mater. 171 (2009) 693–703.
[293] Y. Chen, S.-R. Zhai, N. Liu, Y. Song, Q.-D. An, X.-W. Song, Dye removal of activated carbons prepared from NaOH-pretreated rice husks by low-temperature solution-processed carbonization and $H_3PO_4$ activation, Bioresour. Technol. 144 (2013) 401–409.
[294] K. Mohanty, J.T. Naidu, B. Meikap, M. Biswas, Removal of crystal violet from wastewater by activated carbons prepared from rice husk, Ind. Eng. Chem. Res. 45 (2006) 5165–5171.
[295] X. Song, Y. Zhang, C. Chang, Novel method for preparing activated carbons with high specific surface area from rice husk, Ind. Eng. Chem. Res. 51 (2012) 15075–15081.
[296] S. Uçar, M. Erdem, T. Tay, S. Karagöz, Preparation and characterization of activated carbon produced from pomegranate seeds by $ZnCl_2$ activation, Appl. Surf. Sci. 255 (2009) 8890–8896.
[297] Ö. Gerçel, A. Özcan, A.S. Özcan, H.F. Gerçel, Preparation of activated carbon from a renewable bio-plant of Euphorbia rigida by $H_2SO_4$ activation and its adsorption behavior in aqueous solutions, Appl. Surf. Sci. 253 (2007) 4843–4852.

[298] A. Basta, V. Fierro, H. Saied, A. Celzard, Effect of deashing rice straws on their derived activated carbons produced by phosphoric acid activation, Biomass Bioenergy 35 (2011) 1954–1959.

[299] H. Deng, G. Li, H. Yang, J. Tang, J. Tang, Preparation of activated carbons from cotton stalk by microwave assisted KOH and $K_2CO_3$ activation, Chem. Eng. J. 163 (2010) 373–381.

[300] A. Puziy, O. Poddubnaya, A. Martınez-Alonso, F. Suarez-Garcıa, J. Tascón, Synthetic carbons activated with phosphoric acid: I. Surface chemistry and ion binding properties, Carbon 40 (2002) 1493–1505.

[301] M. Hussein, R. Tarmizi, Z. Zainal, R. Ibrahim, M. Badri, Preparation and characterization of active carbons from oil palm shells, Carbon 34 (1996) 1447–1449.

[302] F. Kapteijn, G. Abbel, J.A. Moulijn, $CO_2$ gasification of carbon catalysed by alkali metals: reactivity and mechanism, Fuel 63 (1984) 1036–1042.

[303] L.J. Kennedy, J.J. Vijaya, K. Kayalvizhi, G. Sekaran, Adsorption of phenol from aqueous solutions using mesoporous carbon prepared by two-stage process, Chem. Eng. J. 132 (2007) 279–287.

[304] L.J. Kennedy, J.J. Vijaya, G. Sekaran, Effect of two-stage process on the preparation and characterization of porous carbon composite from rice husk by phosphoric acid activation, Ind. Eng. Chem. Res. 43 (2004) 1832–1838.

[305] G.Y. Peng, Y.S. Fang, Z.J. Zhe, W.Z. Chen, Z.M. Yu, Preparation of active carbon with high specific surface area from rice husks, Chem. Res. Chin. Univ. 3 (2000) 001.

[306] Y. Guo, S. Yang, K. Yu, J. Zhao, Z. Wang, H. Xu, The preparation and mechanism studies of rice husk based porous carbon, Mater. Chem. Phys. 74 (2002) 320–323.

[307] M.M. Yeganeh, T. Kaghazchi, M. Soleimani, Effect of raw materials on properties of activated carbons, Chem. Eng. Technol. 29 (2006) 1247–1251.

[308] D. Kalderis, S. Bethanis, P. Paraskeva, E. Diamadopoulos, Production of activated carbon from bagasse and rice husk by a single-stage chemical activation method at low retention times, Bioresour. Technol. 99 (2008) 6809–6816.

[309] Y. Guo, K. Yu, Z. Wang, H. Xu, Effects of activation conditions on preparation of porous carbon from rice husk, Carbon 41 (2003) 1645–1647.

[310] C.H. Yun, Y.H. Park, C.R. Park, Effects of pre-carbonization on porosity development of activated carbons from rice straw, Carbon 39 (2001) 559–567.

[311] P. Yeletsky, V. Yakovlev, M. Mel'gunov, V. Parmon, Synthesis of mesoporous carbons by leaching out natural silica templates of rice husk, Microporous Mesoporous Mater. 121 (2009) 34–40.

[312] G.H. Oh, C.R. Park, Preparation and characteristics of rice-straw-based porous carbons with high adsorption capacity, Fuel 81 (2002) 327–336.

[313] M.J. Ahmed, S.K. Theydan, Microporous activated carbon from Siris seed pods by microwave-induced KOH activation for metronidazole adsorption, J. Anal. Appl. Pyrol. 99 (2013) 101–109.

[314] D.N. Han, D. Xie, Y. Gao, Q. Zhang, J. Zhu, Response surface method to optimize pretreatment of rice husk by microwave-assisted NaOH solution, Adv. Mater. Res. 550 (2012) 1486–1490.

[315] X. He, P. Ling, M. Yu, X. Wang, X. Zhang, M. Zheng, Rice husk-derived porous carbons with high capacitance by $ZnCl_2$ activation for supercapacitors, Electrochim. Acta 105 (2013) 635–641.

[316] L.J. Bellamy, The infra-red spectra of complex molecules, (1958).

[317] C.J. Pouchert, The Aldrich library of infrared spectra, (1975).

[318] H. Preiss, L.-M. Berger, K. Szulzewsky, Thermal treatment of binary carbonaceous/zirconia gels and formation of Zr (C, O, N) solid solutions, Carbon 34 (1996) 109–119.

[319] D. Basa, F. Smith, Annealing and crystallization processes in a hydrogenated amorphous Si–C alloy film, Thin Solid Films 192 (1990) 121–133.

[320] Y. Juan, Q. Ke-Qiang, Preparation of activated carbon by chemical activation under vacuum, Environ. Sci. Technol. 43 (2009) 3385–3390.

[321] A.L. Smith, D.R. Anderson, Vibrational spectra of $Me_2SiCl_2$, $Me_3SiCl$, $Me_3SiOSiMe_3$, $(Me_2SiO)_3$, $(Me_2SiO)_4$, $(Me_2SiO)_x$, and their deuterated analogs, Appl. Spectrosc. 38 (1984) 822–834.

[322] J.L. Nieto, Infrared determination of quartz, kaolin, corundum, silicon carbide and orthoclase in respirable dust from grinding wheels, Analyst 103 (1978) 128–133.

[323] K. Sato, F. Kurosawa, O. Kammori, Effect of particle size on infrared spectra of inorganic powders, Bull. Chem. Soc. Jpn. 42 (1969) 3593–3596.

[324] C.F. Bohren, D.R. Huffman, Absorption and Scattering of Light by Small Particles, Wiley VCH, 1983. 82–129.

[325] M. Falk, S. Karunanithy, Determination of $SiO_2$ in SiC whiskers by infrared absorption spectroscopy, Mater. Sci. Eng., A 114 (1989) 209–212.

[326] G. Lucovsky, J. Yang, S. Chao, J. Tyler, W. Czubatyj, Oxygen-bonding environments in glow-discharge-deposited amorphous silicon-hydrogen alloy films, Phys. Rev. B 28 (1983) 3225.

[327] N. Yalçın, V. Sevinc, Studies of the surface area and porosity of activated carbons prepared from rice husks, Carbon 38 (2000) 1943–1945.

[328] M. Lillo-Ródenas, D. Cazorla-Amorós, A. Linares-Solano, Understanding chemical reactions between carbons and NaOH and KOH: an insight into the chemical activation mechanism, Carbon 41 (2003) 267–275.

[329] A. Daifullah, B. Girgis, H. Gad, A study of the factors affecting the removal of humic acid by activated carbon prepared from biomass material, Colloids Surf., A 235 (2004) 1–10.

[330] Y. Guo, D.A. Rockstraw, Activated carbons prepared from rice hull by one-step phosphoric acid activation, Microporous Mesoporous Mater. 100 (2007) 12–19.

[331] A. Basta, V. Fierro, H. El-Saied, A. Celzard, 2-Steps KOH activation of rice straw: an efficient method for preparing high-performance activated carbons, Bioresour. Technol. 100 (2009) 3941–3947.

[332] J. Chen, G. Hou, Preparation of active carbon with high specific surface area from rice husks via KOH, Mater. Rev. 10 (2009) 032.

[333] D. An, Y. Guo, B. Zou, Y. Zhu, Z. Wang, A study on the consecutive preparation of silica powders and active carbon from rice husk ash, Biomass Bioenergy 35 (2011) 1227–1234.

[334] J. Sahu, S. Agarwal, B. Meikap, M. Biswas, Performance of a modified multi-stage bubble column reactor for lead (II) and biological oxygen demand removal from wastewater using activated rice husk, J. Hazard. Mater. 161 (2009) 317–324.